Russian Chemical Reviews **74** (10) 937 – 967 (2005) © 2005 Russian Academy of Sciences and Turpion Ltd

DOI 10.1070/RC2005v074n10ABEH001168

Topological structure and relaxation properties of polymers †

V I Irzhak

Contents

I.	Introduction	937
II.	Relaxation spectrometry	938
III.	Manifestation of the topological structure of polymers in their relaxation properties	940
IV.	The relaxation time spectrum as a means of correct characterisation of topological structure	949
V.	Conclusion	963

Abstract. The experimental data and theoretical views on the relations between the relaxation properties and structure of polymers are generalised. The attention is focused on the topological structural level, in particular, characteristics including the molecular mass, the molecular mass distribution, the degree of branching, and the covalent and equilibrium network parameters. In relation to the discussion of the relaxation spectrometry concept, the physical meaning of the kinetic parameters of local transitions and the nature of β-relaxation are considered. Methods of calculation of the continuous and discrete relaxation spectra from the results of relaxation and rheological experiments are described. Data establishing the relation between the relaxation spectrum and the topological structure of a polymer are analysed. The bibliography includes 282 references.

I. Introduction

The relaxation properties of polymeric materials determine the possibility of using them in practice.[1,2] Of course, the nature and character of relaxation processes depend on the polymer structure. However, the concept of polymer structure requires a clear definition.

A feature of high-molecular-mass compounds is that their complex structure cannot be described in a certain single fashion. Conditionally, it is possible to consider three interrelated structural levels, namely, a molecular, a topological and a supramolecular level.[3] Characterisation of each level requires the use of a specific approach.

The molecular level covers the chemical and isomeric structure, *i.e.*, all aspects that can be described by structural formulae accepted in chemistry. On this level polymers are not basically different from low-molecular-mass compounds (of course, if we are dealing with rather complex molecules). While on the subject of chemical structure, the case in point is mainly the local organisation of compounds (at least on the length scale of a unit). At the same time introduction of the notion of sequences (blocks) comprising units of different chemical structure (including isomeric states) (copolymers) is due to the chain nature of high-molecular-mass compounds. Besides, chain molecules (in contrast to the molecules of low-molecular-mass compounds) can have stereoisomers, *i.e.*, include isotactic and syndiotactic groups and correspondingly, blocks comprised of them. Therefore, characterisation of the molecular structure of a polymer requires the use of not only 'chemical language' but also complex concepts, which provide a quantitative description of sequences comprising different types of units.

The second, topological, level is immediately related to the concept of polymer chains. Here, we abstract from particular chemical meaning and consider polymers as sets of chains. Chains can have different lengths and different molecular mass distributions (MMDs), be linear or branched or have a complex cyclic structure (including chemically nonbonded molecules, *e.g.*, catenanes); they can also form a continuous three-dimensional network. It is the topological structure that is responsible for many physical properties of polymeric materials.[1,3–5] The concept of local structural organisation of molecules is insufficient for an understanding of the polymer structure on the topological level. Apparently, the chemical notation is inappropriate for the description of the topological structure, which has a particular geometrical meaning. The topological structure is characterised by graphs which include such elements as vertices (branching points), edges (chains), *etc.* The graph theory ignores the edge length, but the chain length and the chain length distribution are quite important for the topological structure of polymers.

The topological structural level 'abstracts' from the spatial arrangement of macromolecules, which characterises the supramolecular structure of the polymer. In essence, this is a macroscopic level; nevertheless, the local structural organisation is an important factor. For instance, the local density strongly depends on the energy of intermolecular interaction (chemical nature of the polymer units). The topology also plays a significant role; for instance, the degree of polymer crystallinity is very responsive to the degree of chain branching, *i.e.*, to the structural level in question.

The chemical level of the polymer structure is basic (eventually, chain formation involves formation of chemical bonds; the possibility or impossibility of ring formation or branching in macromolecules is essentially a chemical problem). However, when considering the relations between the structure and properties of a polymer, it is convenient to discuss the effect of each level separately.

V I Irzhak Institute of Problems of Chemical Physics, Russian Academy of Sciences, 142432 Chernogolovka, Moscow Region, Russian Federation. Fax (7-496) 515 32 44, tel. (7-496) 522 21 63, e-mail: irzhak@icp.ac.ru

Received 14 September 2004
Uspekhi Khimii **74** (10) 1025 – 1056 (2005); translated by A M Raevskiy

† The review is dedicated to the memory of Grigorii L'vovich Slonimskii, the author of pioneering studies on polymer relaxation.

The relaxation properties characterise the ability of a compound disturbed from the equilibrium state to return to the equilibrium state. They are determined by the sum of all types of motions of molecular groups, chain fragments and macromolecules, that is, rotational, vibrational and translational motions. Representation of a relaxation process by the sum of such motions makes it possible to obtain an idea of a spectral characteristic of the compound.

If a process can be expressed by the sum of n independent elementary relaxation transitions, the kinetics of the process can formally be expressed as follows:

$$g(t) = \sum_{i=1}^{n} h_i e^{-t/\lambda_i},$$

where $g(t)$ is the kinetic modulus, t is the running time, h_i is the relaxation spectrum and λ_i is the relaxation time.

In the continuous case one has

$$g(t) = \int_0^\infty h(\lambda) e^{-t/\lambda} d\lambda . \quad (1)$$

Sometimes the relaxation spectrum h_i or $h(\lambda)$, as a function of the relaxation time λ_i (or λ), is denoted as $H(\lambda) = \lambda h(\lambda)$. A very broad range of relaxation times can be described in a more compact form, namely, in the logarithmic scale

$$g(t) = \int_{-\infty}^{\infty} H(\lambda) e^{-t/\lambda} d \ln\lambda . \quad (1a)$$

The frequency dependence of a relaxation process is represented by a Fourier transform of expression (1), namely

$$G^*(\omega) = i\omega \int_0^\infty g(t) e^{-i\omega t} dt, \quad (2)$$

where $G^*(\omega)$ is the complex frequency modulus and ω is the frequency.

As can be seen, there is a one-to-one correspondence between $G^*(\omega)$ and $g(t)$, *i.e.*, knowledge of one parameter permits determination of the other. Since expression (1) is an integral Laplace transform of the spectrum $h(\lambda)$,‡ there is also a one-to-one correspondence between these quantities. A difficulty consists in that the experimentally measured $G^*(\omega)$ and $g(t)$ values (i) usually include random (noise) or systematic errors and (ii) are obtained within limited time and frequency intervals. The integral operator on the right side of equality (1) is a smoothing operator, *i.e.*, intensive perturbations in the $h(\lambda)$ function are considerably smoothed in the $g(t)$ function. But this also means that minor disturbances (*e.g.*, errors) in experimental data can introduce a large uncertainty into solution of the problem of determination of the relaxation spectrum $h(\lambda)$. Cutting off the integration limits due to limitations imposed by experimental techniques can also be a source of errors introduced into the results of the inverse Laplace transform and Fourier transform.

The complex frequency modulus $G^*(\omega)$ is usually expressed through its real and imaginary components

$$G^*(\omega) = G'(\omega) + iG''(\omega), \quad (3)$$

$$G'(\omega) = \int_0^\infty h(\lambda) \frac{\omega^2\lambda^2}{1+\omega^2\lambda^2} d\lambda ,$$

$$G''(\omega) = \int_0^\infty h(\lambda) \frac{\omega\lambda}{1+\omega^2\lambda^2} d\lambda ,$$

Their ratio, called the (mechanical, dielectric, *etc.*) loss factor and given by

$$\tan\delta = \frac{G''(\omega)}{G'(\omega)}, \quad (4)$$

is often used for the determination of individual relaxation transitions. In this case the amplitude (intensity) of a peak in the tanδ-*vs.*-temperature (T) or in the tan δ-*vs.*-frequency plots is usually related to the content of the relaxing element (relaxer).

II. Relaxation spectrometry

In order to describe and classify local relaxation transitions, G M Bartenev put forward a concept of relaxation spectrometry.[1,2,5] As it was written in a monograph [1] that 'relaxation spectrometry itself, as a specific kind of kinetic spectroscopy,... is in the early stage of its development and at present not all principles of relaxation spectrometry can be considered rigorously substantiated'.§

In fact, local character of relaxation processes means that each process occurs (and, correspondingly, can be considered) independently. Parameters of each process (in particular, the relaxation times) are determined by the local polymer structure, which in turn can be characterised by these parameters. This is a distinctive feature of relaxation spectrometry as a method for studying the polymer structure.

A more or less broad spectrum of local relaxation times is due to the fact that even in the simplest macromolecules (such as polyethylene, polyethylene oxide and polystyrene molecules) one can select a set of relaxers. Torsional motions of atoms and side groups and crankshaft rotations of various intrachain atomic groups are characterised by different relaxation times. Complication of the molecular structure leads to broadening of the relaxation spectrum.

Structural description of local relaxation transitions is usually performed by relating the position of the maximum in the temperature dependence of loss factor, at a given frequency or temperature scan rate, to the presence of particular molecular groups in the polymer chain. At the point of maximum, the condition $\omega\lambda = 1$ or $W(T)\lambda = 1$ is met, where $W(T)$ is the temperature scan rate. This makes it possible to determine the relaxation time λ.

According to Bartenev,[2] a relaxation transition can be represented by a jump of a relaxer through an activation barrier, *i.e.*, the temperature dependence of relaxation time obeys an Arrhenius equation

$$\lambda = B \exp\frac{E}{RT} .$$

The barrier height is governed by the activation energy E while the pre-exponent B characterises the volume of the relaxing element (relaxer)

$$B = \frac{\upsilon^{5/6}}{(6kT/\rho)^{1/2}}, \quad (5)$$

where υ is the volume and ρ is the relaxer density.

Processes due to motions of small molecular groups (group size is much less than the size of a chain segment) belong to the smallest-scale γ-processes. Typical values of the kinetic parameters characteristic of this type of motion are as follows: $B \approx 10^{-9}-10^{-12}$ s and $E_\gamma = 10-20$ kJ mol^{-1}.

Larger-scale β-relaxation is characterised by B values of the order of 2×10^{-13} s and E_β values lying between 30 and 70 kJ mol^{-1}. α-Relaxation also belongs to local processes. Usually, the temperature dependence of the α-relaxation time does not obey the Arrhenius equation. However, in a limited temperature

‡ Strictly speaking, the Laplace integral transform of the function $h(1/s)/s^2$, where $s = \lambda^{-1}$.

§ See page 297 in Ref. 1.

interval it is characterised by the parameters $B \sim 5 \times 10^{-12}$ s and $E_\alpha = 50-70$ kJ mol^{-1}.

It should be noted that almost all local transitions can be detected by both high-frequency (NMR, EPR, acoustic, dielectric and various mechanical dynamical methods) and low-frequency [the same mechanical dynamical methods in the low-frequency range, thermomechanical analysis (TMA), differential scanning calorimetry (DSC), *etc.*] methods.[1,2,6] For instance, knowledge of the temperature dependence of the damping constant or of the mechanical loss factor at a frequency of about 1 Hz (or fractions of a Hertz) makes it possible to find out all these transitions.[2,5]

As a rule, local relaxation transitions correspond to structural transitions. For instance, it was shown[7] that the thermal expansion coefficients of the polymers listed below change stepwise at the following temperatures (°C):

poly(methyl methacrylate)	15, 100
poly(methacrylate)	−115, −15, 25, 60
poly(n-propyl methacrylate)	−85, −35, 15, 30
poly(n-butyl methacrylate)	−95, −55, −25, 20

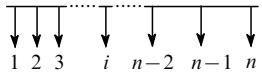
The last-mentioned temperatures correspond to α-transitions and the lower temperatures correspond to small-scale local transitions.

1. Model of coupled rotators

The Frenkel–Eyring discrete model of activated diffusion provides the basis for relaxation spectrometry. According to this model, a diffusion act involves three consecutive stages. These are (i) reorganisation of the environment of the diffusing species involving formation of a 'hole' of comparable volume, (ii) the jump of the particle through the activation barrier to the 'hole' formed and (iii) reorganisation of the environment to remove the 'hole'.

According to modern concepts of the diffusion mechanism (see, *e.g.*, Ref. 2), the motion of a particle occurs simultaneously with local reorganisation of the environment. The particle moves gradually by 'elbowing' particles of the environment rather than by hopping over distances of the order of the particle size. According to this continuous model, the particle executes a number of steps during the hopping time and thus travels a distance comparable with the particle size. Thus, formally both models lead to the same results. However, the kinetic parameters of the process ('hole' volume, energy of 'hole' formation, activation energy for hopping) and, correspondingly, the parameters B [see Eqn (5)] and E in the Arrhenius equation have a different physical meaning.[8–10]

The model of elastically coupled rotators[11,12] was first proposed by Mansfield.[13] It is based on the physically more substantiated mechanism of local relaxation.



Rotators (asterisked) execute torsional motions near the equilibrium positions in the plane normal to the axis. The character of motion is determined by the local (torsional) friction coefficient ζ_i and by the rigidity, K_i, of the bond being twisted (rotators are enumerated from the left, so the bonds are enumerated from zero to n). The two outermost bonds can have a zero rigidity (free chain) or a finite rigidity (chain is embedded into a framework, *e.g.*, a network).

The equations describing relaxation of this system, have the form

$$\begin{aligned}
\dot{x}_1 &= -K_0 x_1 - K_1(x_1 - x_2) - \tau_1^{-1} x_1 = \\
&= -x_1(K_0 + K_1 + \tau_1^{-1}) + K_1 x_2, \\
\dot{x}_2 &= K_1(x_1 - x_2) - K_2(x_2 - x_3) - \tau_2^{-1} x_2 = \\
&= K_1 x_1 - x_2(K_1 + K_2 + \tau_2^{-1}) + K_2 x_3, \\
\dot{x}_3 &= K_2(x_2 - x_3) - K_3(x_3 - x_4) - \tau_3^{-1} x_3 = \\
&= K_2 x_2 - x_3(K_2 + K_3 + \tau_3^{-1}) + K_3 x_4, \\
&\cdots\cdots\cdots\cdots\cdots\cdots\cdots\cdots\cdots\cdots\cdots\cdots \\
\dot{x}_i &= K_{i-1} x_{i-1} - x_i(K_{i-1} + K_i + \tau_i^{-1}) + K_i x_{i+1} \\
&\cdots\cdots\cdots\cdots\cdots\cdots\cdots\cdots\cdots\cdots\cdots\cdots \\
\dot{x}_{n-1} &= K_{n-2} x_{n-2} - x_{n-1}(K_{n-2} + K_{n-1} + \tau_{n-1}^{-1}) + K_{n-1} x_n, \\
\dot{x}_n &= K_{n-1} x_{n-1} - x_n(K_{n-1} + K_n + \tau_n^{-1}),
\end{aligned} \tag{6}$$

where x_i is the angle of deviation of the dipole from its equilibrium position and τ_i is treated as the effective relaxation time of the ith dipole, which is proportional to the friction coefficient ζ_i.

The solution is written as expansion into a series

$$x_i = \sum_{j=1}^{n} a_{ij} \exp(-p_i t). \tag{7}$$

The relaxation time $\lambda_i = p_i^{-1}$ is determined by the equation

$$D_n = \begin{vmatrix}
\varphi_{11} & \varphi_{12} & 0 & 0 & \ldots & 0 & 0 \\
\varphi_{21} & \varphi_{22} & \varphi_{23} & 0 & \ldots & 0 & 0 \\
0 & \varphi_{32} & \varphi_{33} & \varphi_{34} & \ldots & 0 & 0 \\
\cdots & \cdots & \cdots & \cdots & \cdots & \cdots & \cdots \\
0 & 0 & \varphi_{i,i-1} & \varphi_{i,i} & \ldots & 0 & 0 \\
\cdots & \cdots & \cdots & \cdots & \cdots & \cdots & \cdots \\
0 & 0 & \ldots & \ldots & \ldots & \varphi_{n,n-1} & \varphi_{n,n}
\end{vmatrix} = 0 \tag{8}$$

where $\varphi_{11} = z_1 - (\tau_1^{-1} + K_0 + K_1)$; $\varphi_{12} = K_1$; $\varphi_{21} = K_1$; $\varphi_{22} = z_2 - (\tau_2^{-1} + K_1 + K_2)$; $\varphi_{23} = K_2$; $\varphi_{i,i-1} = K_{i-1}$; $\varphi_{i,i} = z_1 - (\tau_i^{-1} + K_{i-1} + K_i)$; $\varphi_{i,i+1} = K_i$; $\varphi_{n,n-1} = K_{n-1}$; $\varphi_{n,n} = z_n - \tau_n^{-1} + K_{n-1} + K_n)$; $z_i = 1/\lambda_i$.

Analysis of the solution of Eqn (8) showed that if $K_i \ll 1$ for any i, the elements relax independently with $\lambda_i = \tau_i$. In other words, in this case the relaxation is governed solely by the physical nature and by the magnitude of the local friction coefficient ζ_i, *i.e.*, by the level of local intermolecular interaction. If $K_i \gg 1$ for any i, the structure of the D_n matrix will be identical to the structure of the Rouse matrix for a free chain (at $K_0 = K_n = 0$) or for an end-to-end cross-linked chain (at K_0 and $K_n \neq 0$). However, in this case the relaxation times increase by a factor of K. Thus, intrachain interaction causes relaxation of each element to be characterised by a spectrum of relaxation times.

To obtain a detailed description of the relaxation kinetics of the system in the framework of the model of coupled rotators, one should allow for the Brownian force[11] exerted on each element in the system. Therefore, each equation in system (6) should be augmented with the corresponding term.

Analysis of the solution of the modified system (6) showed[12] that, at times shorter than $\lambda_{\min}$ (minimum relaxation time of the chain of rotators), the correlator $\langle \cos x_j(t) \cos x_j(0) \rangle$ decreases exponentially with the characteristic time λ_1. In this region the effect of the neighbours of a given rotator can be ignored and the motion occurs as rotational diffusion, which is not affected by chain rigidity

$$\lambda_{\min} = \frac{\zeta^{\text{rot}}}{4K^{\text{rot}}}, \qquad \lambda_1 = \frac{\zeta^{\text{rot}}}{4kT} = \frac{1}{4D}.$$

Here $\zeta_1 = \zeta_2 = \ldots = \zeta_i = \ldots = \zeta^{\text{rot}}$ is the torsional friction coefficient, $K_1 = K_2 = \ldots = K_i = \ldots = K^{\text{rot}}$ is the twisting rigidity of the chain and D is the rotational diffusion coefficient.

At times longer than $\lambda_{\min}$, relaxation is described by a 'stretched' exponent: $\sim \exp[-(t/\lambda_2)^{1/2}]$, where

$$\lambda_2 = \frac{\pi \zeta^{\text{rot}} K^{\text{rot}}}{(4kT)^2}.$$

In this time interval the motion of a rotator is strongly affected by the neighbouring rotators (manifestation of chain rigidity), the

length scale of the motion being equal to the length of the rigid chain fragment.

Note that the relations given above are valid for an infinite chain where the effect of the end groups can be ignored. Finite chains have also been studied.[12]

Thus, the character of local relaxation transitions is first of all determined by the local viscosity. An important additional factor is intrachain interaction, which manifests itself as the twisting rigidity of the chain. In all cases the activation model is inadequate.

2. On the nature of α- and β-relaxation

At present there are two antipodes of opinion of the nature of α- and β-relaxation. On the one hand, it is traditionally accepted (see references cited in Ref. 2) that different molecular groups are responsible for these transitions. Namely, α-transition is due to segmental motion while β-transition is due to a smaller-scale motion of relaxers (here, the molecular mass of the relaxer is five to ten times smaller than that of a chain segment).

According to the other point of view (see Refs 14, 15), relaxation in the corresponding temperature and frequency ranges is due to the same chain fragments, namely, chain segments. This is reasoned by the following:

1. Amorphous low-molecular-mass glasses with rigid molecules (in *e.g.*, solutions of chlorobenzene, *o*-dichlorobenzene and 1-chloronaphthalene in decalin, blends of chlorobenzene with pyridine, blends of tetrahydrofuran with bromobenzene and 1-chloronaphthalene, *etc.*) exhibit not only the α-transition but also a low-temperature transition, which can be associated with β-relaxation.[16–23] The systems in question contain no other relaxers, except for the rigid molecules, capable of moving as a whole. Therefore, both relaxation transitions are due to the same structural elements. Characteristics of the low-temperature transition are similar to those of β-relaxation in polymeric systems, namely, it obeys an Arrhenius-type temperature dependence with an activation energy lying in the range 17–33 kJ mol^{-1}. As the temperature increases, both transitions approach each other. Finally, both relaxation processes in the system including low-molecular-mass components are also observed in the polymeric reaction product, but here the relaxation times are longer, which is quite natural.[22]

2. Bershtein *et al.*[15,24–26] showed that for certain polymers the dependences of the heats of the β- and α-transitions on the number, n, of monomer units are given by similar curves that reach the plateau zone at the same n value. This is indicative of the identity of the β- and α-relaxers in polymeric systems.

3. Liquid systems characterised by one relaxation transition, namely, the glass transition, show a second low-temperature transition upon compression.[27] Apparently, new relaxers cannot appear under these conditions. A possible reason is an increase in the density of the system and, as a consequence, an increase in the concentration of high-density fluctuations.

4. Theoretical analysis[14,28,29] of the relaxation of bulk amorphous systems that show a unique structural feature (density fluctuations) showed the following.

The temporal correlation function $\psi(t)$ is given by the Kohlrausch–Williams–Watts (KWW) formula

$$\psi(t) = \alpha_1 \exp\left[-\left(\frac{t}{\tau_1}\right)^{\beta_1}\right] + \alpha_2 \exp\left[-\left(\frac{t}{\tau_2}\right)^{\beta_2}\right], \qquad (9)$$

where α_1 and α_2 are the pre-exponents, $\beta_1 = 0.33$ and $\beta_2 = 0.14–0.27$.

Analysis of expression (9) revealed the existence of two relaxation regions. The first region corresponds to a short relaxation time, being almost temperature independent, while the second region corresponds to a long relaxation time and extends with temperature. The temperature dependence of τ_1 obeys an Arrhenius relationship while that of τ_2 is described by the Williams–Landell–Ferry (WLF) equation, which is typical of α-relaxation. It was also found that the activation energy for the first region $E_1 = 35$ kJ mol^{-1} and $80 \leqslant E_2 \leqslant 139$ kJ mol^{-1} for the second region.

The frequency dependence of the imaginary component of the bulk modulus exhibits two maxima. The temperature dependence of the high-frequency peak obeys an Arrhenius relation and that of the low-frequency peak obeys the WLF equation.

These processes, α- and β-relaxations, are characteristic of all amorphous systems and both transitions can be initiated by the same elements. The appearance of two regions is due to a nonuniform density distribution, *viz.*, α-relaxation occurs in the high-density fluctuations while β-relaxation occurs in the low-density ones. The former process is essentially a co-operative one for which an important role is played by structural rearrangements in the environment; as a consequence, the temperature dependence is of the WLF type. The latter process is non-co-operative; therefore it is described by the Arrhenius equation.

Recent studies of the structure and properties of thin polymer films (see, *e.g.*, Ref. 30) showed that the glass transition temperature decreases appreciably if the thickness of the polymer film approaches the diameter of the unperturbed coil. It was assumed that this effect is due to violation of the co-operative character of molecular motion in thin films (namely, α-transition manifests itself as a β-transition). If by this is understood a known decrease in the packing density in near-surface layers and thin films, this assumption can be considered quite reasonable.

The aforesaid does not mean that β-relaxation in polymeric systems always has segmental character. Some other mechanism, which is due to the presence of other molecular groups, *i.e.*, a complex structure of polymer chains, can also be involved in addition to the mechanism described above.

III. Manifestation of the topological structure of polymers in their relaxation properties

Certain structural meaning can be assigned with ease to local relaxation transitions that are mainly responsible for the level of internal friction in a polymeric material. This level governs, *e.g.*, the brittleness of the material. At the same time the relaxation properties in a broad sense determine the deformability, long-term strength and other characteristics related to the conformational rearrangements and motions of macromolecules. Apparently, the topological structure plays the key role in this case. But it is a rather complicated task to relate the topological structure to the relaxation behaviour of the polymer, although this problem is undoubtedly topical. In addition it is the relaxation techniques that can become basic to the development of non-destructive methods of structural characterisation of polymeric materials.[31–34]

1. Molecular mass

For linear polymers the dependence of the melt viscosity, η, on the average molecular mass ($\bar{M}$) has the form[4]

$$\eta = K\bar{M}^{\nu}, \qquad (10)$$

where $\nu = 1$ at $\bar{M} \leqslant 2M_e$, $\nu = 3.5 \pm 0.2$ at $\bar{M} > 2M_e$ and M_e is the molecular mass of the chain between entanglements in terms of the Doi–Edwards theory.[11,34]

Expression (10) is a particular case of a more general dependence[3,35,36]

$$\eta \propto [\eta]^{\nu}$$

or

$$\eta \propto R^{\nu},$$

where $[\eta]$ is the characteristic viscosity, the exponent ν lies between 6 and 7 and R is the coil radius. Validity of these relationships was shown for various types of polymers, *viz.*, linear polymers of different rigidity; cyclic, star-branched with different numbers of arms and comb-like polymers, randomly branched chains and

highly cross-linked polymer globules.[3, 37–42] Therefore, the viscosity cannot serve as a unique characteristic of the molecular mass of a polymer. Other parameters of the topological structure, namely, the molecular mass distribution and the degree of branching also play a significant role.

The flow curves obtained for linear monodisperse polymers exhibit a specific shape.[43, 44] At relatively low shear rates $\dot{\gamma}$ (and, correspondingly, strain τ), one deals with a Newtonian flow, *i.e.*, $\tau = \eta_0\dot{\gamma}$, where $\eta_0 = KM^v$. However, at a certain critical shear strain, τ_c, the flow character changes. Here, flow breakdown occurs or the strain abruptly decreases with an increase in the shear rate (the former is characteristic of monodisperse polymers while the latter is typical of polydisperse polymers). The τ_c value is independent of the molecular mass of the polymer. At the same time the shear rate corresponding to the τ_c value can serve as a measure of the molecular mass of monodisperse polymers

$$\dot{\gamma}_c(M) = \frac{\tau_c}{KM^v}.$$

Knowing the temperature dependence of the stress, ε, of linear polymers (TMA method), it is possible to relate the molecular mass to the relaxation properties. Kargin and Slonimskii[45] first showed that the extension of a portion of the $\varepsilon(T)$ curve, which is nearly parallel to the temperature axis (rubbery plateau zone, $\Delta T = T - T_g$, where T is the flow onset temperature and T_g is the glass transition temperature) is related to the molecular mass as follows

$$\log\left(\frac{M}{M_s}\right) \propto \frac{\Delta T}{C + \Delta T}, \qquad (11)$$

where M_s is the molecular mass of the chain segment and C is a constant.

It should be noted that determination of the parameter ΔT faces some difficulties, which are due to the diffuse character of the transition from the glassy to the rubbery state and from the rubbery state to a melt flow. The character of these transient regions depends on the width of the MMD. The validity of relationship (11) was confirmed[46–48] for a broad range of polymers. The authors studied narrow-MMD polymers, which made it possible to attain abrupt glass – elastomer and elastomer – melt transitions. The plot of the dependence (11) is shown in Fig. 1.

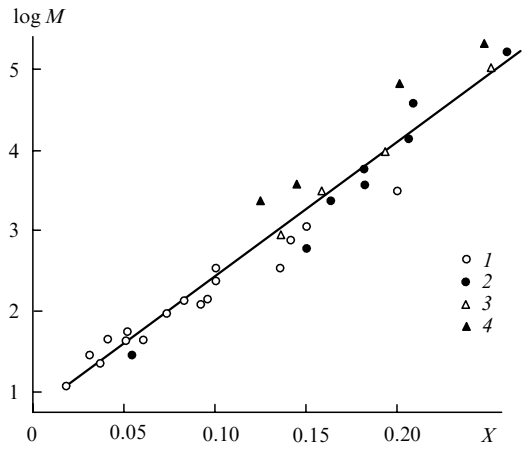


Figure 1. Correlation between the temperature interval corresponding to the rubbery plateau and the molecular mass of polymers plotted in the coordinates of Eqn (11) [X is the numerical value of the right side of Eqn (11), $C = T_g$].[48]
Polymers: polybutadiene (*1*), polyurethane-based polymers (*2*, *3*) at T_g = 215 (*2*) and 250 K (*3*) and polyacrylonitrile (*4*).

Using the temporal and the frequency dependences of the elastic modulus, one can also relate the relaxation properties of polymers to their molecular masses. Since the rubbery plateau zone extends from the minimum (λ_{min}) to the maximum (λ_{max}) relaxation time (see Refs 1, 24, 34), the λ_{min} value being independent of the molecular mass and much shorter than λ_{max}, the extension of the plateau zone is nearly equal (in time or frequency units) to λ_{max}. But

$$\lambda_{max} \propto M^v,$$

where the exponent v can take different values. Usually, it is assumed that $v = 3.4$. At the same time analysis of strain relaxation data showed[49] that $v \approx 4$. From the shift of the relaxation curves as functions of the molecular mass of the polymer (Fig. 2, lines *1*, *2*), *i.e.*, based on the estimate of the extension of the rubbery plateau zone, it was found that the v value lies between 3.3 and 3.5. Analysis of the frequency dependence of the elastic modulus revealed a similar v value ($v = 3.5$ from the real component of the modulus, see Fig. 2, line *3*, data were taken from Ref. 50). It should be noted that the maximum in the $G''(\omega)$ plot correlates with the critical shear strain τ_c (see Ref. 44), *i.e.*, it also characterises the molecular mass of linear monodisperse polymers, namely, $v \approx 3.3$ (from the position of the maximum G'' value).

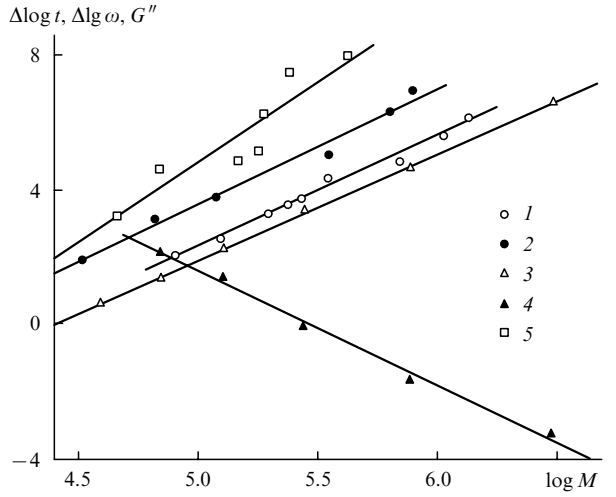


Figure 2. Relaxation parameters of linear polymers (*1–4*) and a four-arm star-branched polymer (*5*) plotted *vs.* molecular mass using the data taken from different studies.
Parameter: $\Delta\log t$ (*1*, *2*), $\Delta\log\omega$ (*3*, *5*) and G''_{max} (*4*); the plateau extension is denoted by Δ; *e.g.*, $\Delta\log t = \log t_{max} - \log t_{min}$.

The molecular mass is closely related to parameters of the terminal zone of the complex frequency modulus curves $G^*(\omega)$.[4, 51–54] The effective relaxation time

$$\lambda_{ef,\,w}(\omega) = \frac{G'(\omega)}{\omega G''(\omega)} \qquad (12)$$

in the terminal zone takes the limiting value, which is frequency independent and equals the ratio of the second to the first moment of the relaxation time distribution, *i.e.*, is the weight-average relaxation time

$$\langle\lambda\rangle_w = \frac{\sum_i h_i(\lambda)\lambda_i^2}{\sum_i h_i(\lambda)\lambda_i}. \qquad (13)$$

At $\omega \to 0$, the effective relaxation time given by

$$\lambda_{\text{ef, n}}(\omega) = \frac{G''(\omega)}{\omega[G_N^0 - G'(\omega)]}, \quad (14)$$

is the number-average relaxation time, which is also frequency independent (G_N^0 is the modulus corresponding to the rubbery plateau zone),

$$\langle\lambda\rangle_{\text{n}} = \frac{\sum_i h_i(\lambda)\lambda_i}{\sum_i h_i(\lambda)}. \quad (15)$$

It is well known that the average relaxation times in the terminal zone correlate with the rheological properties of polymers, namely, the number-average relaxation time correlates with viscosity and the product of the viscosity and the compliance correlates with the weight-average relaxation time. From here it follows that these relaxation times depend on the molecular mass. The data for a number of monodisperse polymers are listed in Table 1.

Table 1. Dependence of the average relaxation times in the terminal region on the molecular mass of polymers.

Polymer	$\langle\lambda\rangle_{\text{n}}$	$\langle\lambda\rangle_{\text{w}}$	Ref.
Polystyrene	$M^{3.4}$	$M^{3.7}$	50
Poly(methyl methacrylate)	$M^{3.4}$	$M^{3.65}$	53
cis-Polyisoprene [a]	$M^{3.62}$	$M^{3.69}$	54
1,4-Polybutadiene	$M^{3.37}$	$M^{3.52}$	55, 56

[a] Data from dielectric measurements.

The parameters of dielectric relaxation are related to the molecular masses of polymers in a similar way. Here one should keep in mind that this can concern only those polymers in which the dipoles and chains are aligned (A-type polymers according to Stockmayer [57]).

The effective dielectric relaxation times are defined as follows:

$$\langle\lambda_{\text{e}}\rangle_{\text{w}} = \frac{\varepsilon_0 - \varepsilon'(\omega)}{\omega\varepsilon''(\omega)}, \quad \langle\lambda_{\text{e}}\rangle_{\text{n}} = \frac{\varepsilon''(\omega)}{\omega\Delta\varepsilon}, \quad \omega \to 0, \quad (16)$$

where ε_0 is the conductivity, ε' and ε'' are the real and imaginary components of the complex dielectric permittivity, $\Delta\varepsilon$ is the intensity of dielectric relaxation for the motion of the entire chain (analogue of G_N^0 in mechanical relaxation).

The position of the maximum in the $\varepsilon''(\omega)$ curve on the frequency axis is also related to the molecular mass by a power law (for *cis*-polyisoprene, the exponent is 3.8 [58]).

The spin–spin relaxation measured by pulsed NMR spectroscopy is sensitive to the molecular mass of linear polymers.[59–62] At a sufficiently high temperature ($T > T_g + 100$), the free induction decay, $G(t)$, is defined by

$$G(t) = \int_1^N \int_0^{\pi/2} \{[g(N,\theta,t)\ P(N)\ \sin\theta]\mathrm{d}\theta\}\mathrm{d}N, \quad (17)$$

where

$$g(N,\theta,t) \approx \exp\left[-\omega_1^2(3\cos^2\theta - 1)^2 t^2 \frac{\ln N}{N^2}\right],$$

N is the number of segments in the chain and θ is the angle between the vector connecting the chain ends and the direction of external magnetic field; ω_1 is the second moment of the free induction decay curve, expressed in frequency units and $P(N)$ is the numerical MMD function.

However, since NMR spectroscopy is a high-frequency method, Eqn (17) is valid for the macromolecules with molecular masses smaller than M_e.

2. The molecular mass distribution

The problem of establishment of correlations between the MMD and the relaxation properties of polymers has a long history;[2, 4, 34, 63–66] however, no unambiguous solution has been reported so far.[31, 32] Only qualitative dependences were determined. For instance, it is assumed [4] that MMD is correctly allowed for in the following relationship for the viscosity

$$\eta \propto \bar{M}_{\text{w}}^{v},$$

where $\bar{M}_{\text{w}} = \sum_M \omega(M)M$, $\omega(M)$ is the mass fraction of the polymer with molecular mass M and $v \approx 3, 4$. More complicated expressions, which take into account higher moments of the MMD function, are also used. For instance, the following expressions were proposed for creep compliance J_e:[64–66]

$$J_e \approx \frac{\bar{M}_{z+1}\bar{M}_z}{\bar{M}_{\text{w}}\bar{M}_{\text{n}}}$$

or

$$J_e \approx \left(\frac{\bar{M}_z}{\bar{M}_{\text{w}}}\right)^b,$$

Here $\bar{M}_{\text{n}} = \mu_1/\mu_0$, $\bar{M}_z = \mu_3/\mu_2$, $\bar{M}_{z+1} = \mu_4/\mu_3$, $\mu_k = \sum_M \omega(M)\ M^{k-1}$ is the kth distribution moment; and $b = 3.5–3.7$.

As an example Fig. 3 presents the dependences of the compliance $J_e = \langle\lambda\rangle_{\text{w}}/\langle\lambda\rangle_{\text{n}}$ and polydispersity index $\bar{M}_{\text{w}}/\bar{M}_{\text{n}}$ on the composition of a bidisperse blend of polystyrenes with molecular masses 4.27×10^5 and 3.89×10^4 (data were taken from Ref. 67).

Because of polydispersity of the polymer the flow curve changes its shape.[31, 68–71] A sharp kink near the critical shear strain disappears and the viscosity gradually decreases from a constant value with an increase in the shear rate. The curves of the temporal and frequency dependences of the relaxation modulus behave analogously.[32–34, 72–78] In the rubbery plateau zone the modulus becomes time (or frequency) dependent; the wider the MMD, the stronger this dependence. Broadening of the MMD

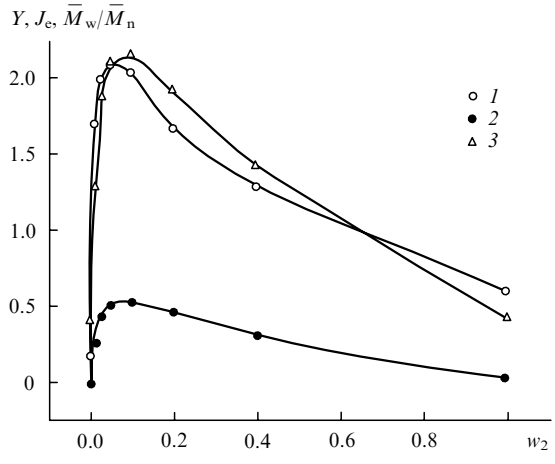


Figure 3. Compliance-*vs.*-polydispersity index correlations for polystyrene.[67]
J_e (*1*) and $\bar{M}_{\text{w}}/\bar{M}_{\text{n}}$ ratio (*2*) plotted *vs.* compositions of bidisperse polystyrene blends with the molecular masses $M_1 = 3.89 \times 10^4$ and $M_2 = 4.27 \times 10^5$, where w_2 is the mass fraction of the second component, and the $Y = 0.2 + 3.4\log(\bar{M}_{\text{w}}/\bar{M}_{\text{n}})$ plot (*3*).

also leads to fundamental changes in the character of the temperature dependence of strain;[32, 48, 79–82] namely, the wider the MMD of the polymer, the less pronounced the transition from the rubbery state to flow.

Numerous attempts at establishing quantitative relations between the character of the MMD and the relaxation behaviour of polymers are usually based on the assumption of additivity of the contributions of each polymer fraction to the properties. For instance, it was proposed to describe the flow curve of a polydisperse polymer by the following relationship [68, 71]

$$\eta(\dot{\gamma}) = \left[\int_0^{M_c} \omega(\mu)\mu \mathrm{d}\mu + M_c \int_{M_c}^{\infty} \omega(\mu)\mathrm{d}\mu\right]^v, \quad M_c = \left(\frac{\tau_c}{K\dot{\gamma}_c}\right)^{1/v},$$

where μ is the integration variable.

The dynamical theory of polymers, which is based on the fixed tube model, predicts [34] that the relaxation modulus of a bidisperse polymer blend equals the weight-average of the relaxation moduli of the components. Correction of the model made it possible to derive much more complicated relationships.[83] Generalisation of various theoretical and experimental approaches led to the following strain relaxation equation [84, 85]

$$G(t) = G_N^0 \left[\int_{\ln M_e}^{\infty} G^{1/\beta}(t, M)\, \omega(M) \mathrm{d}\ln M\right]^{\beta},$$

where $G(t,M)$ is the function describing the relaxation behaviour of the polymer fraction with molecular mass M and the parameter β characterises the mixing rule (it allows for the mutual influence of macromolecules of different size).

It is this factor that allows the additivity principle to be used. However, opinions are different as to the mutual influence of macromolecules or its manifestation in the relaxation properties of polydisperse polymers. On the one hand, there is no denying a strong chain–chain interaction in polymeric systems, which is allowed for by the concepts of entanglements [65, 66] or physical networks.[37, 86–89] It was experimentally shown [83, 84, 90–93] that the longest relaxation time depends on the composition of bidisperse polymer blends.

On the other hand it was assumed [52, 94, 95] that the effect of this interaction can be ignored in the case of slow relaxation processes. This was substantiated by the results of IR dichroism studies [96, 97] of chain orientation relaxation in bidisperse blends of ethylene-*co*-propylene copolymers comprised of monodisperse fractions with the molecular masses $M_S = 5.3 \times 10^4$, $M_M = 1.25 \times 10^5$ and $M_L = 3.7 \times 10^5$. It was shown that the maximum effective relaxation time of long chains is virtually independent of the composition of the system (Fig. 4). As can be seen, the presence of shorter chains has almost no effect on the relaxation of long chains (curves *1*, *2*, *4*) if the concentration of the long chains is not too low.[93] At the same time the relaxation times of the chains of different length are significantly different (*cf*. curves *1*, *2* and curve *3*).

The notion of a 'low-molecular-mass' component of a bidisperse blend is conditional. Probably, under certain conditions this component should be considered as a solvent, which dramatically decreases the concentration of entanglements in a physical network. It was suggested [98] that this occurs at $M_L M_e^2 / M_S^3 < 0.1$.

As applied to thermomechanical experiments, the additivity principle can expressed as follows:[48, 81]

$$J_T = J_0[1 - \omega(M)]^{-1}, \quad \omega(M) = \sum_M \varphi(M)\chi(T, M),$$

where J_T and J_0 are the compliances of the polydisperse polymer and of a hypothetical polymer with infinite molecular mass (base line), $\omega(M)$ is the integral MMD function, $\varphi(M)$ is the differential MMD function and χ is the Heaviside step function

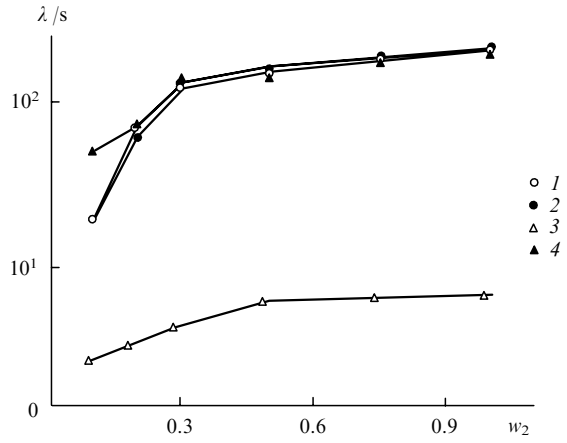


Figure 4. Effective long-chain orientation relaxation time plotted *vs*. volume fraction of long chains in a bidisperse polymer blend.
Molecular mass of the polymer: $M_S = 5.3 \times 10^4$, $M_M = 1.25 \times 10^5$ and $M_L = 3.7 \times 10^5$. Curve *1* was plotted using the data taken from Ref. 97 and curves *2–4* were plotted using the data taken from Ref. 98.
(*1*, *2*) $M_S + M_L$, (*3*) $M_S + M_M$, (*4*) $M_M + M_L$.

$$\chi(T, M) = \begin{cases} 0 & \text{for } T < T_{f,M} \\ 1 & \text{for } T \geqslant T_{f,M} \end{cases},$$

where $T_{f,M}$ is the temperature at which the transition from the rubbery state to the flow of the polymer fraction with the molecular mass M occurs.

Only a few studies on relations between the character of dielectric relaxation and the MMD are available (see the bibliography in a review [52]). Probably, this is due to a narrow range of objects (A-type polymers). Studies of (mainly) bidisperse *cis*-polyisoprene blends showed [99–104] that the MMD manifests itself in dielectric and mechanical relaxation in a similar way, *i.e*.,

$$\frac{\varepsilon''(\omega)}{\Delta\varepsilon} \approx \frac{G''(\omega)}{G_N^0},$$

although the mechanisms of these processes are different, namely, dielectric relaxation is governed by orientation correlation of the *i*th and *j*th segments at different time instants while mechanical relaxation is determined by orientation anisotropy of a segment.

NMR experiments showed that the polydispersity of a polymer affects the shape of the free induction decay curve [61, 62] to the extent to which the M_e parameter limits the chain length.

3. Branching

Branching of polymers, as a structural factor, which manifests itself in the relaxation properties, has been much less studied compared to MMD. This problem has attracted attention only recently [105] owing to the extended possibilities of the synthesis of branched chains of a preset topological structure [106] including 'living' radical polymerisation techniques.[107, 108]

As mentioned above, the viscosity of polymers is independent of their topological structure. However, the coil size is highly sensitive to the chain structure, namely, the higher the degree of branching of a macromolecule, the smaller the root-mean-square radius of the coil at the same molecular mass.[1, 4, 11] For instance, the characteristic viscosities $[\eta]$ (THF solution, 30 °C) of polystyrenes of different topological structure are related to their molecular masses by the following expressions:[109]

$[\eta] = 9.6 \times 10^{-5}\, \bar{M}_w^{0.73}$ for a linear polymer,

$[\eta] = 1.42 \times 10^{-4}\, \bar{M}_w^{0.68}$ for eight-arm stars and

$[\eta] = 6.45 \times 10^{-4}\, \bar{M}_w^{0.39}$ for a hyperbranched polymer with more than twenty arms.

The rheological properties of branched molecules differ from those of linear molecules with the same molecular mass.[109–111] Namely, they show lower viscosities and higher critical shear rates, their melts are characterised by enhanced elasticity, which manifests itself in particular in the magnitude of the first normal stress difference. Branched polymers are characterised by high longitudinal viscosities.

A relation derived in the dynamical reptation theory of star-branched chains [34, 112] has the form

$$\eta \propto \left(\frac{M_a}{M_e}\right)^b \exp\left(v\frac{M_a}{M_e}\right),$$

where M_a is the molecular mass of the arm and b and v are the parameters of the model. Indeed, experiments [113] showed that the viscosities of star-branched polymers at equal molecular masses are independent of the number of arms, if this number is greater than three, being at the same time dependent on M_a (see Refs 114 and 115). This also holds for hyperbranched polymers.[116–118] It was also experimentally found [41, 116, 119–121] that $0.5 \leqslant b \leqslant 2$, $v < 1$ (theoretical values are $b = 2$ and $v = 15/8$).

A fundamental distinction of branched chains, which is due to a more compact coil structure compared to linear macromolecules, consists in complex thermorheological behaviour.[41, 122–129] Since the key parameter in rheology is the coil size, the effect of temperature on the viscosity is determined by not only the temperature dependence of the friction coefficient but also the thermal coefficient of the coil size [130]

$$\kappa = \frac{\mathrm{d}\ln\langle r^2\rangle}{\mathrm{d}T},$$

where $\langle r^2\rangle$ is the root-mean-square radius of gyration of the macromolecule. The coefficient κ increases as the degree of branching increases.[41, 125, 126] Because of this the effective activation energy of viscous flow also increases.¶

According to a hypothesis by Graessley,[123] a fraction of the activation energy, which is due to the branching effect, is related to the arm length as follows

$$E_b = \Lambda\frac{M_a}{M_e}. \qquad (18)$$

The Λ coefficient depends on the chemical structure of the macromolecules and the κ parameter. However, the parameters Λ and κ are related in a rather complex fashion and can even not show any correlation (see the data listed in Table 2).

Table 2. Parameters of equation (18).

Polymer	$10^3\kappa\times$ /K^{-1}	M_a/M_e	Λ
Hydrogenated polyisoprene	−1.3	23–33	0.169
Hydrogenated polybuta-1,4-diene	−1.05	12–39	0.25
Polybuta-1,2-diene	~ −1	12	0.17
Polybuta-1,4-diene	0.39	12–13	0.11
Hydrogenated polybuta-1,2-diene	0.5	5–6	0
Polyisoprene	0.3	15–44	0.07 ± 0.02

The extension of the rubbery plateau zone depends on the molecular mass of the branched polymers more strongly than in the case of the linear polymers. For instance, for linear monodisperse polystyrene [50] the exponent, v, equals 3.5 (*cf.*, $v = 4.8$ for four-arm star-branched polyisoprene [131]). It was shown [116] that at equal molecular mass, ($\bar{M}_w \approx 6\times10^4$), the $G'(\omega)$ and $G''(\omega)$ curves plotted for a linear polymer and a three-arm star-branched polymer nearly merge, whereas for an eight-arm star-branched polymer the terminal zone is shifted towards higher frequencies. At the same time the character of the frequency dependence of the relaxation modulus in the terminal zone is retained, namely, $G'(\omega) \propto \omega^2$ and $G''(\omega) \propto \omega$. Hyperbranched polymers (number of arms is about 50) behave in a different fashion, *viz*., in the terminal zone one has $G'(\omega) \propto \omega^{1.12}$ and $G''(\omega) \propto \omega^{0.91}$ ($\bar{M}_w \approx 2.5\times10^5$); $G'(\omega) \propto \omega^{1.1}$ and $G''(\omega) \propto \omega^{0.85}$ ($\bar{M}_w \approx 5.75\times10^5$).

An interesting method of classification of manifestations of the topological structure in the relaxation properties of polymers was proposed.[132] The technique is based on the analysis of the frequency dependence of the shear modulus in the $\delta - G^*$ coordinates [δ is the loss angle, $\delta = \arctan(G''/G')$; G^* is the complex modulus, $G^* = \sqrt{(G')^2 + (G'')^2}/G_N^0$], the so-called van Gurp–Palmen plot.[133] Using experimental data for a rather large number of polymers having different topological structures (asymmetrical and symmetrical star-branched, H-shaped and comb-like, linear chains with variable MMD), a topology map was constructed. The $\delta - G^*$ curves exhibit a characteristic point P_c, which is assigned a meaning of a characteristic of the topological structure of the polymer. The set of points corresponding to a specific topology forms a particular region in the map. Thus, location of the P_c point in a certain region allows characterisation of the polymer structure.

It should be noted that this is an essentially empirical and physically unsubstantiated approach. In addition, the authors [132] pointed out that the boundaries between the areas characterising different topologies in the topology map are not sharp.

In some sense branching and polydispersity influence the relaxation properties of polymers in a similar fashion. The difference is that branching in the terminal zone retards the relaxation processes. In contrast to this, relaxation at high frequencies is accelerated.[105, 134]

4. The gel point

The formation of polymer networks in any way (by polycondensation, polymerisation or cross-linking) is accompanied by considerable broadening of the MMD as the gel point is approached.[3, 135] The attainment of a gel point is associated with the formation of an infinite cluster,[136] which then undergoes a transformation into the gel fraction. This is accompanied by narrowing of the MMDs of the constituents of the sol fraction (they have a finite size).[3, 135] Thus, at the gel point a polymer has a specific topological structure, which can be characterised in terms of fractal theory.[137] The fractal dimension, D_f, of a cluster relates its volume to the mass

$$R \propto M^{1/D_f},$$

where R and M are the radius and the mass of the cluster. For linear 'massless' chains one has $D_f = 2$ ($D_f = 5/3$ with allowance for the excluded volume).[1, 66, 137] In accordance with percolation theory the fractal dimension of clusters in the region of critical conversion is 2.53.[137] Therefore, branched macromolecules in this region are more compact than linear chains.

The relaxation properties of a polymeric system at the gel point are described by a power law rather than an exponential function [138–141]

$$G(t) \propto t^{-n}. \qquad (19)$$

The exponent n is related to the fractal dimension [142]

$$n = \frac{D}{D_f + 2},$$

where D is the dimension of the space ($n = 0.66$ for three-dimensional space).

¶ See page 137 in Ref. 4.

If the degree of conversion α is expressed in the form

$$\varepsilon = \left| \frac{\alpha - \alpha_c}{\alpha_c} \right|,$$

where ε is the relative conversion and α_c is the critical conversion, at $\alpha < \alpha_c$ the viscosity is given by $\eta = \eta_0 \varepsilon^{-s}$ and at $\alpha > \alpha_c$ the shear modulus is given by $G = G_0 \alpha^r$ (see Refs 143–146). The exponents s and r are related to n as follows:

$$n = \frac{r}{s+r}.$$

A consequence of relationship (19) is that the frequency dependence of the shear modulus obeys a power law

$$G' \propto \omega^n \cos\left(\frac{\pi n}{2}\right), \quad G'' \propto \omega^n \sin\left(\frac{\pi n}{2}\right).$$

Therefore, tan δ is frequency independent

$$\delta = \frac{\pi n}{2}.$$

Theoretical estimates [146] give $n = 0.706$.

These relations were repeatedly confirmed by three-dimensional polymerisation of methacrylate-based oligomers [147] and by end-to-end cross-linking of poly(dimethylsiloxane),[148] *i.e.*, for irreversible processes. Similar behaviour is also characteristic of biopolymers;[149, 150] here, reversible formation of an equilibrium network is due to a change in the physical conditions, *e.g.*, the temperature, pH value and concentrations of components. For instance, when xanthane interacts with Al^{3+} ions, the exponent ρ in the expression

$$\tan\delta \propto \omega^{\rho}$$

varies from -0.1 to 0.08 depending on the solution temperature and becomes equal to zero at 32 °C.[150] The ρ value varies within nearly the same limits as the pH value changes (critical pH value is 2.9).

A decrease in the temperature of spherical particles of *N*-isopropylacrylamide microgel in a water–methanol solution leads to a gel–sol transition (lowest critical solution temperature is 32 °C).[151] In this case the exponent ρ behaves in a similar way and takes a zero value at about 29 °C.

It should be noted that almost all transitions from the liquid to the solid state pass through critical regions where critical clusters are formed, *i.e.*, nuclei of the solid phase (here, the notion 'phase' has a kinetic and not necessarily thermodynamical meaning), which have a similar fractal structure.[152]

The numerical value of the exponent n varies depending on the system. For instance, for polymerisation of methacrylate oligomers n varies from 0.4 ± 0.2 to 0.6 ± 0.1 and increases as the degree of functionality of the initial oligomer increases.[147] In cross-linking of bifunctional oligo(dimethylsiloxane) having vinyl terminal groups, with a polyfunctional reagent (degrees of functionality were equal to 4 and 11) containing $\equiv$SiH reactive groups, the n value varies from 0.69 to 0.76 depending on the system. The cross-linking of poly(dimethylsiloxane) is characterised by $n = 0.5$ (see Ref. 140) and curing of an epoxy resin by $n = 0.7$ (see Ref. 153). The n values for an equilibrium gel formation are much lower, namely, 0.225 (see Ref. 150) and 0.06 (see Ref. 151).

Components of the complex modulus of branched polyethylene are related to frequency by a power law, *i.e.*, here we deal with a similar dependence and, therefore, the loss factor is frequency independent [105, 154, 155] if the number of branches is larger than one per 10^5 carbon atoms in the main chain.[155] The fractal characteristics of the topological structure of the critical cluster and the branched polymer chains are fundamentally different.

5. Structural parameters of polymer networks

The topological structure of a polymer network is usually treated as a set of cross-link points, chain fragments between cross-link points and 'tails' (pendant chains).[3] The classical theory of the rubbery state relates the equilibrium modulus to the concentration of chains and, in the framework of the simplest model of network structure, to the concentration of cross-link points.[1, 3] However, only active chains contribute to the elasticity of a polymer. Therefore, typical of sparse polymer networks are such cross-link points whose effective functionalities are lower than it follows from chemical considerations.[3, 156–158] (Here, the functionality of a cross-link point is the number of attached elastically active chains.) The concentration of such chains is lower than the concentration of chain fragments between cross-link points, as is determined by the topological structure. The concentration of active chains in highly cross-linked polymer networks is larger than it follows from the calculations involving the concentration of cross-link points in the network, because in this case entanglements also contribute to the relaxation modulus.[3] Nonuniform spatial distribution of cross-link points manifests itself in the properties of polymer networks;[159, 160] however, even qualitative structure–property relations have not been established as yet. At the same time the relaxation behaviour of polymer networks is immediately related to parameters of the topological structure.

Indeed, it was shown [161–163] that the $g(t)$, $G'(\omega)$ and $G''(\omega)$ relaxation curves are rather 'sensitive' to the content and molecular mass of 'pendant' chains [polymer networks were prepared by co-polycondensation of divinyl- and monovinylpoly(dimethylsiloxanes) with tris(dimethylsiloxy)phenylsilane]. The results obtained were analysed using the empirical equation [164]

$$g(t) = g_\infty \left[1 + \varphi \left(\frac{\tau_c}{t} \right)^m \right],$$

where g_∞ is the equilibrium modulus, φ is the concentration of 'pendant' chains and τ_c and m are the empirical parameters dependent on the structure of the polymer network and on the molecular mass of the monofunctional modifier, respectively.

Since polymer networks are characterised by the equilibrium modulus, the thermomechanical curve will reach some limiting equilibrium compliance value with an increase in temperature. By studying the transition from the rubbery state to the equilibrium state it is possible to extract information on the topological structure of the polymer similarly to the case of non-cross-linked systems.

In this case the additivity principle is expressed as follows:[48]

$$J_T = J_0 \left[1 - \left(1 - \frac{J_0}{J_{eq}} \right) \sum_m \varphi(m)\, \chi(T, m) \right]^{-1}, \qquad (20)$$

where J_T, J_0 and J_{eq} are the compliance of the polymer network at temperature T, the compliance of a hypothetical polymer with an infinite molecular mass (base line) and the limiting (equilibrium) compliance, respectively.

Based on experimental facts, it was assumed [48] that, similarly to linear macromolecules, the gel fraction includes chain fragments between cross-link points, which are characterised by some molecular masses. However, the hypothesis was based on a model of a perfect network, *i.e.*, the authors assumed that (i) the bulk of the polymer consisted of chain fragments between cross-link points, (ii) there were no pendant 'tails' and (iii) all cross-link points were characterised by the same degree of functionality. A real polymer network has an incomparably more complex topological structure and contains not only chain fragments between cross-link points but also the sol fraction, pendant chains ('tails'), loops and cross-link points of different functionality. All these structural elements are also characterised by certain melt flow transition temperatures. Apparently, at equal molecular masses the 'tails' will 'flow' at a lower temperature than chain fragments between cross-link points. In the polymer network the macro-

molecules not attached to the network are characterised by a lower mobility compared to the mobility in a block polymer.[165] Therefore, Eqn (20) characterises the mass distribution of elements of the topological structure of a polymer network over the relaxation times express through the corresponding flow temperatures. The relations between the flow temperature and the elements of the topological structure should be established independently in special-purpose experiments.

While on the subject of thermomechanical properties, we must consider the relation between the glass transition temperature of a polymer and the concentration, n_c, of cross-link points in the network.

The glass transition temperature, T_g, increases as n_c increases (see, *e.g.*, Refs 156, 166). One can assume that this is a specific manifestation of the topological structure. However, a number of methods have been developed, which allow the glass transition temperature to be calculated from the chemical structure of the polymer.[167–169] In this case it is assumed that the variations of n_c affect only changes in the chemical structure of the polymer. For instance, the epoxy ring opening in the course of curing of epoxy oligomers with amines produces hydroxyl groups whose concentration increases with an increase in n_c. It is this parameter, which strongly affects the level of intermolecular interaction, that determines the glass transition temperature. At the same time the glass transition is immediately affected by such factors as the supramolecular structure, packing character and density fluctuations.[14] With inclusion of all these factors we find that the topological structure itself does not influence the glass transition but the changes in the topological structure cause changes in the character of packing and in the fraction of the free volume. For instance, it is this effect that is attained by varying the topological structure of epoxy amine polymers by (i) introducing monofunctional reagents and (ii) changing the ratio of functional groups.[170] Using dielectric spectroscopy and dynamical light scattering, it was established [171] that the parameters of the α-transition, which vary in the course of curing of the diglycidyl ether of diphenylolpropane with diethylenetriamine, depend on the density fluctuations. Thus, the topological structure at the glass transition of polymers manifests itself indirectly.

Compared to non-cross-linked polymers, polymer networks in the region of the rubbery plateau exhibit a weaker dependence of the relaxation modulus on time

$$G(t) \propto t^{-m}, \tag{21}$$

i.e., the exponent m decreases with an increase in the degree of cross-linking of the polymer.[146, 153, 172] At the same time in the terminal zone (long relaxation times or low frequencies) the $G^*(\omega)$ and $G(t)$ curves for the relaxation modulus and the $J^*(\omega)$ and $J(t)$ curves for compliance reach the limiting values corresponding to the equilibrium strain.[173, 174]

The relaxation behaviour of polymers is described by the Kohlrausch–Williams–Watts (9) [175] and Havriliak–Negami (HN) [176–179] equations

$$G^*(\omega) = G_{\lim} + \frac{G_0 - G_{\lim}}{\left[1 + (i\,\omega\,\tau_0)^{\alpha}\right]^{\beta}},$$

where α and β are empirical constants related to the character of the relaxation spectrum.[177] Here G_0 and $G_{\lim}$ are the limiting values of the elastic modulus corresponding to the low and high frequencies, respectively, and τ_0 is an empirical parameter which can be associated with the relaxation time. The HN equation is more often used when analysing dielectric relaxation data.

Numerical values of the empirical parameters of the KWW and HN equations depend on the polymer structure including its topology. For instance, the parameter β (for the KWW equation containing only one term) decreases with an increase in the concentration of cross-link points (Table 3).[179, 180]

Similar results were also obtained in a broadband dielectric spectroscopy study of the curing of the diglycidyl ether of diphenylolpropane with bis(4-aminophenyl)methane.[181] Although the KWW dependence was obeyed only approximately, the following β values were obtained for the 10%, 20%, 40% and 70% conversions: 0.53, 0.45–0.52, 0.3–0.4 and 0.17–0.2, respectively. Despite the fact that the network is formed at degrees of conversion exceeding 60%, it is reasonable to assume that the trend disclosed also holds in this range of conversions. At the same time the increase in the parameter β during the chemical reaction gives grounds to assume whether or not the network density is an indirectly affecting factor, whereas the chemical structure has a direct effect on the parameter β.

Table 3. Effect of chain length between cross-link points (M_c) on the parameter β.[179, 180]

Polytetrahydrofuran		Polyvinylethylene	
M_c	β	M_c	β
650	0.40	11100	0.34
1000	0.43	1500	0.35
2040	0.49	3800	0.37
2900	0.58	non-cross-linked	0.41

A decrease in β means that the higher the concentration of cross-link points, the smaller the decrease in the modulus with time. This is in qualitative agreement with the data described by relationship (21), namely, an increase in the degree of cross-linking of the polymer leads to a decrease in the exponent m.

The parameters of the HN equation also depend on the degree of cross-linking of the polymer network. For G_0, this dependence is obvious, *viz.*, the value of this equilibrium elastic modulus is proportional to the concentration of chains. For instance, it was shown [182] that changes in the ratio of functional groups in the reaction of polyoxypropylenetriol (POPT) with bis(4-aminophenyl)methane cause appreciable changes in the compliance J_0 and elastic modulus G_0 (Table 4).

Table 4. Effect of stoichiometric ratio of OH and NCO functional groups on the J_0 and G_0 values in the terminal region.[182]

r = [OH]/[NCO]	J_0 /MPa^{-1}	log G_0 (Pa)
POPT with a molecular mass of 710		
0.67	6.27	5.207
0.8	1.67	5.777
1.0	0.40	6.399
1.3	1.42	5.848
1.5	7.45	5.128
POPT with a molecular mass of 2670		
0.67	227.04	3.652
0.8	6.59	5.185
1.0	1.39	5.857
1.2	5.25	5.280
1.35	35.62	4.449

The effect of cross-liking on the parameters α and β can be followed using the data for the curing of the diglycidyl ether of diphenylolpropane with bis(4-aminophenyl)sulfone at 140 °C (see Table 5).[183] As can be seen, the parameter α, which characterises the width of the relaxation time distribution,[181, 184, 185] decreases with an increase in the concentration of cross-link points (the calculated degree of critical conversion for this system is 0.57), whereas the parameter β, which characterises the asymmetry of the distribution function, remains unchanged. Probably, changes in the chemical structure of the system in the course of the reaction and, as a consequence, the glass transition also play a significant role in this case.[186] Indeed, it was shown [184] that an epoxy system (the diglycidyl ether of diphenylolpropane + diethylenetriamine), which undergoes a glass transition in the course of curing, is

Table 5. Dependence of the HN equation parameters on the degree of cross-linking of a polymer network.[183]

Conversion	α	Conversion	α
0.79	0.665	0.83	0.581
0.80	0.651	0.84	0.554
0.81	0.615	0.85	0.532
0.82	0.607		

Note. At all conversion values, $\beta = 0.9$.

characterised by a decrease in the parameter α and an increase in the parameter β. At the same time a study of the formation of an elastic urethane network in the reaction of hexamethylenediisocyanate with a poly(oxypropylene)-based triol revealed an identical trend in changes in the parameters α and β with time, but these changes were small. An attempt[181] to establish a correlation between the degree of cross-linking and the α value for a related system failed. Thus, it is hard to draw an unambiguous conclusion about the relation between the parameters of the HN equation and the cross-link density of polymer networks based on the results presented above.

The topological structure of polymers is correctly reproduced in their relaxation properties, which can be studied by NMR spectroscopy.[59, 187, 188] Gotlib *et al.*[189] established that the temperature dependence of the spin–spin relaxation time T_2 in polymer networks reaches a plateau with an increase in temperature, the $T_{2\,\mathrm{lim}}$ being proportional to the average chain mass (length) between cross-link points, $\overline{M}_c$.

Studies[190, 191] of polymer networks based on poly(tetrahydrofuran) and polyfurite [poly(oxytetramethylene glycol)] showed that the shape of the free induction decay curve depends on the MMD chains of the network

$$G(t) = \int_0^\infty P(N)\, G_0(t, N)\mathrm{d}N\,, \qquad (22)$$

where $G_0(t, N)$ is the dependence of the free induction decay for a monodisperse polymer with chain length N.

The theory of NMR spectra[190, 191] allows this function to be described as a solution to the problem inverse to problem (22). Some examples illustrating a relation between the MMD of the chain fragments between the cross-link points of polymer networks and the NMR data were considered in a review.[187]

Apparently, estimates of the MMD function by this method are of limited use due to at least two reasons. First, one should take into account physical junction points (entanglements), which behave as cross-link points in long chains. This factor 'cuts off' the high-molecular-mass region of the MMD function (see, *e.g.*, Ref. 192). The second reason is the difference of the actual set of topologies from that given by an ideal model of a network. The cross-link points in real polymers are characterised by different degrees of functionality[3, 156–158] and, hence, by different mobilities.[156] The latter was directly shown in pulsed NMR studies.[193–195] Analysis of the free induction decay curves in epoxy amine polymers modified by adding the monoepoxy component or by varying the ratio of epoxy/amine functional groups revealed the presence of two (and more) kinetic phases with different mobilities. It was found that the proton concentration in these phases is proportional to the concentration of cross-links having different functionalities and that the mobilities of the cross-links correlate with the mobilities of the chains emerging from the cross-links. This was shown[180, 196] by, *e.g.*, ^{31}P NMR, taking the reaction of poly(tetrahydrofuran) polymer network with tris(4-isocyanatophenyl)thiophosphate as an example (the latter compound served as the component for cross-link point formation in the polymer network).

6. Equilibrium (physical) networks

The topological structures of the equilibrium networks have been the subject of theoretical and experimental research.[197–203] According to Flory,[204] physical gels can be classified as follows:

— well ordered lamellar structures;

— completely disordered covalent polymer networks;

— mainly disordered polymer networks formed by aggregation and containing ordered regions; and

— specific disordered structures.

As can be seen, polymeric systems with cross-links formed by clustering are also included. Conventional non-cross-linked polymers, which exhibit, in a particular relaxation time interval, the properties of three-dimensional polymers due to formation of physical junction points (*e.g.*, entanglements and/or orientation clusters)[85, 87, 205] as well as labile networks with equilibrium cross-links are left out of consideration. It is the last-mentioned type of network that is of particular interest, because they can be treated as models for covalent networks on the one hand and for non-cross-linked polymers on the other hand.

In contrast to cross-link points in a polymer network, which represent more or less complex fragments of the molecular structure,[3, 169] the junction points in a reversible network are 'points' in essence. Their concentration can be described by a simple equilibrium[201, 206–209]

$$2X \rightleftharpoons X_2\,, \qquad (23)$$

where X is the content of the functional groups capable of forming chemical bonds, whose concentration equals X_2. Such bonds are labile cross-links.

In contrast to the cross-link points in a reversible network, the temporary junctions in a non-cross-linked polymer, which manifest themselves within a particular relaxation time interval (rubbery plateau zone), are not related to the chemical nature of the polymer. Indeed, entanglements, which are usually treated as temporary junction points,[34] are only due to impenetrability of chains. The formation of nematic clusters, which can also play the role of temporary junction points,[85, 87, 205] is due to natural properties of polymers (segment anisotropy and confined space available for arrangement of a polymer chain due to the excluded volume effect) rather than some specific intermolecular interaction.[205]

Thus, the junction points of reversible networks are similar to and at the same time different from cross-link points in non-cross-linked and three-dimensional polymers (Table 6). The relaxation properties of these three types of networks are qualitatively compared in Fig. 5 (see also Ref. 201). Curve *1* is the temporal

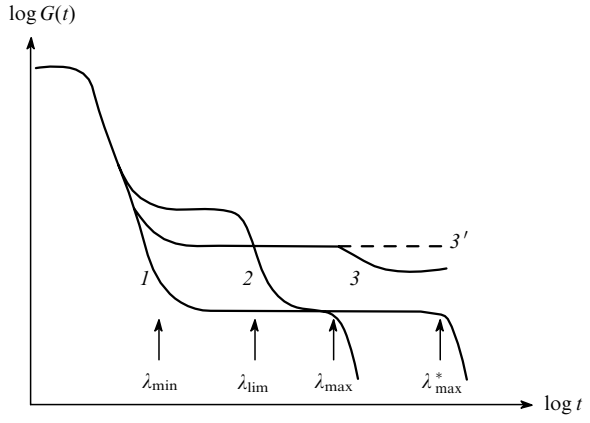


Figure 5. Relaxation elastic modulus plotted *vs.* time for a non-cross-linked polymer (*1*) and equilibrium (*2*) and non-equilibrium (*3* and *3′*) networks.

Table 6. Characteristics of cross-links in different types of networks.

Chain entanglements (non-cross-linked polymers) [a]	Physical network [a]	Chemical network (three-dimensional polymers)
Chemical structure of the polymer is immaterial	presence of polar H-bonding groups on the chains is essential	presence of functional groups that can chemically react with one another
No energy is involved during cross-link creation – loss ($\sim RT$)	energy of the order of units of kJ per mole ($\leqslant 10\,RT$) is involved during creation – loss	energy of the order of tens of kJ per mole ($\geqslant 100\,RT$) is involved during creation – loss
Formation and loss are non-specific	formation of cross-links requires specific site orientation and cooperative network mobility	formation of cross-links obeys kinetic laws that are often complicated by diffusion and other processes
Non-cooperative	cooperativity effects are significant during zipping and unzipping of ladder-like structures	usually, co-operative effects are ignored
Solvent does not affect physical networks	solvent effects can be crucial for the equilibrium constant	conventional kinetic solvent effect

[a] According to Ref. 199.

dependence of the relaxation modulus of elasticity of a non-cross-linked polymer. In a particular relaxation time interval, from λ_{min} to λ_{max}, in the rubbery plateau zone, the polymer exhibits the properties of a network. Then, in the terminal zone, an abrupt decrease in the relaxation modulus characterises the transition to a viscous flow state. The relaxation modulus of a three-dimensional polymer (curve *3*) in the vicinity of λ_{max} either remains at the plateau level (highly cross-linked polymers for which chemical cross-link points and labile junction points are summed, curve *3′*), or goes to the level of the equilibrium modulus (sparse networks for which only chemical cross-links are significant). Reversible networks (curve *2*) are characterised by two plateau zones. The former corresponds to a physical network, in which an important role is played by both types of labile cross-link points. At relaxation times longer than λ_{lim}, the relaxation modulus is determined by the concentration of the same cross-link points as in the non-cross-linked polymer. However, in the presence of functional groups interacting with one another to form cross-links with average lifetimes shorter than λ_{lim}, the λ_{max} value appreciably increases [201]

$$\lambda^*_{max} = \lambda_{max}\frac{2S^2p^2}{12 - 9p + p^2},$$

where S is the average number of functional groups per chain and p is the probability of formation of a cross-link. The reason for the lowering of the relaxation rate is retardation of the diffusion motion of chains by the newly forming labile cross-links.

The relaxation behaviour of equilibrium polymer networks was studied [206–211] taking polybutadiene modified by 4-phenyl-1,2,4-triazolidine-3,5-dione as an example. On addition to polymers, the latter compound undergoes dimerisation and forms cross-links with a bond energy of 57 ± 15 kJ mol^{-1} (see Ref. 206).

An increase in the concentration of modifier causes an increase in the relaxation modulus G^0_N in the rubbery plateau zone (Table 7).[211] Lowering the temperature leads to an increase in G^0_N, which is apparently due to the temperature dependence of the equilibrium constant (23). A significant effect of temperature on G^0_N is a distinctive feature of the equilibrium networks.[208, 209]

The extension of the rubbery plateau zone and the viscosity of polybutadiene ($M_n = 2.6 \times 10^4$) are plotted *vs.* the concentration of modifier in Fig. 6 using the data taken from Refs 210 and 211. These results qualitatively substantiate theoretical conclusions, namely,[201] an increase in the concentration of active functional groups causes an appreciable increase in the viscosity and, as a consequence, an increase in λ^*_{max}. The effect of temperature is also quite clear, that is, lowering the temperature leads to a corresponding increase in the viscosity. The extension of the rubbery plateau zone also increases.

Table 7. Effect of degree of cross-linking of an equilibrium network on the relaxation modulus in the region of the rubbery plateau at $T = 273$ K.

$10^{-3}\,M_n$	Degree of modification (mol.%)	$10^{-5}\,G^0_N$ /Pa
26	0	6.0
	0.5	6.0
	2	6.9
	5	7.1
	7.5	9.1
28 [a]	2	8.7
	3	9.6
	4	13.6
35	0	7.6
	1	9.1
48.5	0	7.5
	1	8.6
215	0	8.0
	1	9.2

[a] Data taken from Ref. 209 at $T = 237$ K.

The concentration of functional groups also influences the parameters of the HN equation,[208] namely, with an increase in the concentration of functional groups the parameter α slightly increases while the parameter β substantially decreases.

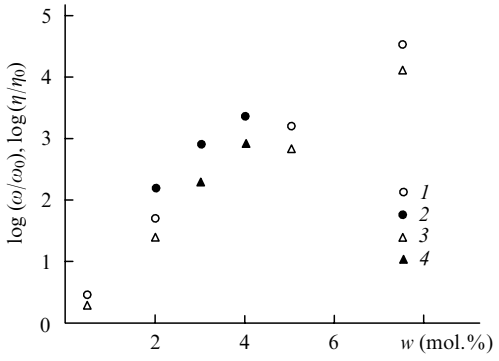


Figure 6. Rubbery plateau extension (*1*, *2*) and viscosity (*3*, *4*) of modified polybutadiene plotted *vs.* concentration of modifier at 273 (*1*, *3*) [210] and 233 K (*2*, *4*).[211]

IV. The relaxation time spectrum as a means of correct characterisation of topological structure

The possibility of obtaining a correct description of the relaxation behaviour of polymers using the relaxation time spectrum was initially considered as a hypothesis only.[63, 64, 212] Rouse[213] first showed that the dynamics of a polymer chain can be described using a discrete set of relaxation times that depend on the chain length (number of dynamical units). The totality of unambiguously determined pre-exponents can also be considered as a relaxation spectrum. Since then a number of models have been proposed, which describe the reptation motion of macromolecules with allowance for various relaxation mechanisms of the 'tube', *i.e.*, a region in which a restrained motion of a specified chain is realised.[4, 11, 34, 52, 214, 215] Each relaxation mechanism corresponded to a particular set of relaxation times and, hence, a relaxation spectrum. Comprehensive analysis of the dynamical models and consequences following from them was reported in a review.[52]

Some authors (see, *e.g.*, Refs 216–220) considered a theory which provides an alternative to the reptation theory. Basic to the new theory is the assumption that restrained chain motions are mainly due to close packing, which leads to intermolecular cooperativity on the length scale of a chain segment, rather than topological junctions. In this case the formation of nematic clusters also plays a significant role.[89]

Thus, in this case the relaxation spectrum, in contrast to local relaxation transitions, has a dynamical meaning. Namely, it is related to the polymer structure indirectly, through correlations between the dynamical properties and topology of macromolecules (of course, with allowance for the conditions under which the motion occurs).

1. Modified Rouse chain

The molecular structure can also to some extent affect parameters of the relaxation spectrum, but again this occurs due to specific features of dynamical processes. For instance, the relaxation properties of the modified Kargin–Slonimskii–Rouse model[45, 213] have been studied.[214, 215, 221, 222] The relaxation behaviour of these models was also analysed in other studies (see Refs 223 and 224), but this concerned the frequency or temporal dependences of the relaxation modulus while the effect of chain modification on the relaxation spectrum was not considered.

The modification consisted of the chain units being ascribed different friction coefficients. Stress relaxation of an unbalanced chain comprising n units is described by a system of n equations

$$\begin{aligned}
&\tau_1\dot{x}_1 = -x_1 + x_2\\
&\tau_2\dot{x}_2 = x_1 - 2x_2 + x_3\\
&\ldots\ldots\ldots\ldots\ldots\ldots\ldots\ldots\\
&\tau_i\dot{x}_i = x_{i-1} - 2x_i + x_{i+1}\\
&\ldots\ldots\ldots\ldots\ldots\ldots\ldots\ldots\\
&\tau_n\dot{x}_n = x_{n-1} - x_n,
\end{aligned} \tag{24}$$

where x_i is the coordinate of the ith unit; the relaxation characteristics of the units, which are due to different friction coefficients (*i.e.*, the interaction between the units and the environment), are described by the parameter τ_i. Having solved the system (24), it is possible to derive the equations of motion for all units of the chain and to determine the change in the chain length, $L = x_n - x_1$, provided that the initial conditions are specified. An example of the initial conditions is given by $L(0) = 1$ $x_i(0) = (i-1)/(n-1)$, which corresponds to a uniformly stretched equidistant chain.

The solution of system (24) in the form of a combination of exponents for relaxation of the chain length

$$L(t) = \sum_{i=1}^{n} h_i \exp(-p_i t),$$

where h_i is the relaxation time spectrum, is given by the roots $z_i = \tau_i p_i$ of the polynomial $D_n = 0$, where D_n is the modified Rouse matrix

$$D_n = \begin{vmatrix}
z_1 - 1 & 1 & 0 & 0 & \ldots & 0 & 0 & 0\\
1 & z_2 - 2 & 1 & 0 & \ldots & 0 & 0 & 0\\
 & & & & & & & \\
0 & 0 & 0 & 0 & \ldots & 1 & z_{n-1} - 2 & 1\\
0 & 0 & 0 & 0 & \ldots & 0 & 1 & z_{n-1}
\end{vmatrix} \tag{25}$$

Numerical solution of Eqn (25) makes it possible to obtain a total of $(n-1)$ roots $p_1, p_2, \ldots, p_i, \ldots, p_{n-1}$, which represent the reciprocal relaxation times ($p_i = \lambda_i^{-1}$) characterising the relaxation behaviour of the entire chain. In the case of identical units the results obtained are exactly described by the Rouse relations

$$\lambda_i^{-1} = 4\sin^2\left(\frac{\pi}{2}\frac{i}{n+1}\right),$$

$$h_i = \frac{1}{2n}\left[\tan\left(\frac{i\pi}{2n}\right)\right]^{-2},$$

where i is the mode number ($i = 0$ corresponds to the maximum relaxation time); $h_i = 0$ for the even i values.

Insertion of units with higher friction coefficients (type a units; type b was ascribed to unmodified units) into the chain causes significant changes in the set of relaxation modes. Figures 7 and 8 show that the total number of modes increases with an increase in the number of type a units, which divide the chain into blocks comprised of units with a low friction coefficient. However, higher-frequency modes are grouped into 'packets', *i.e.*, form groups characterised by similar relaxation times; a distinctive feature is that the higher the friction coefficient of the type a units, the smaller the separation between such modes (see Fig. 7). It is hard to assign the relaxation modes in the relaxation time spectrum characterising the Rouse chain to particular units. If the relaxation properties of the type a units inserted into the chain differ only slightly from those of the type b units ($\tau_a/\tau_b = 2$), it is possible to select 'packets' of relaxation modes, which, although they have different parameters, are 'clustered' near the values characteristic of the type b blocks. The larger the τ_a/τ_b ratio, the smaller the separation between the modes in 'packets' (see Fig. 7). In the limiting case, chain elongation due to an increase in the number of blocks leads to a decrease in the number of modes,

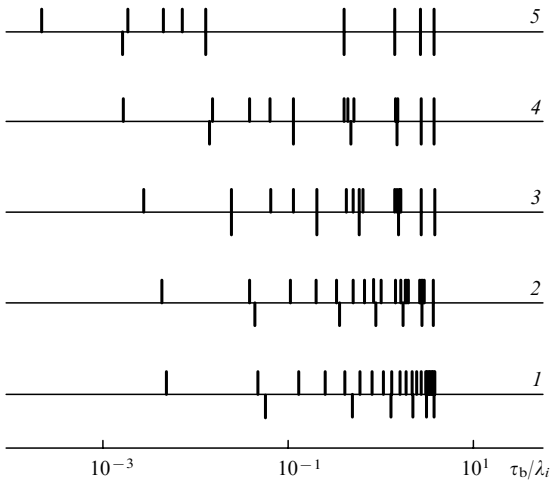


Figure 7. Relaxation modes for monoblock (below horizontal lines) and tetrablock chains (above horizontal lines) for the $a-(b-b-b-b-b-a)_m$ structure.[215]
$\tau_a/\tau_b = 1$ (*1*), 2 (*2*), 5 (*3*), 10 (*4*) and 100 (*5*).

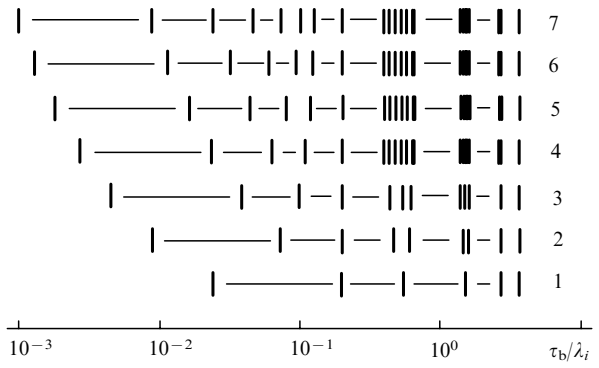


Figure 8. Relaxation modes for the $a-(b-b-b-b-b-a)_m$ structure.[215]
$\tau_a/\tau_b = 2$. Figures denote the m values.

which becomes smaller than the total number of units because high-frequency modes merge.

A comparison of polyblock chains with a 'monoblock' one (see Fig. 8) showed that high-frequency relaxation modes are grouped near the values characteristic of the corresponding block. The number of relaxation modes in a 'packet' becomes equal to the number of blocks. (In Fig. 8 we present the data for $\tau_a/\tau_b = 2$ in order to distinguish between components of the 'packet'.) Thus, the units with a high friction coefficient separate blocks from one another; because of this, the relaxation modes characterising the units possessing different relaxation properties can be separated in the relaxation spectrum of any chain.

The relaxation spectra of the chains having the structures described in Table 8 are shown in Fig. 9.

If the modified unit is present in the terminal zone of the chain, the λ_{max} value somewhat increases, but the statistical weight of the corresponding mode decreases. Separation of the blocks comprised of units with higher mobility by the units of lower mobility

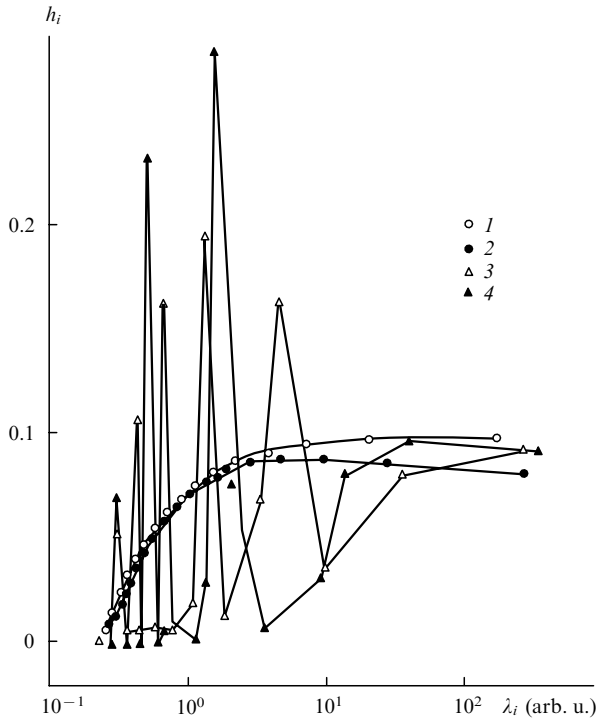


Figure 9. Relaxation modes for chains of different structure. For notations (*1*–*4*), see Table 8.

Table 8. Effect of the structure of the modified Rouse chain on the parameters of the relaxation spectrum (in arbitrary units).[215]

No.	Chain structure [a]	λ_{max}	$\langle\lambda\rangle_w$	$\langle\lambda\rangle_n$
1	$1-(1)_{18}-1 \rightarrow F$	174	143	20
2	$5-(1)_{18}-1 \rightarrow F$	265	224	25
3	$5-(1)_{12}-5-(1)_5-1 \rightarrow F$	261	232	27
4	$5-(1)_3-5-(1)_6-5-(1)_4-5-(1)_2-1 \rightarrow F$	331	282	36

[a] Figures are the ratios of the friction coefficients of the units a and b; subscripts denote the number of units in the block and F is the force exerted on the chain.

leads to the appearance of peaks in the relaxation spectra, the number of peaks being changed antiparallel to the number of blocks. This is due to a decrease in the block length.

Thus, this example allowed us to follow how the 'molecular' structure manifests itself in the relaxation time spectra through the mobilities of units.

Analysis [214, 215] showed that the strain and stress relaxation processes affect not only the relaxation spectrum (this was shown earlier for the uniform Rouse model, see, *e.g.*, Ref. 34) but also the set of relaxation times. This is illustrated in Fig. 10. Apparently, this is a consequence of an indirect relation between the relaxation spectrum and the polymer structure through the macromolecular

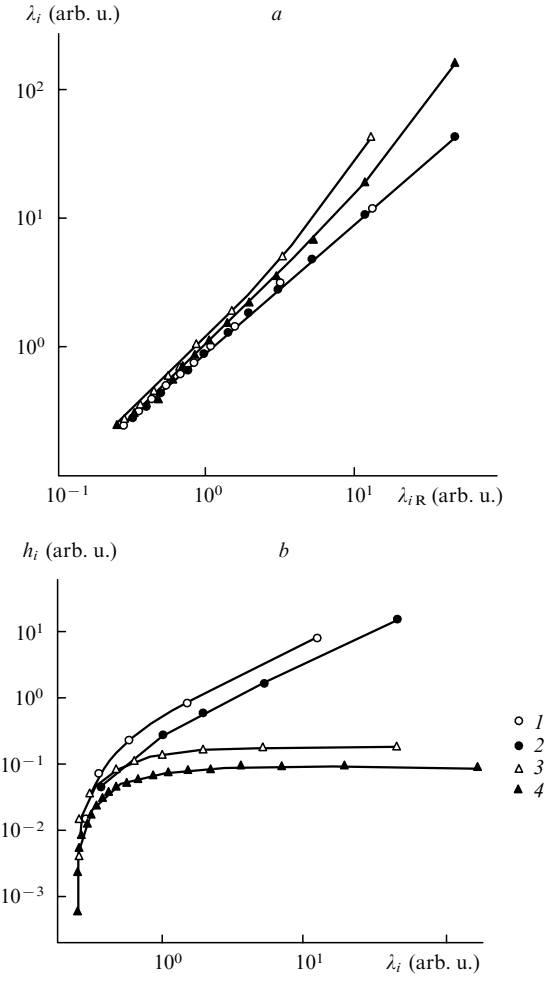


Figure 10. Correlation between the relaxation times λ_i and λ_{iR} (a) and the stress relaxation spectra (b, curves *1* and *2*) and deformation relaxation spectra (b, curves *3* and *4*) obtained for chains comprising ten (*1*, *3*) and twenty (*2*, *4*) units.

dynamics. This is also indicated by the fact that physically substantiated spectrum cannot be obtained under any initial relaxation conditions. For instance, if in the initial state the chain units are arranged nonuniformly, a number of pre-exponents can take negative values.[225]

2. Methods of calculation of the relaxation spectra from experimental data

The viscoelastic behaviour of polymers can be conveniently characterised by a spectrum of relaxation times. Usually, it is believed [4, 5] that one can determine and predict the viscoelastic behaviour of polymers under any strain and loading conditions from the known relaxation spectrum. However, the relaxation spectrum was obtained in explicit form only for molecular models (see above). Comparison of the results of modelling with experimental data on certain relaxation properties gives no assurance of correctness of the former. In order to assess the ability of a theoretical model to describe experimental data, one should compare the model relaxation spectra with the experimental ones, which thus play the role of a generalised characteristic. Therefore, methods of calculation of relaxation spectra, which are based on analysis of experimental data (mainly temporal and frequency dependences of the elastic modulus) have been continuously developing.[226]

Calculations of the relaxation time spectrum from the known real and imaginary components of the elastic modulus belong to the class of ill-posed problems; therefore, the uniqueness problem of the results obtained poses.[226–229]

a. Effective relaxation time as a characteristic of the relaxation spectrum

Is it always necessary to represent the relaxation time distribution function in explicit form? It was shown [49, 51, 88] that as a quantitative characteristic it is sufficient to use the effective relaxation time λ_{ef}

$$\frac{1}{\lambda_{ef}} = -\frac{d \ln G(t)}{dt} = \frac{\sum_i h_i \lambda_i^{-1} \exp(-t/\lambda_i)}{\sum_i h_i \exp(-t/\lambda_i)} = \sum_i w_i(t) \lambda_i^{-1} ,$$

where h_i is the relaxation spectrum and $w_i(t)$ is the relaxation time distribution function in the time domain, which is related to h_i at $t = 0$ as follows

$$w_i = \frac{h_i}{\sum_i h_i} .$$

The use of the parameter λ_{ef} for comparison of experimental stress relaxation data with the dependences obtained using the polymer dynamics models led to good results.[49, 51] For instance, the Rouse and Doi–Edwards models with the known (and different!) relaxation spectra give significantly different dependences $\lambda_{ef}(t)$. In the Rouse model the parameter λ_{ef} is proportional to t at $\lambda_{min} \leqslant t \leqslant \lambda_{max}$, *i.e.*, in the region where the relaxation modulus of elasticity is proportional to $t^{-1/2}$. In the Doi–Edwards model the parameter λ_{ef} in the rubbery plateau zone is proportional to $t^{1/2}$.

The temporal dependences of the relaxation shear modulus and the effective relaxation time of narrow-MMD polystyrene ($M_w/M_n = 1.03$) plotted using the data taken from Ref. 230 are shown in Fig. 11. In the transient region corresponding to transition from the glassy state to the rubbery plateau zone the parameter λ_{ef} is nearly proportional to the square root of time, the dependence in the rubbery plateau zone is nearly linear (the exponent is 1.2) and then it becomes weaker in the region where the effect of the molecular mass becomes pronounced. Eventually, the parameter λ_{ef} takes a constant value equal to the maximum relaxation time. It was shown [49] that the stress relaxation behaviour of other monodisperse polystyrenes (see Refs 74, 231, 232) also obeys these laws, with the maximum relaxation time being

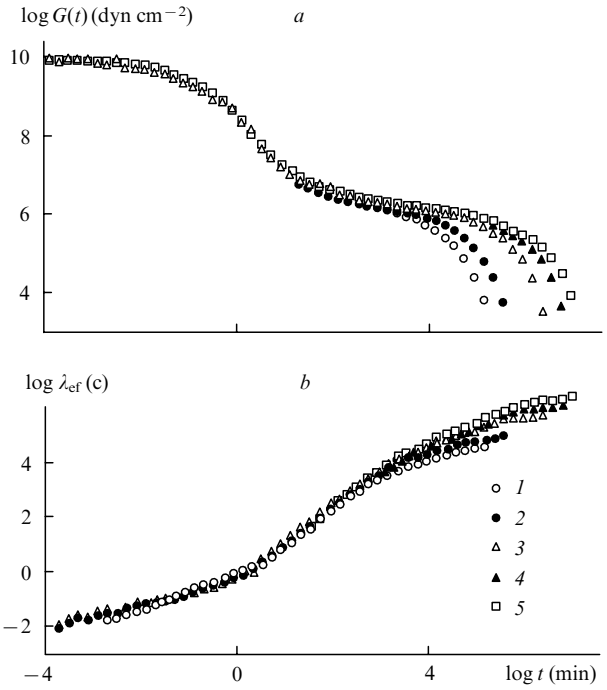


Figure 11. Shear modulus (*a*) and effective relaxation time (*b*) of polystyrene plotted *vs.* time.[230]
$M_w \times 10^{-3} = 80$ (*1*), 125 (*2*), 193 (*3*), 239 (*4*), 267 (*5*). The reduction temperature was 129 °C.

proportional to M^4 (Fig. 12). This dependence cannot always be revealed. Indeed, if the molecular masses vary with a not too large interval, the dependence mentioned above can be distorted. Besides, if the molecular mass of a polymer varies over a broad range, the relaxation measurements are usually carried out at appreciably different temperatures and then their results are reduced to a certain specified temperature using the principle of temperature–time superposition. Small uncertainties introduced when using this procedure can lead (and do lead, see the data shown in Fig. 12) to errors. Analysis of the whole array of experimental data showed validity of the power law mentioned above. This dependence was also reported in other studies.[104, 233]

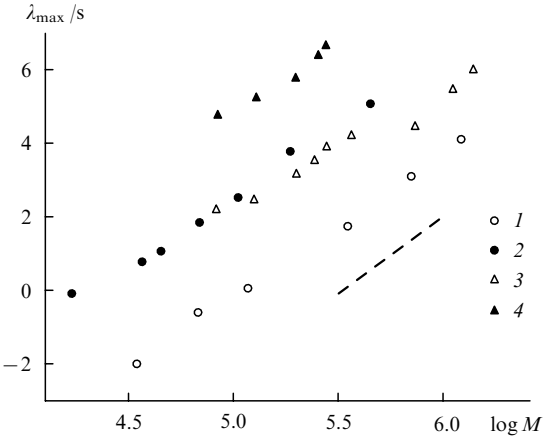


Figure 12. Maximum relaxation time plotted *vs.* molecular mass of polystyrene (*1–4*) using the data taken from Refs 231, 74, 230 and 232, respectively.
Reduced temperature /°C: 160 (*1*), 139 (*2*, *3*) and 127 (*4*).
The dashed line describes the dependence $\lambda_{max} \propto M^4$.

The fact that for monodisperse polymers λ_{ef} in the rubbery plateau zone is proportional to $I^{1.2}$ can indicate that the relaxation spectra of these compounds are more similar to the Rouse spectrum with respect to this characteristic.

Knowing the frequency dependence of the effective relaxation time, it is possible to determine [51] two parameters with different degrees of averaging over the relaxation times. In this case analysis is carried out using the real $G'(\omega)$ and the imaginary $G''(\omega)$ components of the relaxation modulus of elasticity separately.

Similarly to the case of the frequency dependence of the relaxation modulus, the frequency domain is divided into three zones with respect to the character of the frequency dependence of the effective relaxation time. These are the terminal zone (zone *I*, low frequencies), the rubbery plateau zone (zone *II*) and the high-frequency zone (zone *III*) .

As mentioned above [see expression (12)] the effective relaxation time $\lambda_{ef\,w}(\omega)$ in the terminal zone *I* reaches a limiting value, which is frequency independent and equals the ratio of the second to the first moment of the relaxation time distribution, *i.e.*, is the weight-average relaxation time [see relationship (13)].

In zone *III* at $\omega \to \infty$ one has

$$\lambda_{w\,III} = \frac{\sum_i h_i}{\sum_i (h_i/\lambda_i)}.$$

Since short relaxation times make a greater contribution to the last-mentioned expression, one gets $\lambda_{w\,III} < \lambda_{w\,I}$ and the $\lambda_{w\,II}(\omega)$ dependence in zone *II* (rubbery plateau zone) is a decreasing function of frequency.

The effective relaxation time [see expression (14)] at $\omega \to 0$ (region *I*) is the number-average relaxation time, which is also frequency independent

$$\langle\lambda\rangle_{n\,I} = \frac{\sum_i h_i(\lambda)\lambda_i}{\sum_i h_i(\lambda)}.$$

In region *III* one has

$$\lambda_{ef\,n}(\omega) \to \frac{\sum_i h_i/\lambda_i}{\sum_i h_i/\lambda_i^2}.$$

This value can be either small or rather large depending on the character of the relaxation spectrum. Therefore, in region *II* the $\lambda_{ef\,n}(\omega)$ dependence can show rather complex behaviour.

Thus, analysis of the frequency dependence of the effective relaxation time makes it possible to estimate the relaxation time spectrum using a number of distribution moments. In particular, the ratio

$$\gamma_I = \frac{\langle\lambda\rangle_{w\,I}}{\langle\lambda\rangle_{n\,I}}$$

characterises the width of the relaxation time distribution in region *I*.

The relaxation spectrum of the Rouse model is given [33] by the relationship $h_i = n^{-1}$, where n is the chain length. Therefore, in the terminal zone one gets

$$\langle\lambda\rangle_{w\,I} = \lambda_{max}\frac{\sum_{i=1}^{n} i^{-4}}{\sum_{i=1}^{n} i^{-2}} \approx \lambda_{max}$$

and

$$\langle\lambda\rangle_{n\,I} = \frac{\lambda_{max}}{n}\sum_{i=1}^{n} i^{-2} \approx \frac{\lambda_{max}}{n}.$$

Table 9. Dependences of characteristics of the effective relaxation time on the chain length for various models.[51]

Model	$\langle\lambda\rangle_{n\,I}$	$\langle\lambda\rangle_{w\,I}$	λ_{max}	γ_{max}	ω_{max}	γ_I
Rouse model	n^1	n^2	n^2	–	–	n^1
Doi – Edwards model	n^3	n^3	n^3	–	–	n^0
Modified Rouse model	n^1	$n^{1.66}$	$n^{1.7}$	$n^{0.58}$	$n^{-2.2}$	$n^{0.66}$

Because, in accord with the Rouse model, λ_{max} is proportional to n^2, the parameter $\langle\lambda\rangle_{w\,I}$ also increases in proportion to n^2 and $\langle\lambda\rangle_{n\,I}$ increases in proportion to n. The distribution width, γ_I, increases proportionally to the polymer chain length (Table 9).

The following relationships are valid in zone *III*:

$$\langle\lambda\rangle_{w\,III} = \lambda_{max}\frac{n}{\sum_{i=1}^{n} i^2} \approx \frac{\lambda_{max}}{n^2},$$

$$\langle\lambda\rangle_{n\,III} = \lambda_{max}\frac{\sum_{i=1}^{n} i^2}{\sum_{i=1}^{n} i^4} \approx \frac{\lambda_{max}}{n^2},$$

Thus, the distribution width γ is independent of chain length in this frequency region.

In the Doi – Edwards reptation model the relaxation spectrum is given [34] by the expression $h_i = i^{-2}$; therefore, in zone *I* one has

$$\langle\lambda\rangle_{w\,I} = \lambda_{max}\frac{\sum_{i=1,3\ldots}^{n} i^{-6}}{\sum_{i=1,3\ldots}^{n} i^{-4}} \approx \lambda_{max},$$

$$\langle\lambda\rangle_{n\,I} = \frac{8}{\pi^2}\lambda_{max}\sum_{i=1,3\ldots}^{n} i^{-4} \approx \lambda_{max}.$$

The distribution width γ_I is independent of chain length.

For zone *III* one has

$$\langle\lambda\rangle_{n\,III} = \lambda_{max}\frac{n}{\sum_{i=1}^{n} i^2} \approx \frac{\lambda_{max}}{n^2},$$

$$\langle\lambda\rangle_{w\,III} = \lambda_{max}\frac{\sum_{i=1}^{n} i^{-2}}{n} \approx \frac{\lambda_{max}}{n},$$

and γ_{III} increases in proportion to n.

In the rubbery plateau zone (zone *II*) the parameter $\lambda_{w\,II}$ is proportional to ω^{-1} for the Rouse model and to $\omega^{-1/2}$ for the Doi – Edwards model; respectively, $\lambda_{n\,II} \propto \omega^{-1/2}$ and $\lambda_{n\,II} \propto \omega^{-1}$. From here the ratios of the average relaxation times for these models are also different, namely, the parameter γ_{II} decreases in the former and increases in the latter case nearly proportionally to the square root of the frequency.

Thus, different frequency dependences of the average relaxation times and their ratios reflect significant differences between the relaxation spectra of the models under consideration.

The average relaxation times and their ratios depend on the structures of the polymer chains. This dependence can be illustrated taking nonuniform Rouse chains (see above) as an example. We will consider chains whose structures can be expressed through the friction coefficients of units as follows:

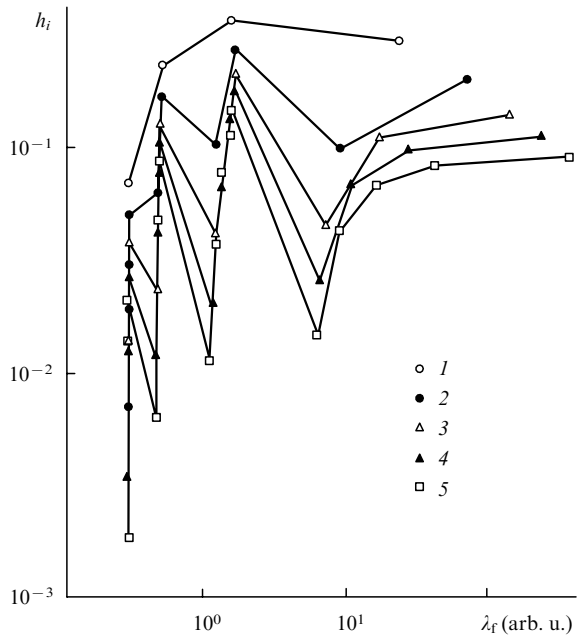


Figure 13. Relaxation spectra calculated for modified Rouse chains $F \leftarrow (1-1-1-5)_m-1-1-1-5$ with $m = 0$ (*1*), 1 (*2*), 2 (*3*), 3 (*4*) and 4 (*5*).[51]

$F \leftarrow (1-1-1-5)_m-1-1-1-5$, where $m = 0$, 1, 2, 3, 4. The relaxation spectra calculated for these model chains are shown in Fig. 13. As can be seen, in contrast to the Rouse and the Doi–Edwards models, the nonuniform Rouse chain model leads to the formation of an essentially non-monotonic discrete relaxation spectrum. Qualitatively, the frequency dependences of the average relaxation times (Fig. 14) obey the same pattern as the analogous theoretical dependences shown above. However, the $\gamma(\omega)$ dependence is basically different, namely, pronounced maxima appear in the curves. Quantitative relation of these parameters to the chain length also differs from the corresponding relations derived for the models considered above (see Table 9).

In the frequency regions *I* and *III* the parameters $\langle\lambda\rangle_w$, $\langle\lambda\rangle_n$ and γ take constant values, the average relaxation times in zone *I* being proportional to the chain length $n = 4(m+1)$ raised to the power 1.66 and 1.00 for $\langle\lambda\rangle_{w\,I}$ and $\langle\lambda\rangle_{n\,I}$, respectively; here for the average relaxation time ratio one has $\gamma_I \propto n^{0.66}$ (see Table 9); in zone *III* the parameters $\langle\lambda\rangle_{w\,III}$ and $\langle\lambda\rangle_{n\,III}$ are independent of n. The frequency dependence of the ratio of the average relaxation times in the rubbery plateau zone can be quite accurately described by a power law with an exponent of about 0.5. The height of the maximum and its position on the frequency axis depend on the chain length, namely, $\gamma_{max} \propto n^{0.58}$ and $\omega_{max} \propto n^{-2.2}$.

Thus, the nonuniform Rouse chain model is intermediate between the Rouse and the Doi–Edwards models with respect to the relaxation properties. This shows that the relaxation characteristics in question (effective relaxation times and their ratio) are rather sensitive to both the type of motion (the Rouse and Doi–Edwards models) and the chain structure (the classical and nonuniform Rouse models).

As an example Fig. 15 presents the frequency dependences of the effective relaxation times of polystyrene, obtained [51] using the tabulated data.[50] In the terminal zone the effective relaxation times are frequency independent and can be determined as the average values $\langle\lambda\rangle_{w\,I}$ and $\langle\lambda\rangle_{n\,I}$.

The dependence of the average relaxation times on the molecular mass is described by a power law $\langle\lambda\rangle \sim M^a$. The exponents for $\langle\lambda\rangle_{w\,I}$ and $\langle\lambda\rangle_{n\,I}$ differ from each other (see Table 9), being in the former case larger than in the latter. For all polymers under study (data were taken from Refs 53, 57, 58)

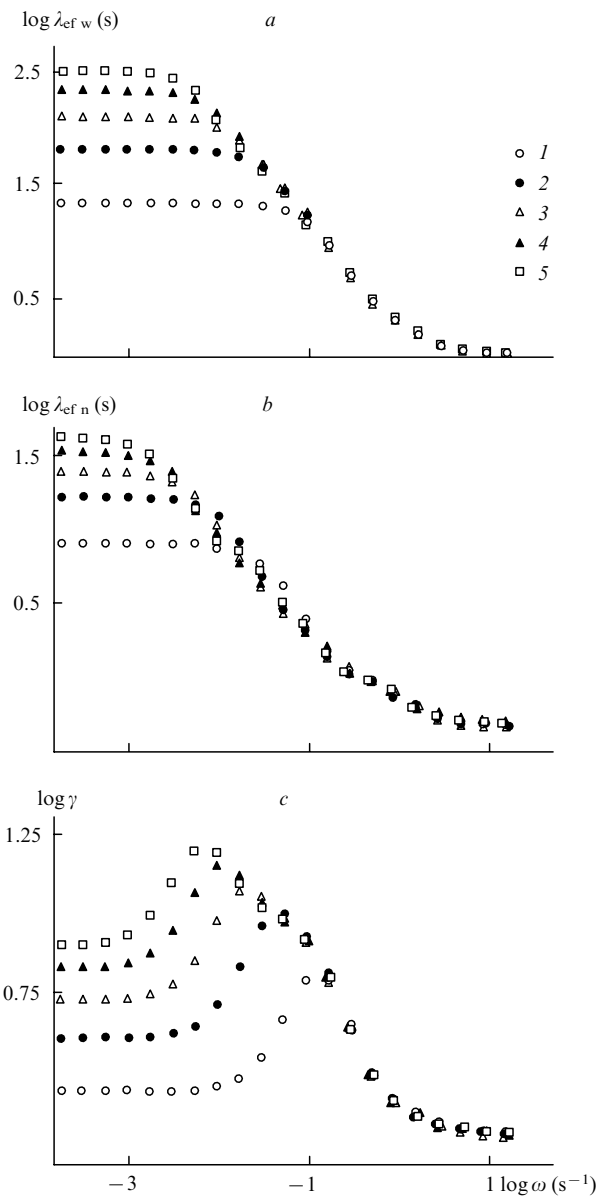


Figure 14. Frequency dependences of average relaxation times (*a*, *b*) and their ratios (*c*) obtained for the modified Rouse chains whose relaxation spectra are shown in Fig. 13.[51]
Notations (*1–5*) correspond to those used in Fig. 13.

the dependence of $\langle\lambda\rangle_{n\,I}$ on the molecular mass is characterised by an a value of about 3.4. The same exponent value is also characteristic of the known dependence of viscosity on the molecular mass.[4]

The value of the exponent at M depends on the procedure of averaging over the relaxation times. This concerns both the limiting values and the rubbery plateau zone. Analysis of the dependences presented in Fig. 15 showed that at all molecular masses an increase in frequency causes a nearly linear (more exactly, the exponent approaches a value of 0.9) decrease in $\langle\lambda\rangle_{n\,II}$ while $\langle\lambda\rangle_{w\,II}$ is proportional to $\omega^{-0.75}$, so the corresponding ratio increases in proportion to $\omega^{0.15}$. With allowance for this dependence, which is common to all narrow-MMD polymers, one can assume that their relaxation spectra are intermediate between broad relaxation spectra characteristic of the Rouse model and narrow relaxation spectra characteristic of the Doi–Edwards model. The shape of the $\gamma(\omega)$ plots points to a similarity between the relaxation spectra of real polymers and those of the polymers corresponding to the modified Rouse model.

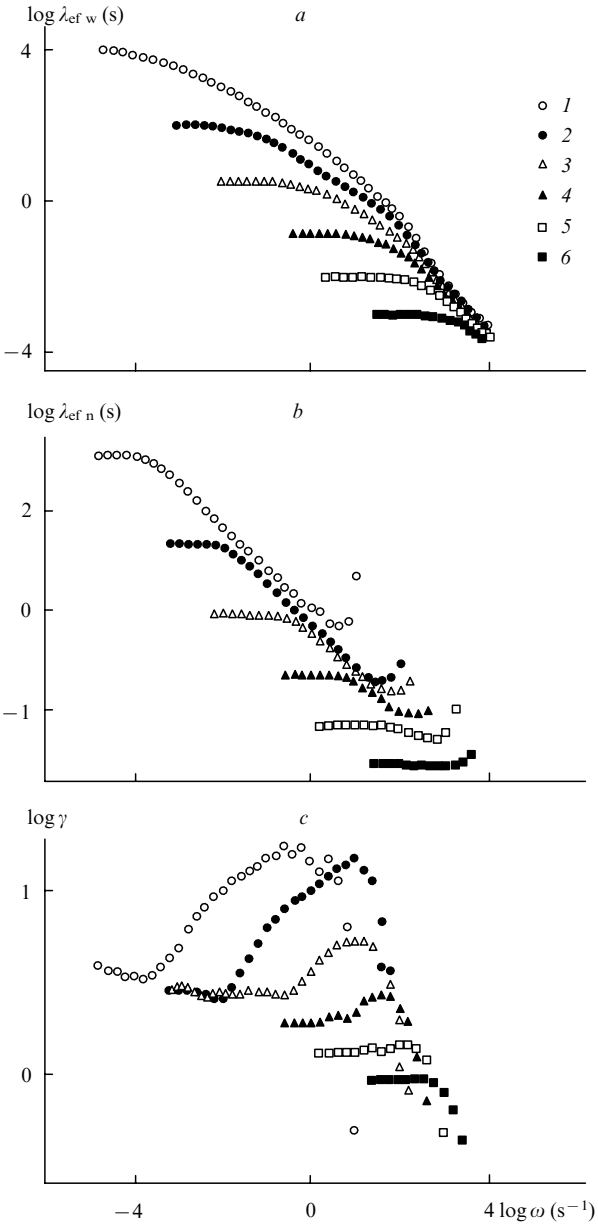


Figure 15. Frequency dependences of average relaxation times (*a*, *b*) and their ratio (*c*) at $T = 180$ °C obtained for monodisperse polystyrene using the data taken from Ref. 50.
$M \times 10^{-3} = 3000$ (*1*), 770 (*2*), 275 (*3*), 128 (*4*), 70 (*5*) and 39 (*6*).

Comparison of the distribution parameters in zone *III* is complicated by the fact that real polymers undergo glass transitions in this frequency region. In contrast to a similar dependence obtained in model calculations, here a pronounced maximum in the frequency dependence of the parameter γ_{II} is not an artifact; rather, it has a particular physical meaning. Probably, the appearance of this maximum characterises the glass transition. Thus, the $\gamma(\omega)$ dependence, as well as the loss factor $\tan\delta$, can be used for the description of this transition.

Depending on the molecular mass, the transition points are located at different positions on the frequency axis (see Fig. 15 *c*), namely, an increase in the molecular mass leads to a shift of the transition point towards lower frequencies. The position of the maximum on the frequency axis is nearly proportional to M^{-2}; the exponent being almost equal to that for the nonuniform Rouse model ($n^{-2.2}$).

b. Continuous relaxation spectrum

In fact, the development of the Kargin – Slonimskii – Rouse model led to the idea that the relaxation spectrum characterising the viscoelastic properties of polymers is a continuous function,[213] because the number of modes in the Rouse spectrum equals the number of chain units and the difference between the relaxation times of the 'neighbouring' modes is much less than the relaxation times, *i.e.*, $(\lambda_{i+1} - \lambda_i) \ll \lambda_i$. This concept dominated in the polymer science in the 1950s – 1960s.[63,212] The relaxation behaviour of polymers was described using relaxation spectra, which were represented by a wedge, 'box' or their combination.[212] Even at present some authors often use a continuous function instead of the calculated discrete spectrum (see, *e.g.*, Ref. 234) assuming that only this representation is physically substantiated. Moreover, an opinion was offered [228] that discretisation is a necessary prerequisite for using numerical methods of solving the problem of determination of continuous relaxation spectrum from experimental data.

In mathematics, the determination of a spectrum is reduced to inversion of the Laplace transforms (1), (1a) or the Fourier transform (2), *i.e.*, this is a quite solvable problem

$$H(\lambda) = \hat{H}(s) = \frac{1}{2\pi i}\int_0^\infty g(t)e^{st}dt, \tag{26}$$

where $s = 1/\lambda$.

The difference is that (if we ignore the problems of accuracy and ambiguity of experimental data), first, the integration limits in expressions (1a) and (26) are limited by the experimental conditions; second, the $g(t)$ and $G^*(\omega)$ curves are non-analytical curves and therefore integral (26) can be calculated only using approximate numerical methods.

Probably, the most efficient [235] and, at the same time, the oldest [236] is the method based on the use of the expansion of the inverse Laplace transform (1a) into a series [237]

$$H_n(\lambda) = \frac{1}{(n-1)!}\sum_{i=1}^{n}(-1)^i a_m \left.\frac{d^i g(t)}{d(\ln t)^i}\right|_{t=i\lambda}, \tag{27}$$

which is a particular case of a general relationship

$$h(\lambda) = \lim_{n\to\infty}\left[(-1)^n \frac{nt^{n-1}}{(n-1)!}\left.\frac{d^n h(t)}{dt^n}\right|_{t=n\lambda}\right].$$

The a_{ni} coefficients are calculated using the recurrent relation

$$a_{ni} = (n-1)a_{n-1,i} + a_{n-1,i-1},$$

$i \leqslant n$.

Usually, only two first terms of the series (27) are included in calculations of the relaxation spectra, therefore

$$H(\lambda) = -\left.\frac{dg(t)}{d\ln t}\right|_{t=\lambda} + \left.\frac{d^2 g(t)}{d(\ln t)^2}\right|_{t=2\lambda}. \tag{28}$$

Recently, this method was evaluated and then widely used for the characterisation of the structures and for the prediction of the properties of materials based on polyolefins in the studies by Kimel'blat *et al.*[238–242] The initial data represented the curves of the pressure drop in the cylinder of a capillary viscosimeter in the non-steady-state flow of a polymer melt through a capillary after stopping the plunger. The authors believed that the pressure drop and a parallel decrease in the shear rate were due to the mechanism proposed by Vinogradov [43,44] with allowance for a broad relaxation time spectrum due to polydispersity of the polymer.[68–71]

Thus, the calculated characteristics of the relaxation spectrum, namely, the average relaxation times $\langle\lambda\rangle_n$, $\langle\lambda\rangle_w$ and $\langle\lambda\rangle_z$ should correlate with characteristics of the MMD of the polymer. For instance, it was stated [243] that 'dispersion in the MMD and

dispersion in the relaxation spectrum go hand in hand'. Indeed, corresponding correlations were established for polyethylene and polyethylene copolymers.[242] For instance in the case of high-density polyethylene one has

$$\log M_n = 4.14 + 0{,}147 \log \langle\lambda\rangle_n$$

with the correlation coefficient $r^2 = 0.89$,

$$\lg M_w = 4.64 + 0.839 \lg \langle\lambda\rangle_w$$

with the correlation coefficient $r^2 = 0.96$ and

$$\lg M_z = 4.57 + 1.131 \lg \langle\lambda\rangle_z$$

with the correlation coefficient $r^2 = 0.92$.

Here

$$\langle\lambda\rangle_n = \frac{\int H(\lambda)\mathrm{d}\ln\lambda}{\int [H(\lambda)/\lambda]\mathrm{d}\ln\lambda}, \quad \langle\lambda\rangle_w = \frac{\int \lambda H(\lambda)\mathrm{d}\ln\lambda}{\int H(\lambda)\mathrm{d}\ln\lambda},$$

$$\langle\lambda\rangle_z = \frac{\int \lambda^2 H(\lambda)\mathrm{d}\ln\lambda}{\int \lambda H(\lambda)\mathrm{d}\ln\lambda}.$$

Correlations between characteristics of the relaxation spectrum and the topological structures of polymers are illustrated in Fig. 16 where the average relaxation times are plotted *vs.* the composition of polymer blends with different molecular masses (Fig. 16 *a*) and *vs.* the degree of cross-linking (Fig. 16 *b*).

Numerous examples of correlations between characteristic features of the relaxation spectrum and the technological and physicomechanical properties of materials based on polyolefins can be found in a monograph.[242] It is the shape analysis of the spectral curve that allowed the author of the monograph [242] to optimise the procedure of welding of high-density polyethylene pipes and predict the lifetime of such pipes. The curves of the relaxation spectra of ethylene–propylene rubbers served as criteria in evaluating the stability of the synthesis of such materials. Optimisation of the composition of thermoplastic composites and weldment are also based on analysis of specific features of the shape of the relaxation spectra. It is important that it was the relaxation spectra rather than the experimental pressure drop curves that were used as sensitive tools in the above-mentioned and similar research and development studies.

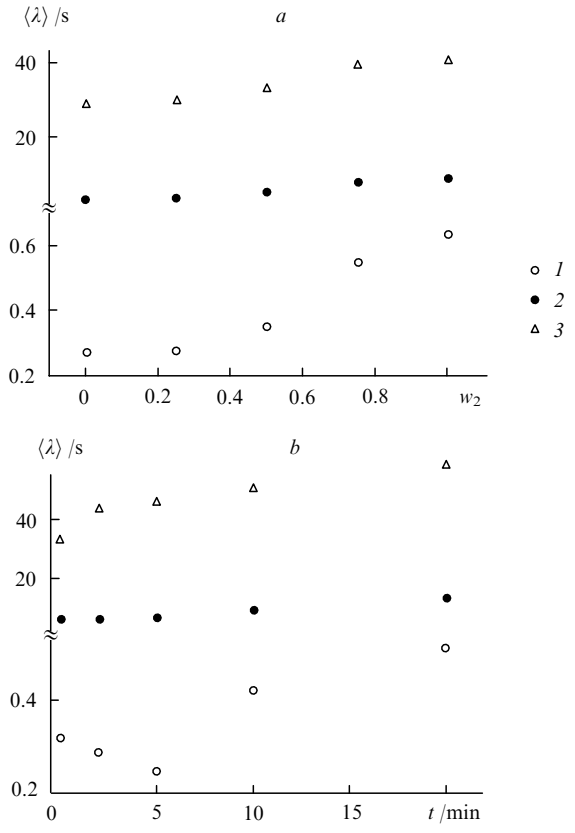


Figure 16. Average relaxation times $\langle\lambda\rangle_n$ (*1*), $\langle\lambda\rangle_w$ (*2*) and $\langle\lambda\rangle_z$ (*3*) plotted *vs.* composition of a bidisperse blend of low-density polyethylenes (LDPE) (*a*) and vulcanisation time of butyl rubber (*b*).[242]
Polymer blend: component 1 is LDPE-277 ($\bar{M}_w = 6 \times 10^4$, $\bar{M}_w/\bar{M}_n \approx 5$), component 2 is LDPE-273 ($\bar{M}_w = 2 \times 10^5$, $\bar{M}_w/\bar{M}_n \approx 15$).

c. Discrete relaxation spectrum. Regularisation methods

Methods of determination of a discrete relaxation spectrum have been analysed in detail in a review by Malkin [226] who tried to show that the determination of a relaxation spectrum in order to interpret experimental data has no physical meaning in the general case because the final result is not unique. Therefore, in comparing the properties of materials with different topological structures it is more appropriate to lean upon characteristic data points obtained in direct relaxation experiments rather than the relaxation spectrum calculated using these data, because, according to Malkin,[226] the relaxation spectrum is 'nothing more than a method of possible approximation of experimental data within the limits of measurement error, which is convenient for various applications in the framework of the theory of viscoelasticity of continuous media'. Nevertheless, numerous calculations of the relaxation spectra have been and are being reported.

Physically, an approach [244] widely used in the analysis of the free induction decay curves (see, *e.g.*, Ref. 193) seems to be the most evident. The method involves successive determination of the exponents and pre-exponents of the $\ln[g(t)]$ function at $t \to \infty$. In this case the kinetics of the decay is governed by the exponent with the longest relaxation time. Of course, such a division of the relaxation curve is quite rough and exponents with similar decay constants are indistinguishable.[212, 244] However, calculations of model functions (in particular, the Rouse relaxation curve) showed that the first three terms of the relaxation spectrum (with the longest relaxation times) can be determined quite accurately. The advantage of this approach is the possibility of estimating the maximum relaxation time. In particular, the relation $\lambda_{max} \propto M^4$ was established [230] using this procedure.

Essentially the same strategy was used in another study.[245] The orientation relaxation curve of polystyrene samples, expressed by the Legendre polynomial $P_2(t)$, was approximated by three exponents, which provided the best agreement with the experimental data. The relaxation times thus obtained were significantly different, *e.g.*, $\lambda_1 = 0.7$, $\lambda_2 = 39$ and $\lambda_3 = 1.65 \times 10^4$ s (obtained for a polymer with a molecular mass of 2.34×10^6 at a temperature, which is 20° higher than the glass transition temperature). The relaxation time λ_1 was independent of the molecular mass while the other two relaxation times were related to M as follows: $\lambda_2 \propto M^{0.5}$ and $\lambda_3 = 2\lambda_1 M^{1.6}$.

To determine a relaxation spectrum is to find the solution to a problem inverse to problem (1). To this end, the following relation is used:

$$g(t) = K[h(\lambda)](t) + \varepsilon(t),$$

where K is the operator relating the function h to the experimental data g, and $\varepsilon(t)$ is the error. Often, K is a linear operator, which corresponds to the Fredholm integral equation. Examples of linear inverse problems are provided by the analysis of experimental data obtained by NMR spectroscopy, static light scattering and results of resistor conductivity measurements. The linear rubbery state theory also includes nonlinear problems. Besides, as mentioned above (see Introduction), inevitable experimental errors complicate calculations of the relaxation spectrum using expression (1). Finally, experimental data are always available within a limited range of argument values. Taken altogether, this makes the problem of calculating the relaxation spectrum an ill-posed problem.[226, 246–248]

The case for the problem inverse to the problem described by Eqn (3) is somewhat different. Indeed, Winter showed [228] that the frequency dependence of the relaxation modulus, $G^*(\omega)$, is the best source of initial experimental data for calculating the relaxation spectra. Also, mention was made [228] that the $g(t)$ function can be determined more accurately from the same $G^*(\omega)$ dependence rather than direct measurements. Systematic and statistical errors can be corrected using the Kramers – Kronig relation

$$\frac{G'(\omega)}{\omega^2} = \frac{2}{\pi}\int_0^\infty \frac{G''(x)}{\omega^2 - x^2}\,\mathrm{d}x\,,$$

(x is the integration variable), which leads to the following equality (at $h > 0$)

$$\frac{\lambda}{1+(\omega\lambda)^2} = \frac{2}{\pi}\int_0^\infty \frac{x}{1+(x\lambda)^2}\,\frac{\mathrm{d}x}{\omega^2 - x^2}$$

for any λ.

Listed below are criteria which an algorithm for calculating a relaxation spectrum should satisfy. The choice of these criteria is an expression of personal preference rather than objective definition. The preferences of the author of Ref. 228 are as follows:

— good fit of experimental data;

— the algorithm should be able to find the optimum amount of detail which can be extracted from experimental data without producing artifacts;

— the format of the relaxation spectrum should not be predetermined; it has to be freely adjustable during the processing of the experimental data;

— the resulting parameters should have physical meaning;

— minimisation of the experimental data truncation errors;

— checking of experimental data quality is required (the data are always inconsistent to some extent, because the signal-to-noise ratios differ for G' and G''; this may cause a large discrepancy between fit and experimental data);

— the relaxation spectrum $H(\lambda)$ should be expressed by a function or a sum of functions, which can be integrated easily;

— the number of parameters of the model functions should not be large;

— the computation time should be short.

Calculations are based on the assumption that there exists a function $H(\lambda)$, which is sufficiently smooth that it can be taken as linear within small intervals $[\lambda_i^-, \lambda_i^+]$ around λ_i.

To carry out calculations with a computer, the function $g(t)$ should be discretised

$$g(t) = \int_0^\infty H(\lambda)\,\mathrm{d}\ln\lambda = \sum_{i=1}^{\infty}\int_{\lambda_{i-1}}^{\lambda_{i+1}} H(\lambda_i)\,\mathrm{d}\ln\lambda_i = \sum_{i=1}^{\infty} H(\lambda_1)\,\Delta_1,$$

where

$$\Delta_i = \frac{1}{2}\ln\frac{\lambda_{i-1}}{\lambda_{i+1}}\,.$$

The discretising frequency is given by $\omega_i = 1/\Delta_i$. The expression for $g(t)$ takes the form

$$g(t) = g_0 + \sum_{i=1}^{N} h_i \exp\left(-\frac{t}{\lambda_i}\right), \qquad (29)$$

where $h_i = H(\lambda_i)\Delta_i$.

The use of two data series (G' and G'') eliminates the problem of ill-posedness. For the same reason simultaneous use of the g modulus and compliance data leads to the same result.[249] The uniqueness of the solution to the problem is due to the fact that the g modulus and compliance are interrelated.

The key point in calculations is minimisation of an error functional

$$\frac{1}{Z}\sum_{i=1}^{Z}\left[\left(\frac{G'(\omega_i)}{\hat{G}'_i} - 1\right)^2 + \left(\frac{G''(\omega_i)}{\hat{G}''_i} - 1\right)^2\right] = \min,$$

where

$$G' = \sum_{i=1}^{N} h_i \frac{(\omega\lambda_i)^2}{1+(\omega\lambda_i)^2}\,,\quad G'' = \sum_{i=1}^{N} h_i \frac{\omega\lambda_i}{1+(\omega\lambda_i)^2}\,,$$

and $\hat{G}'_i$ and $\hat{G}''_i$ are the data measured at Z frequencies ω_i.
The parameters λ_i. h_i, N are freely adjustable during the minimisation.

Analysis showed that the results of minimisation depend on the N value, but a stable solution is reached after a reasonably short time (in this case the error functional becomes independent of N). Thus, the number of modes in the relaxation spectrum is limited by the minimum N value responsible for stability of the solution. Usually, $N \leqslant 20$.

A 'parsimonious' relaxation spectrum thus obtained is unique in the sense that different discrete sets of h_i and λ_i values lead to the same continuous function $H(\lambda)$.

Based on the results of experimental studies of polypropylene,[250] polybutadiene [56, 141, 251] and polystyrene,[141, 234] using the IRIS program (please visit a website at URL http://128.119.197/Lab/IRIS.html) it was concluded that the relaxation spectra of monodisperse polymers can be represented by two arms, a decreasing arm at $\lambda \leqslant \lambda_1$ (λ_1 corresponds to the inflection point) and an increasing arm at $\lambda \geqslant \lambda_1$

$$H(\lambda) = \begin{cases} mG_N^0\left[\left(\dfrac{\lambda}{\lambda_c}\right)^{-n_g} + \left(\dfrac{\lambda}{\lambda_{max}}\right)^{n_e}\right] \text{ at } \lambda \leqslant \lambda_{max}, \\ 0 \text{ at } \lambda > \lambda_{max}. \end{cases} \qquad (30)$$

The λ_c value is determined from the equality $H(\lambda_c) = H(\lambda_{max}) = mG_N^0$ (the subscripts 'g' and 'e' at the exponents denote 'glass' and 'elastic', respectively).

Figure 17 presents some examples of this type of relaxation spectra, which are called the BSW spectra.†

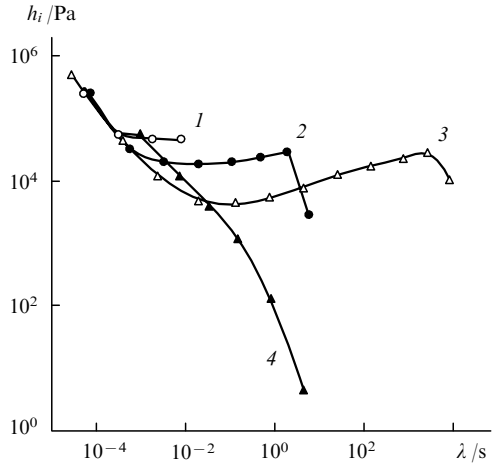


Figure 17. Continuous relaxation spectra of polystyrene [50] (*1–3*) and low-density polyethylene [263] (*4*).
$M \times 10^{-3} = 39$ (*1*), 275 (*2*) and 3000 (*3*).

Taking polybutadienes with different topological structures as examples, it was shown [251] that the BSW relaxation spectra consist of three regions, *viz*., a decreasing arm at $\lambda \leqslant \lambda_1$, an increasing arm at $\lambda_1 \leqslant \lambda \leqslant \lambda_{max}$ and an abrupt cut-off region at $\lambda > \lambda_{max}$

† BSW abbreviation is an using the first letters in the surnames of the authors of Ref. 234.

$$H(\lambda) = \left[H_g\left(\frac{\lambda}{\lambda_c}\right)^{-n_g} + n_e G_N^0\left(\frac{\lambda}{\lambda_{max}}\right)^{n_e}\right]\exp\left[-\left(\frac{\lambda}{\lambda_{max}}\right)^{\beta}\right], \qquad (31)$$

where

$$H_g = n_e G_N^0\left(\frac{\lambda}{\lambda_{max}}\right)^{n_e}\left(\frac{\lambda_1}{\lambda_c}\right)^{n_g},$$

and λ_1 is the instant at which the first two branches merge (or intersect). Usually, $n_g \approx 0.67$, $n_e \approx 0.30$ and $\beta = 2$.

It should be noted that the relaxation spectrum described by Eqn (31) does not meet the smoothness condition. At the λ_{max} point, the curve exhibits an abrupt kink. In particular, if in the double logarithmic coordinates the spectrum is sectionally linear but has abrupt wings, the method cannot be used. It was shown [252] that in this case one should use regularisation methods .

A regularisation method involves minimisation of the error function $V_\xi(\ln h)$ (see Refs 252 and 253).

$$V_\xi(\ln h) = \sum_{i=1}^{M}\frac{1}{(\sigma'_1)^2}\left[G'_\sigma(\omega_i) - \int_{-\infty}^{\infty}\frac{(\omega_i\lambda)^2}{1+(\omega_i\lambda)^2}H(\lambda)\mathrm{d}\ln\lambda\right]^2 +$$

$$+\sum_{i=1}^{M}\frac{1}{(\sigma''_1)^2}\left[G''_\sigma(\omega_i) - \int_{-\infty}^{\infty}\frac{\omega_i\lambda}{1+(\omega_i\lambda)^2}H(\lambda)\mathrm{d}\ln\lambda\right]^2 + \xi R(\ln h),$$

where σ is the standard deviation of the Gaussian error function. The regularisation term, $R(\ln h)$, imposes constraints based on the *a priori* information on the shape of the relaxation spectrum. The regularisation parameter ξ 'weights' the constraints with allowance for the *a priori* knowledge.

At present, a number of program packages ‡ (*e.g.*, NLREG,[254] GENEREG,[253] CONTIN [255] and FTIKREG [256]) developed for solving ill-posed problems by the regularisation method are available.

The assumption of smoothness means that

$$R(\ln h) = \int_{-\infty}^{\infty}\left[\frac{\mathrm{d}^2\ln h}{\mathrm{d}(\ln\lambda)^2}\right]^2\mathrm{d}\ln\lambda\,.$$

Taking into account abrupt changes in the function in the wings leads to a more general expression for R

$$R(\ln h) = \int_{-\infty}^{\infty}\frac{[\mathrm{d}^2\ln h/\mathrm{d}(\ln\lambda)^2]^2}{\sqrt{1+[\alpha\mathrm{d}^2\ln h/\mathrm{d}(\ln\lambda)^2]^2}}\mathrm{d}\ln\lambda\ ,\ \alpha \geqslant 0.$$

The problem thus formulated was solved [252] using the Edge Preserving Regularisation (EPR) and Edge Preserving Nonlinear Regularisation (EPNREG) programs. The approach considered here can be employed if there are reasons to assume that the relaxation spectrum is smooth except for the inflection points in the λ_1 and λ_{max} regions (at 10^{-4} and 10^0 s, respectively). A decrease in the long-time region was reported [154] to be a linear function in the double logarithmic coordinates (slope is ~ -10). It should be noted that both the EPR and IRIS calculations give nearly identical results in the region $\lambda \leqslant \lambda_{max}$.

In essence, the criterion for uniqueness of solution formulated by Winter [228] means that the set of relaxation times is insignificant for the determination of a continuous relaxation spectrum. Therefore, a relaxation spectrum can be determined as a solution of the 'semi-inverse' problem (*i.e.*, a problem with a prescribed set of relaxation times). It is this solution that was proposed in Refs 257 and 258.

‡ These programs are available on the Internet at URLs http://www.itp.ac.cn/english/itpnet/cpcindex/cpcindex.html and http://cpc.cs.qub.ac.uk/simmaries/ADOQ.

Liu [257] reported a mathematical approach to the determination of a discrete relaxation spectrum from the temporal dependence of the relaxation modulus or creep compliance. The method is based on approximation theory.[259] According to Liu, 'discrete relaxation and retardation times do not necessarily have any physical meaning since the continuous relaxation modulus and creep compliance can be approximated arbitrarily closely by discrete variables with different sets of relaxation and retardation times'. Starting from this point, Liu experimented with the following sets of relaxation times: $\lambda_k = \lambda/k$, $\lambda_k = \lambda/k^2$, $\lambda_k = \lambda/\rho^k$ (k is the mode number and ρ is an empirical constant). The function was minimised using the non-negative least squares method and the MATLAB software package,

$$F(g_0, g_1, ..., g_n) = \sum_{i=1}^{m} w_i[G^*(t_i, n) - G(t_i)]^2\,,$$

where $F(G_0, G_1, ..., G_n) = \min F(g_0, g_1, ..., g_n)$ at $g_0, g_1, ..., g_n \geqslant 0$, $w_1, w_2, ..., w_m$ are non-negative weights,

$$G^*(t, n) = g_0 + \sum_{j=1}^{n} g_j e^{-t/\lambda_j}.$$

Yet another set of relaxation times is given by:[258]

$$\lambda_i = \lambda_{min}\left(\frac{\lambda_{max}}{\lambda_{min}}\right)^{(i-1)/(N-1)},$$

where i is the mode number and N is the limiting number of modes.

Then, the function $\|\vec{K}\vec{h} - \vec{G}\|$ was minimised by the least squares method with a constraint $\vec{h} \geqslant 0$.

$$\vec{K}_{i,j} = \frac{(\omega_i\lambda_j)^2}{1+(\omega_i\lambda_j)^2},\ i = 1, ..., m; j = 1, ..., N,$$

$$\vec{h} = \{h_j\},$$

$$G'_i = h'_i(\omega_i),\ i = 1, ..., m,$$

$$G''_i = h''_i(\omega_i),\ i = m+1, ..., 2m,$$

$$m \geqslant N.$$

Experimental data on the frequency dependence of the relaxation modulus $G^*(\omega)$ of poly(dimethylsiloxane) were used as the input data. The relaxation spectrum thus determined was used for calculating the viscosity η_0 and compliance J_e^0 as follows

$$\eta_0 = \sum_{i=1}^{N} h_i\lambda_i\,, \qquad J_e^0 = \frac{1}{\eta_0^2}\sum_{i=1}^{N} h_i\lambda_i^2\,.$$

The results obtained were in good agreement with experimental data,

$$\eta_0 = \frac{G'(\omega)}{\omega},\ \ \omega \to 0\,;\ \ J_e^0 = \frac{G''(\omega)}{[G'(\omega)]^2},\ \ \omega \to 0.$$

An interesting method of calculation of a relaxation spectrum was proposed by Davies and Anderssen.[260, 261] The relaxation spectrum $h(\lambda)$ was related to

$$g_{ab} = \int_a^b h(\lambda)\mathrm{d}\lambda = \int_{\ln a}^{\ln b} H(\lambda)\mathrm{d}\ln\lambda\,.$$

A narrow frequency range [ab] was divided into a small odd ($2L-1$, $L = 2, 3, 4$) number of intervals and centred on an experimental frequency range, which in turn was divided into k discrete frequencies $\omega_k = \omega_0\exp(kr)$. Usually, one had $\omega_0 = 10^{-3}-10^{-2}$ and $r = \pi/(2L-1)$. The expressions for the relaxation modulus components were as follows

$$g'_j = -\frac{1}{2}\int_{\ln\omega_{j-1}-\pi/2}^{\ln\omega_{j+1}+\pi/2}\left[E''\left(\ln\frac{\omega}{\omega_j}+r\right)-E''\left(\ln\frac{\omega}{\omega_j}-r\right)\right]G'(\omega)\mathrm{d}\ln\omega\,,$$

$$g''_j = -\frac{1}{2}\int_{\ln\omega_{j-1}-\pi/2}^{\ln\omega_{j+1}+\pi/2}\left[E'\left(\ln\frac{\omega}{\omega_j}+r\right)-E'\left(\ln\frac{\omega}{\omega_j}-r\right)\right]G''(\omega)\mathrm{d}\ln\omega\,,$$

$$E'(x) = E'_\varepsilon(x), \quad E''(x) = E''_\varepsilon(x), \quad \varepsilon\to 0\,,$$

$$E^*_\varepsilon(x) = E'_\varepsilon(x) + \mathrm{i}E''_\varepsilon(x) = \frac{1}{\pi}\mathrm{erf}\left(\frac{x+\pi\mathrm{i}/2}{\sqrt{2\varepsilon}}\right), \quad \varepsilon>0\,.$$

As can be seen, this method also does not require a search for discrete relaxation times; it involves calculations of the function $h(\lambda_i)$ for a set of relaxation times λ_i.

Among the key sources of ill-posedness of the problem of determination of a discrete relaxation spectrum is that the function being minimised is linear with respect to $h(\lambda)$ and nonlinear with respect to λ. A method [262] of linearisation of functions involves transformation of the components of the complex modulus into new functions U_n and V_n using the polynomial P_n

$$U_n(\omega)^2 = G'(\omega)\prod_{i=1}^{n}(1+\lambda_i^2\omega^2) = \sum_{i=1}^{n}u_i(\omega^2)^i\,,$$

$$V_n(\omega)^2 = \omega G''(\omega)\prod_{i=1}^{n}(1+\lambda_i^2\omega^2) = \sum_{i=1}^{n}v_i(\omega^2)^i\,,$$

$$P_n(\omega)^2 = \prod_{i=1}^{n}(1+\lambda_i^2\omega^2) = \sum_{i=1}^{n}p_i(\omega^2)^i\,.$$

Now we have a linear problem, *viz*., search for the coefficients p_i and u_i or p_i and v_i, which can be solved using the least squares method. Each pair of these coefficients is in mutually unique correspondence with the pair λ_i and $h(\lambda_i)$, which is given by a system of simple algebraic equations.

Applicability of this linearisation technique was demonstrated by comparing an artificially constructed relaxation spectrum with a relaxation spectrum calculated from the corresponding relaxation function. Besides, calculations of the relaxation spectrum from G' and G'' (polystyrene, 179 °C) gave almost coinciding results (Fig. 18).

Finally, Jensen [263] reported determination of a relaxation spectrum using a version of the Monte Carlo method called 'simulating annealing'.§ The technique involves the generation of trial values of h_i and λ_i and the search for a global minimum of the error function. The method imposes no constraints on the relaxation spectrum and does not require smoothness or even continuity. A drawback of the technique is a rather long computation time (in some cases more than 10^6 functions should be calculated in order to reach a global minimum). Similarly to the study by Winter [228], the number of modes was limited to avoid fitting of noise, so the so-called 'parsimonious' relaxation spectrum was determined. The number of modes was chosen to be equal to that at which the dependence of the minimum value on the number of modes reached a plateau.

The relaxation spectrum of low-density polyethylene calculated using this technique is presented in Table 10.

§ The program is available at the website http://www.netlib.org.

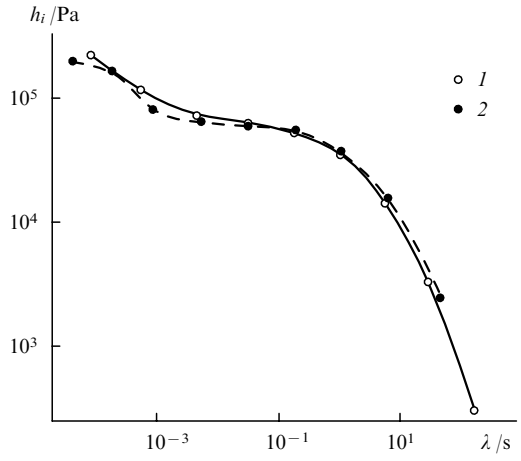


Figure 18. Relaxation spectra of polystyrene calculated from G' (*1*) and G'' (*2*).[262]

Table 10. Relaxation spectrum of low-density polyethylene at 150 °C.[263]

k	λ_k /s	h_k /Pa	k	λ_k /s	h_k /Pa
1	4.22690885	8.6331	4	0.03429959	7770.0291
2	0.90131057	270.2802	5	0.00724564	23416.7956
3	0.15323119	2296.5292	6	0.00089831	111882.6500

The relaxation spectrum was also calculated [103] from dielectric relaxation data using the 'false position' algorithm. The method involves a comparison of experimental dependence (in this case the spectrum of dielectric loss ε'') with a calculated dependence obtained using an arbitrary distribution function. The distribution function is refined by taking into account the error obtained and the iterative procedure is repeated until coincidence of the calculated and experimental data. Of course, the method requires *a priori* knowledge of the form of the distribution function; otherwise, a problem of uniqueness of the results obtained is posed.

Except for the authors of Refs 262 and 263, researchers are inclined to believe that only a continuous relaxation spectrum has physical meaning. In this case the relaxation spectrum can serve for characterisation of both the topological structure and the specific features of macromolecular dynamics. Discretisation can be arbitrary, being no more than a trick for computations. But here, first, it remains unclear how this inference can be related to the results of calculations of the models, which either directly or indirectly lead to the concept of a discrete relaxation spectrum. Second, a comparison of the continuous relaxation spectra shown in Figs 17 and 18 reveals ambiguity in the results of calculations. Therefore, one has to conclude that attempts at calculating a discrete relaxation spectrum (at least most of those considered above) failed.

Unfortunately, it is impossible to put forward a criterion for 'correctness' of a relaxation spectrum, because it can be determined if the condition for coincidence of the calculated and experimental data for $g(t)$ or $G^*(\omega)$ with certain accuracy is met. This inevitably means fulfillment of rheological characteristics, because the stress tensor components σ_{ij} are related to the relaxation function $g(t)$ (see Ref. 4)

$$\sigma_{12} = \sigma_{21} = \dot\gamma\int_0^t g(t-t_1)\mathrm{d}t_1,$$

$$\sigma_{11} - \sigma_{22} = 2\dot{\gamma}^2 \int_0^t (t - t_1) \cdot g(t - t_1) \mathrm{d}t_1,$$

where $\dot{\gamma}$ is the shear rate.

We believe that discussion of relaxation spectrum calculations concerns in fact two independent problems. One of them is concerned with the physical correctness of the mathematical models describing interrelations between viscoelastic characteristics and based on the concept of a relaxation spectrum. The other problem is to develop a corresponding mathematically correct formalism. Of course, it is irrational to criticise and reject a convenient fundamental concept of the relaxation spectrum on the basis of non-reliable results of spectrum reconstruction obtained in the framework of (mathematically) unstable models. Therefore, in the text below we will consider a stable method of calculation of a relaxation spectrum.

3. Stable method of calculation of a relaxation spectrum. The relaxation times distribution function

An approach [264, 265] to the representation of a relaxation spectrum using the distribution functions [266] and Stieltjes integral [267] provides an alternative to the methods considered above. Let $P(\lambda)$ denote the integrated intensity of a relaxation spectrum. Then, the functions $g(t)$ and $G(\omega)$ can be expressed *via* the Stieltjes integral with respect to $P(\lambda)$

$$g(t) = \int_0^\infty \exp\left(-\frac{t}{\lambda}\right) \mathrm{d}P(\lambda) , \tag{32}$$

$$G(\omega) = \int_0^\infty \frac{\mathrm{i}\omega\lambda}{1 + \mathrm{i}\omega\lambda} \mathrm{d}P(\lambda) . \tag{33}$$

A discrete relaxation spectrum corresponds to a step distribution function

$$P(\lambda) = \sum_{k=1}^{N} h_k \chi(\lambda - \lambda_k) , \tag{34}$$

where χ is the Heaviside step function. A continuous relaxation spectrum corresponds to the distribution function given by

$$P(\lambda) = \int_0^\lambda h(\xi) \mathrm{d}\xi \tag{35}$$

(ξ is the integration variable), *i.e.*, $P(\lambda)$ is an antiderivative of the density $h(\lambda)$.

The problem of uniqueness of the function $P(\lambda)$ and stability of $P(\lambda)$ to perturbations in $g(t)$ and $G^*(\omega)$ has been studied.[265] In constructing $P(\lambda)$ from the kinetic function $g(t)$ (the procedure for relaxation spectrum reconstruction in the frequency domain differs insignificantly) it was shown that uniqueness of $P(\lambda)$ follows from one-to-one reversibility of the Laplace transform. The notion of stability was formulated in terms of the weak convergence of monotonic functions in the positive semiaxis R_+ as the following continuity principle.[267, 268]

Let $g_n, P_n (n = 1, 2, ...), g, P$ be a sequence of kinetic curves and corresponding distribution functions. Then convergence $g_n(t) \to g(t)$ at any $0 \leqslant t < \infty$ is equivalent to weak convergence $P_n \Rightarrow P$ in R_+.

This statement was proved [265] by combining the Helly selection principle for a converging subsequence of monotonic functions and the property of uniqueness.

The properties of uniqueness and continuity mean that a problem inverse to problem (35) with respect to $P(\lambda)$ rather than $h(\lambda)$ is well-posed and solution to this problem does not require application of a regularisation technique.

The development of a method of stable reconstruction of $P(\lambda)$ from approximate values of the kinetic and frequency moduli required introduction of the notion of a generalised solution as a solution to the problem of error functional minimisation. In the simplest case (quadratic functional) the procedure involves solution of the following problems

$$\int_T v(t) \left[\int_0^\infty \exp\left(-\frac{t}{\lambda}\right) \mathrm{d}P(\lambda) - g(t) \right]^2 \mathrm{d}t \to \min , \tag{36}$$

$$\int_\Omega \mu(\omega) \left[\int_0^\infty \frac{\mathrm{i}\omega\lambda}{1 + \mathrm{i}\omega\lambda} \mathrm{d}P(\lambda) - G(\omega) \right]^2 \mathrm{d}\omega \to \min , \tag{37}$$

where $v(t)$ and $\mu(\omega)$ are some non-negative weighting functions, which determine the error functional, and T and Ω are respectively the domains in which the experimentally measured $g(t)$ and $G(\omega)$ functions are defined. The search for a minimum is carried out in the class of all distribution functions.

A solution $P(\lambda)$ to problems (36) and (37) is called an optimum integral representation (OIR) of the corresponding functions of the kinetic or frequency moduli. In setting these problems it is possible to impose, without significant complication, various constraints that allow for the *a priori* information on the relaxation spectrum. The choice of the weighting functions is free, being governed by the *a priori* knowledge of the distribution of experimental errors. For instance, it is appropriate to use the coefficients $v(t)$ and $\mu(\omega)$ for relatively narrow (2–3 decades) ranges of changes in t and ω, respectively. The choice of the $v(t) = t^{-1}$ and $\mu(\omega) = \omega^{-1}$ weighting functions provides a logarithmically uniform error functional, which can naturally be used in treatment of data characterised by a broad range of changes in t, ω (more than four decades). The properties of existence, uniqueness and stability of OIR have been proved.[264] It was found that the overstability is unexpectedly high, namely, the OIR is stable to both integrally small errors of the functions $g(t)$ and $G(\omega)$ and to white noise of finite amplitude superimposed on these functions. All the results are also valid for a more general combined error functional, which permits reconstruction of $P(\lambda)$ from the real and imaginary components of $G(\omega)$ or from their combination.

Numerical implementation of this method requires a finite set of measuring times $\{t_j\}, j = 1, ..., n$. When a continuous problem is discretised by introducing a grid with a fixed arrangement of nodes $\{\lambda_i\}$, $i = 1, ..., m$, the desired distribution function is approximated by the step function

$$P(\lambda) = \sum_{i=1}^{m} h_i \chi(\lambda - \lambda_i) , \tag{38}$$

where $h = \{h_i\}$, $i = 1, ..., m$ is the set of unknown non-negative coefficients. Application of some linear quadrature formulae to the outer integrals in expressions (36) and (37) gives the following discrete analogues, respectively

$$\sum_{j=1}^{n} v_j \left[\sum_{k=1}^{m} \exp\left(-\frac{t_j}{\lambda_k}\right) h_k - g(t_j) \right]^2 \to \min, \ h \geqslant 0, \tag{39}$$

$$\sum_{j=1}^{n} \mu_j \left[\sum_{k=1}^{m} \frac{\mathrm{i}\omega_j\lambda_k}{1 + \mathrm{i}\omega_j\lambda_k} h_k - G(\omega_j) \right]^2 \to \min, \ h \geqslant 0. \tag{40}$$

Here v_j, μ_j is a set of positive weighting coefficients determined by the totalities of the nodes $\{t_j\}$ and $\{\omega_j\}$. These coefficients are included in the quadrature scheme. For instance, constant weighting coefficients are obtained when the rectangle formula is applied to uniformly distributed nodes at $v(t) = 1$, $\mu(\omega) = 1$ or to logarithmically uniformly distributed nodes at $v(t) = t^{-1}$, $\mu(\omega) = \omega^{-1}$.

Problems (39) and (40) are solved by the quadratic programming technique using some efficient finite-step algorithms incorporated into standard mathematical software (MAPLE, MATLAB) and FORTRAN libraries (IMSL, CXML), including the non-negative least squares method algorithm NNLS.[269] Some

difficulties in numerical solution can arise from the high dimensions of these problems (m and n can be of the order of several hundreds); good approximation of initial continuous problems (36) and (37) by discrete analogues requires about 10 to 30 nodes (t_j, ω_j, λ_k) per decade of corresponding range.

When a relaxation spectrum is reconstructed from model and experimental data, the experimental and calculated grid patterns have no effect on the quality of the solution, only the node density is significant. Different grid patterns require calculations of different sets of weights. The resulting antiderivative step distribution function $P(\lambda)$ coincides with an accuracy determined by the grid densities and errors in $g(t)$ and $G(\omega)$. Non-uniqueness of the solution (this is possible at $m > n$) is of no concern because any set of the parameters h, at which minima of expressions (39) and (40) are reached, gives an equivalent approximation of the relaxation spectrum distribution.

Because the relaxation spectrum distribution functions reconstructed by this method are only stable in a specific 'weak' sense, it is appropriate to mention those characteristics of the relaxation spectrum that are related to this kind of stability. By definition of weak continuity, stable are linear integral average distribution functions of the type

$$\int_{R_+} f(\lambda)\mathrm{d}P(\lambda)\,,$$

where $f(\lambda)$ is some continuous averaging function. A particular case of averaging is provided by the moments for which $f(\lambda) = \lambda^n$. The plot of the distribution function is stable in the sense mentioned above, namely, as 'entire geometric figure'. On the contrary, local numerical characteristics, in particular, the density $h(\lambda) = \mathrm{d}P(\lambda)/\mathrm{d}\lambda$, are unstable. Conversion of a discrete relaxation spectrum into the density function by direct interpolation of a comb-like plot of δ-functions does not lead to 'weak stability', as was postulated by Winter.[141] A correct smoothing of arbitrary, in particular, discrete relaxation spectra requires an integral averaging over one or another kernel.

The working efficiency of this method was exemplified [265] by reconstructing the relaxation spectrum of an oligomeric nonuniform Rouse chain,[214, 215] a continuous BSW-spectrum [141] and the frequency modulus of polystyrene from experimental data.[234]

A model example of relaxation spectrum reconstruction from the relaxation kinetics of the length of an equidistant chain containing $n = 6$ nonuniform units involved calculations of the frequency dependence of the relaxation modulus $G^*(\omega)$ using relationship (2). Noise produced by a software generator of evenly distributed random numbers was applied at the calculated (t, ω) nodes, the noise intensity, ε, being equal to 10^{-2} and 10^{-3} of the corresponding amplitude. The calculated h_i and λ_i coefficients and the corresponding moments

$$\mu_k = \int \lambda^k \mathrm{d}P(\lambda)$$

for $k = 0, 1, 2$ are listed in Table 11. Simulation of experimental data was carried out using $n = 300$ logarithmically uniform time values and frequencies in the ranges $t \in [10^{-4}$ and $10^3]$ $\omega \in [10^{-1}, 10^5]$, respectively, and the spectrum reconstruction was performed following the scheme given by expressions (39) and (40) on a logarithmically uniform grid containing $m = 400$ nodes in the range $\lambda \in [10^{-2}, 10^2]$.

Analysis of the data listed in Table 11 showed that the relaxation spectrum reconstructed from G is more similar to the exact spectrum than the relaxation spectrum reconstructed from the g data. As noise (ε value) decreases, the accuracy of the calculations increase. Although the calculated relaxation spectrum is somewhat different from the theoretical spectrum, in all cases the moments coincide excellently.

Yet another example involved the relaxation spectrum reconstruction from the frequency-dependent stress relaxation modulus determined in a series of experiments.[234] Data for monodisperse polystyrene with $M = 3 \times 10^6$ were analysed using a complex data array ($n = 44$). Calculations following scheme (40) involved a logarithmically uniform grid with $m = 400$ in the range $\lambda \in [10^{-5}, 10^4]$.

A discrete relaxation spectrum reconstructed using the OIR technique is shown in Fig. 19. Experimental data were fitted to the theoretical curve $G(\omega)$ calculated after reconstruction with a quadratic error of about 1% (see Fig. 19 *a*). In Fig. 19 the OIR and IRIS reconstructed plots are superimposed. The errors in the approximation of the frequency-dependent relaxation moduli in both reconstructed relaxation spectra are similar (with respect to the order of magnitude), but the error of the OIR method is 'random' while the plot of the error of the IRIS procedure clearly exhibits systematic 'waves' (see Fig. 19 *b*). The plots of the distribution functions in Fig. 19 *d* are parallel in the range $\lambda \in [10^{-4}, 10^1]$. In this case a parallel shift of the distribution functions owing to initial jumps indicates a significant discrepancy between the reconstructions, which is due to insufficient width of the data window in the high-frequency region.

Thus, in the intermediate range the OIR and IRIS reconstructed relaxation spectra are similar in terms of the distribution functions, although the parameters of individual lines are appreciably different (see Fig. 19 *c*).

Table 11. Parameters of the relaxation spectrum of a modified Rouse chain calculated using the OIR technique (λ in arbitrary units).

Exact spectrum [a]		$\varepsilon = 0.01$				$\varepsilon = 0.001$			
		reconstructed from $g(t)$ [b]		reconstructed from $G(\omega)$ [c]		reconstructed from $g(t)$ [d]		reconstructed from $G(\omega)$ [e]	
λ	$h(\lambda)$	λ	$h(\lambda)$	λ	$h(\lambda)$	λ	$h(\lambda)$	λ	$h(\lambda)$
0.5586×10^0	0.2287×10^{-1}	0.4281×10^{-1}	0.5865×10^{-3}	0.5813×10^0	0.2637×10^{-1}	0.1000×10^{-1}	0.8093×10^{-4}	0.6088×10^0	0.1699×10^{-1}
0.1068×10^1	0.1409×10^{-1}	0.9439×10^0	0.1910×10^{-1}	0.5949×10^0	0.1432×10^{-2}	0.5813×10^0	0.7610×10^{-2}	0.6230×10^0	0.1268×10^{-1}
0.1671×10^1	0.3533×10^{-1}	0.9660×10^0	0.4656×10^{-1}	0.1643×10^1	0.1376×10^{-1}	0.5949×10^0	0.1872×10^{-1}	0.1568×10^1	0.6310×10^{-3}
0.3165×10^1	0.9069×10^{-2}	0.1760×10^1	0.1874×10^{-2}	0.1681×10^1	0.3862×10^{-1}	0.1464×10^1	0.8293×10^{-2}	0.1605×10^1	0.3941×10^{-1}
0.1087×10^2	0.4186×10^0	0.1041×10^2	0.4172×10^0	0.1065×10^2	0.1047×10^{-1}	0.1498×10^1	0.3593×10^{-1}	0.2547×10^1	0.9668×10^{-2}
		0.1066×10^2	0.1067×10^{-1}	0.1090×10^2	0.4086×10^0	0.3360×10^1	0.1036×10^{-1}	0.2606×10^1	0.9614×10^{-3}
		0.1000×10^3	0.3831×10^{-2}	0.1000×10^3	0.1176×10^{-2}	0.3438×10^1	0.7915×10^{-3}	0.1065×10^2	0.8226×10^{-1}
						0.1066×10^2	0.5521×10^{-1}	0.1090×10^2	0.3374×10^0
						0.1090×10^2	0.3630×10^0	0.8910×10^2	0.7645×10^{-6}
								0.9118×10^2	0.3044×10^{-4}

[a] $\mu_0 = 0.5$, $\mu_1 = 4.666$, $\mu_2 = 49.67$; [b] $\mu_0 = 0.4998$, $\mu_1 = 4.907$, $\mu_2 = 84.82$; [c] $\mu_0 = 0.5004$, $\mu_1 = 4.788$, $\mu_2 = 61.69$; [d] $\mu_0 = 0.5$, $\mu_1 = 4.665$, $\mu_2 = 49.66$; [e] $\mu_0 = 0.5$, $\mu_1 = 4.668$, $\mu_2 = 49.9$.

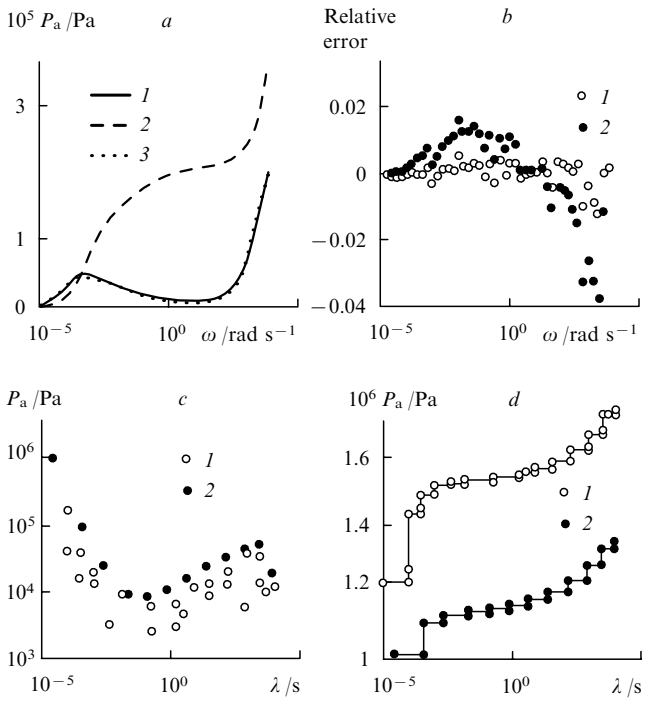


Figure 19. Relaxation spectrum of monodisperse polystyrene with $M = 3 \times 10^6$ reconstructed from the complex frequency modulus $G(\omega)$ using the data taken from Ref. 50.
(*a*) Experimental $G'(\omega)$, $G''(\omega)$ curves (*1*) and the corresponding calculated curves (*2*, *3*); (*b*) relative errors in approximation $G'(\omega)$: error in OIR reconstruction (*1*), error in IRIS reconstruction (*2*); (*c*) reconstructed discrete relaxation spectrum: the OIR spectrum (*1*) and the IRIS spectrum (*2*); (*d*) distribution functions of reconstructed discrete relaxation spectra: the OIR spectrum (*1*) and the IRIS spectrum (*2*) (data were taken from Ref. 265).

The Stieltjes OIR theory provides an explanation for similarity of integral characteristics of seemingly distinct results obtained using different versions of relaxation spectrum reconstructions. Consistency occurs if these results are quite well approximated by experimental data and meet the condition of belonging to a 'convex local weakly compact set', which can be separated out by, *e.g.*, a simple non-negativity condition. In accord with the OIR theory in this case the relaxation spectrum will be similar to the exact spectrum in terms of distribution functions, irrespective of the procedure employed to obtain the spectrum.

It should also be noted that representation of the relaxation spectrum in the form of integral distribution function $P(\lambda)$ eliminates the problem of non-uniqueness of such a representation. Examples given in Ref. 265 show that seemingly different relaxation spectra give almost the same function $P(\lambda)$. Probably, this is the reason why experimental data are 'insensitive' to the local shape of the relaxation spectrum, as was shown in many studies and summarised in a review.[226]

The OIR technique makes it possible to determine stable values of the moments (as well as any integral characteristic) of a relaxation spectrum. Local characteristics of the relaxation spectrum, in particular, the limiting relaxation times, are unstable and of little informativity. Therefore, the dependence of the maximum relaxation time on the procedure for relaxation spectrum reconstruction [226, 229] is insignificant because the relaxation properties are determined by the distribution moments, which are highly stable characteristics.

At the same time this mathematical approach allows experimental methods of determination of relaxation spectra of polymers to be divided into methods producing artifacts and those providing rational results. Formally, the problem of minimisation of an error functional on the class of monotonic distribution functions always has a unique solution, *i.e.*, the OIR. By definition the resulting spectrum provides the best plausible explanation for experimental data when using a linear model with a non-negative relaxation spectrum, which has a physical meaning and is related to the polymer structure. But in linear theory one can face a problem of sign-alternating expansion of the viscoelastic functions in terms of exponential modes. This is indicated by the impossibility of correctly (with an accuracy to noise) reproducing the experimental dependences, $g(t)$ and $G(\omega)$, using the OIR found. For instance, if in the chain retraction problem considered above the initial state of the chain is not equidistant, it is impossible to obtain a non-negative relaxation spectrum reproducing the model relaxation because some pre-exponents in expression (1) are negative. This shows that determination of a relaxation spectrum as a characteristic of the polymer structure requires a particular experimental design.[225] It is known that relaxation of a Rouse chain under stress and strain gives somewhat different relaxation spectra (see Ref. 33 and Fig. 10). Apparently, this is due to the fact that the polymer structure manifests itself indirectly if the entire chain moves (therefore the relaxation spectrum depends on the character of chain motion). This is clearly seen when comparing the Rouse and Doi – Edwards models.[33]

Thus, the problem of reconstruction of a monotonic relaxation time distribution function from the kinetic curve or frequency modulus is mathematically correct. But it should be interpreted in the framework of the OIR method rather than traditional methods for fitting a set of parameters of a point spectrum or as a solution of an integral equation of the first kind with respect to the density function of a continuous spectrum.

Summing up, the method [264, 265] of calculation of relaxation spectra is characterised by the following features.

The accuracies of reconstruction of the relaxation spectrum distribution function and any integral average characteristics of this distribution function are only limited by the systematic error and the 'density' of experimental data.

Theoretically, the OIR technique allows a relaxation spectrum to be reconstructed with arbitrary accuracy from a set of kinetic or frequency data obtained in any range. However, when narrowing such ranges, one should significantly improve the accuracy of data and the size of the data array.

Reliable reconstruction of the relaxation spectrum requires that the experimental data window be wider than the interval in which the relaxation spectrum is located (by 1 – 2 orders of magnitude for the 'kinetic' reconstruction and by 3 – 4 orders of magnitude for the 'frequency' reconstruction). Otherwise the distribution function can be determined with an accuracy of the initial jump, the local structure of which is not informative, and the accuracy of determination of moments decreases abruptly.

Statements that the relaxation spectrum is a fiction are senseless, because they are based on mathematically incorrect formalisms for both discrete and continuous descriptions. Of course, stable OIR mathematical formalism for reconstruction of relaxation spectra from the data of dynamical experiments does not mean that the relaxation spectrum is a physical reality. However, this approach makes revision of the results of relaxation experiments on the basis of stable interpretation of the relaxation spectrum in terms of distribution functions, aimed at establishing the applicability range of the notion of a relaxation spectrum as a fundamental characteristic and its relation to the polymer structure, promising and topical.

4. Manifestation of topological structure in relaxation spectra

Interrelations between the relaxation behaviour and topological structure of polymers have been well documented (see Section III). However, information on immediate relations between the relaxation spectrum and parameters of topological structure is scarce. The reason is quite understandable, that is, ambiguity of calcu-

lations (see Section IV.2). Nevertheless, a little body of data are available.

First of all mention may be made of the studies of the BSW spectra and of the studies carried out by Winter *et al.*[57, 83, 138–141, 152, 172, 228, 234, 250, 251, 270]

The dependence of the characters of the BSW spectra on the molecular masses of the monodisperse polymers [see relationship (31) and Fig. 17] is determined by two parameters, λ_{max} and λ_1. The former parameter is related to M by a conventional expression

$$\lambda_{max} = KM^a,$$

or, according to Ref. 56,

$$\lambda_{max} = \lambda_c \left(\frac{M}{M_c}\right)^a.$$

The λ_{max}/λ_c ratio determines the extension of the rubbery plateau zone, the physical meaning of M_c is similar to that of M_e. Correspondingly, λ_1 is defined by

$$\lambda_1 = \lambda_c \left(\frac{M}{M_c}\right)^{an_e/(n_c+n_g)}.$$

The numerical values of the parameters of the BSW spectra of polystyrene and polybutadiene listed in Table 12 were taken from Refs 57 and 83.

Table 12. Numerical values of parameters of the BSW spectra of polystyrene and polybutadiene.

Parameter	Polystyrene	Polybutadiene
G_N^0 /Pa	2.28×10^5	1.65×10^6
n_e	0.23	0.23
n_g	0.67	0.73
λ_c /s	2×10^{-4}	4.04×10^{-7}
M_c	1.66×10^4	2.714×10^3
a	3.43	3.52
T /°C	180	28

Based on the results of studies of monodisperse polystyrene/monodisperse polybutadiene binary blends,[83, 234] it was concluded that the resulting relaxation spectrum can be expressed as follows

$$H(\lambda) = \sum_i B_i H_i \left(\frac{\lambda}{A_i}\right),$$

where

$$\sum_i B_i = 1,\ B_2 = w_2^2 + aw_1w_2,\ a \approx 0.1,$$

if the molecular masses of the components differ insignificantly and w_i is the mass proportion of the fraction. The A_i coefficients weakly depend on the blend composition. They are related to the molecular masses of the components, namely, $A_i = \lambda_{max,i,b}/\lambda_{max,i}$ is the ratio of the maximum relaxation times of the blend component and of the homopolymer.

Clearly, this ratio is inconsistent with the postulated[34, 271] additivity with respect to relaxation times.

However, it should be noted that the relaxation spectrum of a blend, calculated by the EPR method,[252] has little in common with the BSW spectrum, although for monodisperse polymers both methods, EPR and IRIS, give identical relaxation spectra (see above).

When establishing relations between the relaxation properties and MMD of polymers, the dependences of relaxation times on the molecular mass are often considered. If the case in point is the dependence of λ_{max} or any other average characteristic (*e.g.*, $\langle\lambda\rangle_w$) on the molecular mass of the type $\lambda_{max} \sim M^a$, this is quite understandable. But some authors (see, *e.g.*, Refs 104, 258, 271–273) assume this dependence for each relaxation time in the relaxation spectrum and simply use the function $h(M^a)$ instead of $h(\lambda)$. It can be shown with ease, taking, *e.g.*, the Rouse relaxation spectrum as a simple example, that this replacement is incorrect because a change in the chain length first of all leads to a change in the number of modes.

Studies of star-branched polymers[251] revealed a much more complicated form of the BSW spectrum compared to the spectrum described by the equation of the type (31). Namely, it was found that expression (31) should be augmented with the following term

$$n_0 G_0 \left(\frac{\lambda}{\lambda_0}\right)^{n_0} \exp\left(\frac{\lambda}{\lambda_0}\right)^{\beta}.$$

The relaxation parameters of the (thus) modified BSW spectra of various star-branched polybutadienes of regular structure are listed in Table 13. Within the limits of experimental error, the parameters G_N^0, H_g and λ_c can be considered independent of the molecular mass and the number of arms, whereas the parameters G_0, λ_{max} and λ_1 seem to be stronger dependent on the molecular mass rather than the number of arms. The λ_0 parameter is affected by both structural characteristics. The authors of Ref. 251 believed that these results are consistent with theoretical concepts.[274, 275] However, the available data are insufficient for making quantitative estimates.

Analysis of the relaxation spectra calculated by the OIR technique is also based on a very small amount of data[276, 277] because the problem, as applied to polymers, was formulated only recently.[264, 265]

Figure 20 presents the relaxation spectra of polymers in terms of the integral distribution functions, which were reconstructed using the OIR technique and the data taken from Ref. 50. In this connection a problem is posed by the methods for comparison and, hence, quantitative characterisation of distribution func-

Table 13. Numerical values of parameters of the relaxation spectra of star-branched polybutadienes (for all polymers, $n_g = 0.67$, $n_e = 0.30$ and β lies between 0.8 and 1).[251]

Number of arms	$10^{-3} M_a$	G_N^0 /MPa	λ_c /s	$10^{-4} \lambda_{max}$ /s	λ_1 /s	H_g /MPa	$10^3 G_0$ /MPa	$10^{-6} \lambda_0$ /s
Linear polybutadiene	155	1.65	0.86	90	40.5	0.49	–	–
4	11.25	2.19	0.55	0.4	8.61	0.66	–	–
62	6.3	2.51	0.37	0.015	2.38	0.75	6.08	0.0065
64	23.9	2.00	0.53	0.75	10.2	0.59	17.8	0.55
124	6.8	2.51	0.37	0.015	2.38	0.75	6.08	0.0305
125	13	2.72	0.54	0.3	7.75	0.82	1.48	0.6
114	26.1	2.05	0.66	2.5	17.4	0.62	0.89	4.92
127	47	1.66	1.00	5.4	25.5	0.49	11.2	13.2

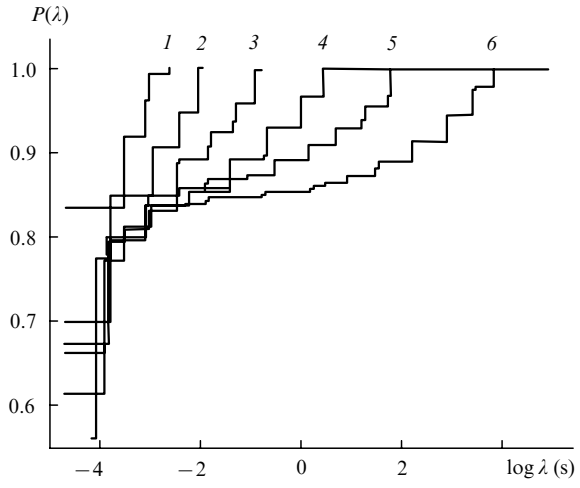


Figure 20. Relaxation spectra of monodisperse polystyrene-based polymers plotted in the form of distribution functions $P(\lambda)$ using the data taken from Ref. 50.
$M \times 10^{-3}$ = 39 (*1*), 70 (*2*), 128 (*3*), 275 (*4*), 770 (*5*) and 3000 (*6*).

tions. The most obvious is the method of central moments,[278] which in the case of the Stieltjes integral are defined by

$$\mu_k(\lambda) = \int (\lambda - \langle\lambda\rangle)^k \mathrm{d}P(\lambda) ,$$

where $\langle\lambda\rangle$ is the arithmetic mean of a random quantity λ. A set of appropriate characteristics includes the dispersion $\sigma = (\mu_2)^{1/2}$, asymmetry (skewness) $\gamma_1 = \mu_3/\sigma^3$ and excess $\gamma_2 = \mu_4/\sigma^4 - 3$. Corresponding characteristics of the distribution functions shown in Fig. 20 are listed in Table 14. As can be seen, the average relaxation times and dispersions depend on the molecular mass (see also Table 1), whereas the asymmetry and excess show no dependence within the limits of data scatter. Therefore, one can state that the relaxation spectra of monodisperse polymers with different molecular masses, expressed in terms of the distribution function $P(\lambda)$, are similar.

The data listed in Table 15 show that the MMD of polymers affects their relaxation spectra. This manifests itself not only in the average and maximum relaxation times and dispersion but also in the γ_1 and γ_2 values (relaxation spectra were constructed using the OIR technique and the results reported by Watanabe and Kotaka [67]). A comparison with various polymer blends showed that the additivity principle is not valid for at least one binary blend (molecular masses were 4.27×10^5 and 3.89×10^4). Namely, the maximum relaxation time was composition independent; correspondingly, the dispersion was much larger than the value characteristic of the polymer blend.

Table 14. Characteristics of the distribution functions $P(\lambda)$ for monodisperse polystyrene-based polymers having different molecular masses.

M	$\langle\lambda\rangle_n$ /s	$\langle\lambda\rangle_w$ /s	σ	γ_1	γ_2
3 000 000	2070	20750	31200	1.34	−0.181
770 000	19.93	56.05	32.01	1.702	4.566
275 000	0.916	3.245	4.326	2.807	6.387
128 000	0.0465	0.09115	0.0379	−0.984	−0.707
70 000	0.0045	0.00706	0.0029	−0.965	−0.776
39 000	9.456×10^{-4}	6.32×10^{-4}	1.423×10^{-4}	0.834	6.57×10^{-4}

This is qualitatively consistent with the conclusions drawn in another study.[83] Unfortunately, data for quantitative characterisation are insufficient. Nevertheless, it is clear that representation of a relaxation spectrum in the form of the distribution function $P(\lambda)$ can serve as a reliable basis for establishment of interrelation between the relaxation spectrum and the topological structure of the polymer. This research avenue requires intensive development.

V. Conclusion

Many researchers have put forward the idea of using the relaxation properties of a polymer for non-destructive quantitative characterisation of topological structure. This first of all concerns the MMD as the key structural parameter of high-molecular-mass compounds.[31–33] However, experience showed that the use of the relaxation curves leads to incorrect conclusions, because these methods are based on quite different and arbitrary mixing rules.[83] We believe that it would be more appropriate to use the relaxation spectrum, because it is obviously related to the polymer structure. Indeed, '...a normalised relaxation spectrum is a replica of the shape of the MMD curve'.[243] Here, two problems arise, namely, (i) calculations of relaxation spectra from relaxation data and (ii) establishment of a relation between the relaxation spectrum and the polymer structure.

In this review we tried to show some ways of attacking these problems. The OIR technique provides a means of stable calculations of relaxation spectra in the form of the distribution function $P(\lambda)$, which in turn serves as a reliable basis for the establishment of correlations between the relaxation spectrum and the polymer structure.

This approach seems to be not unique. For instance, the Havriliak–Negami equation (see above) is related [177,243] to the empirical relaxation spectrum, which is based on the Cole–Cole model.[279] The spectral parameters thus obtained correlate with the MMDs of some polyethylenes.[243] Probably, other characteristics of the topological structure can also be extracted from this type of relaxation spectra.

Nearly five decades ago G L Slonimskii put forward a basically different approach to analysis of the relaxation properties of polymers.[280] The method involves expression of the

Table 15. Characteristics of the distribution functions $P(\lambda)$ for bidisperse polystyrene blends (processed data taken from Ref. 67).

w_2	λ_{max} /s	$\langle\lambda\rangle_n$ /s	$\langle\lambda\rangle_w$ /s	σ	γ_1	γ_2
1.0	> 10000	1.91	8708	129	77.5	6010
0.4	10000	9.54	4455	206	47.9	2322
0.2	21.5	0.0408	9.895	0.634	33.7	791.15
0.1	13.6	0.0113	6.028	0.261	157.9	2228
0,05	12.4	0.0050	2.263	0.1065	1718	4951
0.01	11.3	0.0025	1.196	0.0546	12450	36500
0	0.022	0.0020	0.0112	0.0043	3.34	11.9
0.4 add	10000	3.95	4609	134.9	73.3	5429.5
0.2 add	10000	1.97	4620	95.38	103.7	10861
0.1 add	10000	1.15	5262	77.78	127.5	16381

relaxation relations between stress σ and strain ε using fractional derivatives

$$\sigma(t) = E\lambda^{\alpha}\frac{\mathrm{d}^{\alpha}\varepsilon(t)}{\mathrm{d}t^{\alpha}},\ 0 \leqslant \alpha \leqslant 1.$$

At $\alpha = 0$, one gets an equation for the Hooke model (pure elasticity) while the equation derived at $\alpha = 1$ describes a Newtonian flow.

However, attempts at using this approach in studies of particular systems (see, *e.g.*, Ref. 281) have been undertaken only recently. Clearly, in this case we deal with quite a new view of the mathematical formalism and physical meaning of the relaxation spectrum. Here, one must keep in mind that '... if modelling is intended to understand or to discover new phenomena, the exact mathematical model should be sufficiently sophisticated, especially when several branches of solutions have different physical meanings. Hence, the study of a sophisticated exact inverse problem may be not only a pure mathematical research but also an applied one, where interactions between ways of modelling and inverse theory are essential'.[282]

This review has been written with financial support from the Russian Foundation for Basic Research and the Government of the Moscow Region (Project r2004naukograd No. 04-01-97202).

References

1. G M Bartenev, S Ya Frenkel' *Fizika Polimerov* (The Physics of Polymers) (Leningrad: Khimiya, 1990)
2. G M Bartenev, A G Barteneva *Relaksatsionnye Svoistva Polimerov* (Relaxation Properties of Polymers) (Moscow: Khimiya, 1992)
3. V I Irzhak, B A Rozenberg, N S Enikolopyan *Setchatye Polimery. Sintez, Struktura, Svoistva* (Cross-linked Polymers. Synthesis, Structure, Properties) (Moscow: Nauka, 1979)
4. G V Vinogradov, A Ya Malkin *Reologiya Polimerov* (Rheology of Polymers) (Moscow: Khimiya, 1977)
5. G M Bartenev *Struktura i Relaksatsionnye Svoistva Elastomerov* (Structure and Relaxation Properties of Elastomers) (Moscow: Khimiya, 1979)
6. V K Kryzhanovskii, V V Burlov *Prikladnaya Fizika Polimernykh Materialov* [Applied Physics of Polymeric Materials [St Petersburg: St Petersburg State Technological Institute (Technical University), 2001]
7. R Hakien, R Simha *J. Appl. Phys.* **39** 1890 (1968)
8. D S Sanditov, S Sh Sangadiev *Vysokomol. Soedin., Ser. A* **41** 977 (1999) [a]
9. D S Sanditov *Dokl. Akad. Nauk* **390** 39 (2003) [b]
10. D S Sanditov, S Sh Sangadiev *Vysokomol. Soedin., Ser.A* **47** 478 (2005) [a]
11. Yu Ya Gotlib, A A Darinskii, Yu E Svetlov *Fizicheskaya Kinetika Makromolekul* (Physical Kinetics of Macromolecules) (Leningrad: Khimiya, 1986)
12. Yu Ya Gotlib, V P Toshchenkov *Vysokomol. Soedin., Ser. A* **43** 833 (2001) [a]
13. M L Mansfield *J. Polym. Sci., Polym. Phys. Ed.* **21** 773 (1983)
14. V G Rostiashvili, V I Irzhak, B A Rozenberg *Steklovanie Polimerov* (Vitrification of Polymers) (Leningrad: Khimiya, 1987)
15. V A Bershtein, V M Egorov *Differentsial'naya Skaniruyushchaya Kalorimetriya v Fizikokhimii Polimerov* (Differential Scanning Calorimetry in Physical Chemistry of Polymers) (Leningrad: Khimiya, 1990)
16. G P Johari, M Goldstein *J. Chem. Phys.* **53** 2372 (1970)
17. G P Johari, M Goldstein *J. Phys. Chem.* **74** 2034 (1970)
18. G P Johari, M Goldstein *J. Chem. Phys.* **55** 4245 (1971)
19. L Hayler, M Goldstein *J. Chem. Phys.* **66** 4736 (1977)
20. G P Johari *J. Chem. Phys.* **58** 176 (1973)
21. G P Johari *J. Chem. Phys.* **77** 4619 (1982)
22. G P Johari, in *Chemistry and Technology of Epoxy Resins. Electrical Properties of Epoxy Resins* Ch. 6 (Ed. B Ellis) (London: Blackie and Sons, 1993)
23. G P Johari *Polymer* **27** 866 (1986)
24. V A Bershtein, V M Egorov, Yu A Emelyanov, V A Stepanov *Polym. Bull.* **9** 98 (1983)
25. V A Bershtein, V M Egorov, V A Stepanov *Dokl. Akad. Nauk SSSR* **269** 627 (1983) [c]
26. V A Bershtein, V M Egorov *Vysokomol. Soedin., Ser. A* **27** 2440 (1985) [a]
27. H Sasabe, S Saito *J. Polym. Sci., Polym. Phys.* **6** 1401 (1968)
28. A R Nekhoda, V G Rostiashvily, V I Irzhak, T F Irzhak *Chem. Phys. Lett.* **108** 363 (1984)
29. A R Nekhoda, V G Rostiashvili, V I Irzhak *Dokl. Akad. Nauk SSSR* **278** 922 (1984) [d]
30. J A Forrest, K Dalnoki-Veress *Adv. Colloid Interface Sci.* **94** 167 (2001)
31. A Ya Malkin *Vysokomol. Soedin., Ser. B* **44** 1720 (2002) [a]
32. V I Irzhak *Usp. Khim.* **69** 780 (2000) [*Russ. Chem. Rev.* **69** 717 (2000)]
33. Y Lui, M T Shaw, W H Tuminello *J. Rheol.* **42** 453 (1998)
34. M Doi, S Edwards *The Theory of Polymer Dynamics* (Oxford: Oxford Univiversity Press, 1988)
35. S H Wasserman *J. Rheol.* **39** 601 (1995)
36. A Ya Malkin *Rheol. Acta* **12** 486 (1973)
37. V I Irzhak *Vysokomol. Soedin., Ser. B* **42** 1616 (2000) [a]
38. M Antonietti, T Pakula, W Bremser *Macromolecules* **28** 4227 (1995)
39. V Foumaraux-Demange, A Brulet, J P Cotton, L Hilliou, P Martinoty, P Keller, F Boue *Macromolecules* **31** 7445 (1998)
40. L A Utracki *J. Polym. Sci., Polym. Lett. Ed.* **11** 717 (1973)
41. P G Santangelo, C M Roland *J. Non-Cryst. Solids* **235 – 237** 709 (1998)
42. D C Baird, R L Ballman *J. Rheol.* **23** 505 (1979)
43. G V Vinogradov *Vysokomol. Soedin., Ser. A* **13** 294 (1971) [a]
44. G V Vinogradov, V N Pokrovsky, Yu G Yanovsky *Rheol. Acta* **11** 258 (1972)
45. V A Kargin, G L Slonimskii *Dokl. Akad. Nauk SSSR* **62** 239 (1948) [d]
46. Russ. P. 2023255; *Byull. Izobret.* (21) 142 (1994)
47. Yu I Matveev, A A Askadskii *Vysokomol. Soedin., Ser. B* **35** 63 (1993) [a]
48. Yu A Ol'khov, V I Irzhak *Vysokomol. Soedin., Ser. B* **40** 1706 (1998) [a]
49. T F Irzhak, L I Kuzub, O V Nikitina, V I Irzhak *Vysokomol. Soedin., Ser. A* **42** 1404 (2000) [a]
50. A Schausberger, G Schindlauer, H Janeschitz-Kriegl *Rheol. Acta* **24** 220 (1985)
51. L I Kuzub, V I Irzhak *Vysokomol. Soedin., Ser. A* **46** 304 (2004) [a]
52. H Watanabe *Prog. Polym. Sci.* **24** 1253 (1999)
53. K Fuchs, Chr Friedrich, J Weese *Macromolecules* **29** 5893 (1996)
54. D W Mead *J. Rheol.* **38** 1769 (1994)
55. J K Jackson, M E De Rosa, H H Winter *Macromolecules* **27** 2426 (1994)
56. R R Rahalkar *Rheol. Acta* **29** 88 (1990)
57. W H Stockmayer *Pure Appl. Chem.* **15** 539 (1967)
58. H Yoshida, K Adachi, H Watanabe, T Kotaka *Polym. J.* **21** 863 (1989)
59. M Andreis, J L Koenig *Adv. Polym. Sci.* **89** 71 (1989)
60. V V Marchenkov, A K Khitrin *Khim. Fiz.* **3** 1399 (1984) [e]
61. G E Karnaukh, A A Lundin, B N Provotorov, K T Summanen *Zh. Eksp. Teor. Fiz.* **91** 2229 (1987) [f]
62. A N Ivanova, B N Provotorov *Zh. Eksp. Teor. Fiz.* **107** 473 (1995) [f]
63. F Bueche *Physical Properties of Polymers* (New York, London: Interscience, 1962)
64. J D Ferry *Viscoelastic Properties of Polymers* (New York: Wiley, 1961)
65. P G de Gennes *Scaling Concepts in Polymer Physics* (Ithaca, London: Cornell University Press, 1979)
66. A Yu Grossberg, A R Khokhlov *Statisticheskaya Fizika Makromolekul* (Statistical Physics of Macromolecules) (Moscow: Nauka, 1989)
67. H Watanabe, T Kotaka *Macromolecules* **17** 2316 (1984)
68. A Ya Malkin, A E Teishev *Vysokomol. Soedin., Ser. A* **29** 2230 (1987) [a]
69. G V Gordon, M T Shaw *Computer Programs for Rheologists* Ch. 4 (Munich, Vienna, New York: Hauser Publ., 1994)

70. W H Tuminello, N Cudre-Mauroux *Polym. Eng. Sci.* **31** 1496 (1991)
71. D Nichetti, I Manas-Zloczower *J. Rheol.* **42** 951 (1998)
72. W H Tuminello *Polym. Eng. Sci.* **26** 1339 (1986)
73. Y Liu, M T Shaw *J. Rheol.* **42** 267 (1998)
74. W J McGrory, W H Tuminello *J. Rheol.* **34** 867 (1990)
75. C Carrot, J Guillet *J. Rheol.* **41** 1203 (1997)
76. F A Morrison, R G Larson *J. Polym. Sci., Polym. Phys.* **30** 943 (1992)
77. M R Nobile, F Cocchini *Rheol. Acta.* **40** 111 (2001)
78. J-Ch Majeste, A Allal, J-P Montfort *Rheol. Acta.* **42** 477 (2003)
79. B Ya Teitel'baum *Termomekhanicheskii Analiz Polimerov* (Thermomechanical Analysis of Polymers) (Moscow: Nauka, 1979)
80. Yu A Ol'khov, S M Baturin, V I Irzhak *Vysokomol. Soedin., Ser. B* **38** 849 (1996) [a]
81. T F Irzhak, S E Varyukhin, Yu A Ol'khov, S M Baturin, V I Irzhak *Vysokomol. Soedin., Ser. A* **39** 671 (1997) [a]
82. E E Al'yanova, N M Bravaya, T I Ponomareva, V I Tsvetkova, P M Nedorezova, V I Irzhak *Vysokomol. Soedin., Ser. B* **40** 1691 (1998) [a]
83. J K Jackson, H H Winter *Macromolecules* **28** 3146 (1995)
84. D Maier, A Eckstein, C. Friedrich, J Honerkamp *J. Rheol.* **42** 1153 (1998)
85. P Cassagnau, J P Montfort, G Marin, P Monge *Rheol. Acta* **32** 156 (1993)
86. V I Irzhak, G V Korolev, M E Solov'ev *Usp. Khim.* **66** 179 (1997) [*Russ. Chem. Rev.* **66** 167 (1997)]
87. S E Varyukhin, V I Irzhak *Dokl. Acad. Nauk* **369** 755 (1999) [b]
88. V I Irzhak *Usp. Khim.* **69** 283 (2000) [*Russ. Chem. Rev.* **69** 261 (2000)]
89. V V Lopatin, A A Askadskii, V G Vasil'ev *Vysokomol. Soedin., Ser. A* **46** 1217 (2004) [a]
90. H Watanabe, T Sakamoto, T Kotaka *Macromolecules* **18** 1436 (1985)
91. A Schausberger *Rheol. Acta* **25** 596 (1986)
92. J Schieber, C Curtiss, R Bird *Ind. Chem. Fundam.* **25** 471 (1986)
93. Y-H Lin, J-H Juang *Macromolecules* **32** 1811 (1999)
94. H Watanabe, T Kotaka, M Tirrell *Macromolecules* **24** 201 (1991)
95. M Doi, H Watanabe *Macromolecules* **24** 740 (1991)
96. J A Kornfield, G G Fuller, D S Pearson *Macromolecules* **22** 1334 (1989)
97. C M Ylitalo, J A Kornfield, G G Fuller, D S Pearson *Macromolecules* **24** 749 (1991)
98. M J Struglinski, W W Graessley *Macromolecules* **18** 2630 (1985)
99. Y Imanishi, K Adachi, T Kotaka *J. Chem. Phys.* **89** 7585 (1988)
100. K Adachi, I Nishi, S Itoh, T Kotaka *Macromolecules* **23** 2550 (1990)
101. K Adachi, I Nishi, I Nishi, T Kotaka *Macromolecules* **23** 2554 (1990)
102. J S Fodor, D A Hill *Macromolecules* **26** 5379 (1993)
103. J S Fodor, D A Hill *J. Phys. Chem.* **98** 7674 (1994)
104. T Kotaka, K Adachi *Polym. Sympos.* **101** 123 (1996)
105. J Vega, M Aguilar, J Peun, D Pastor, J Martnnez-Salazar *e-Polymers* art. no. 046 (2002)
106. S J Teertstra, M Gauthier *Progr. Polym. Sci.* **29** 277 (2004)
107. G V Korolev, A P Marchenko *Usp. Khim.* **69** 447 (2000) [*Russ. Chem. Rev.* **69** 409 (2000)]
108. A Goto, T Fukuda *Progr. Polym. Sci.* **29** 329 (2004)
109. S B Kharchenko, R M Kannan, J J Cernohous, S Venkataramani *Macromolecules* **36** 399 (2003)
110. H M Laun, H Schuch *J. Rheol.* **33** 119 (1989)
111. H M Münstedt, S Kurzbeck, L Egersdofer *Rheol. Acta* **37** 31 (1998)
112. P de Gennes *J. Phys. (Paris)* **36** 1199 (1975)
113. D S Pearson, E Helfand *Macromolecules* **17** 888 (1984)
114. L J Fetters, A D Kiss, D S Pearson, G F Quack, F J Vitus *Macromolecules,* **26** 647 (1993)
115. J M Carella, J T Gotro, W W Graessley *Macromolecules* **19** 659 (1986)
116. S B Kharchenko, R M Kannan *Macromolecules* **36** 407 (2003)
117. C M Nunez, B S Chiou, A L Andrady, S A Khan *Macromolecules* **33** 1720 (2000)
118. I Sendijarevic, A McHugh *Macromolecules* **33** 590 (2000)
119. J Roovers *Polymer* **26** 1091 (1985)
120. G S Grest, L J Fetters, J S Huang, D Richter *Adv. Chem. Phys.* **94** 67 (1996)
121. K L Ngai, D J Plazek *Rubber Chem. Technol.* **68** 376 (1995)
122. P G Santangelo, C M Roland, J E Puskas *Macromolecules* **32** 1972 (1999)
123. W W Graessley *Macromolecules* **15** 1164 (1982)
124. C B Gell, W W Graessley, V Efstratiadis, M Pitsikalis, N Hadjichristidis *J. Polym. Sci., Polym. Phys. Ed.* **35** 1943 (1997)
125. C Bero, C M Roland *Macromolecules* **29** 1562 (1996)
126. C M Roland, C Bero *Macromolecules* **29** 7521 (1996)
127. H Mavridis, R N Shroff *Polym. Eng. Sci.* **32** 1778 (1992)
128. J S Wang, R S Porter *Rheol. Acta* **34** 495 (1995)
129. S G Hatzikiriakos *Polym. Eng. Sci.* **40** 2279 (2000)
130. P J Flory *Statistical Mechanics of Chain Molecules* (New York: Wiley, 1969)
131. S T Milner, T C B McLeish *Macromolecules* **31** 7479 (1998)
132. S Trinkle, P Walter, Ch Friedrich *Rheol. Acta* **41** 103 (2002)
133. S Trinkle, Ch Friedrich *Rheol. Acta* **40** 322 (2001)
134. C He, S Costeux, P Wood-Adams *Polymer* **45** 3747 (2004)
135. V I Irzhak *Usp. Khim.* **73** 275 (2004) [*Russ. Chem. Rev.* **73** 251 (2004)]
136. L Z Rogovina, G L Slonimskoi *Vysokomol. Soedin., Ser. B* **39** 1543 (1997) [a]
137. D Stauffer, A Coniglio, M Adam *Adv. Polym. Sci.* **44** 103 (1982)
138. F Chambon, H H Winter *Polym. Bull.* **13** 499 (1985)
139. F Chambon, H H Winter *J. Rheol.* **31** 683 (1987)
140. M Baumgaertel, H H Winter *Rheol. Acta* **28** 511 (1989)
141. H H Winter *Progr. Coll. Polym. Sci.* **75** 104 (1987)
142. P Tordjeman, C Fargette, P Mutin *J. Rheol.* **45** 995 (2001)
143. M Rubinstein, R Colby, J Gillmor *Polym. Prep.* **30** 81 (1989)
144. D Adolf, J Martin *Macromolecules* **23** 3700 (1990)
145. T Nicolai, H Randrianantoandro, F Prochazka, D Durand *Macromolecules* **30** 5897 (1997)
146. T S Chow *Macromol. Theor. Simul.* **7** 257 (1998)
147. J Lange, M Johansson, C T Kelly, P J Halley *Polymer* **40** 5699 (1999)
148. T Tixier, Ph Tordjeman *Polymer* **44** 6937 (2003)
149. Yu I Matveev *Vysokomol. Soedin., Ser. B* **45** 841 (2003) [a]
150. A B Rodd, J Cooper-White, D E Dunstan, D V Boger *Polymer* **42** 185 (2001)
151. Y Zhao, Y Yang, C Wu *Macromolecules* **36** 855 (2003)
152. H H Winter, M Mours *Adv. Polym. Sci.* **134** 167 (1997)
153. J E Marin, D Adolf, J P Wilcoxon *Phys. Rev. Lett.* **61** 2620 (1988)
154. P M Wood-Adams, J M Dealy, A W de Groot, O D Redwine *Macromolecules* **33** 7489 (2000)
155. C A Garcna-Franco, S Srinivas, D J Lohse, P Brant *Macromolecules* **34** 3115 (2001)
156. B A Rozenberg, V I Irzhak *Prog. Colloid Polym. Sci.* **90** 194 (1992)
157. T R Deberdeev, R M Garipov, R Ya Deberdeev, T F Irzhak, V I Irzhak *Vysokomol. Soedin., Ser. A* **46** 412 (2004) [a]
158. T R Deberdeev, R M Garipov, T F Irzhak, V I Irzhak, R Ya Deberdeev *Dokl. Akad. Nauk* **393** 209 (2003) [d]
159. F Ikkai, M Shibayama *J. Polym. Phys. Ed.* **43** 617 (2005)
160. L Gonzales, A Rodriguez, A Del Campo, A Marcos-Fernandez *Polym. Intern.* **53** 1426 (2004)
161. L E Roth, D A Vega, E M Valles, M A Villar *Polymer* **45** 5923 (2004)
162. M A Villar, E M Valles *Macromolecules* **29** 4081 (1996)
163. D A Vega, M A Villar, J L Alessandrini, E M Valles *Macromolecules* **34** 4591 (2001)
164. R Chasset, P Thirion, in *Proceedings of the Conference on Physics of Non-Crystalline Solids* (Ed. J A Prins) (Amsterdam: North-Holland, 1965) p. 56
165. S Ndoni, A Vorup, O Kramer *Macromolecules* **31** 3353 (1998)
166. B A Rozenberg, E F Oleinik *Usp. Khim.* **53** 273 (1984) [*Russ. Chem. Rev.* **53** 164 (1984)]

167. D W van Krevelen *Properties of Polymers: Correlations with Chemical Structure* (Amsterdam: Elsevier, 1972)
168. A A Askadskii, Yu I Matveev *Khimicheskoe Stroenie i Fizicheskie Svoistva Polimerov* (Chemical Structure and Physical Properties of Polymers) (Moscow: Khimiya, 1977)
169. A A Askadskii *Usp. Khim.* **67** 755 (1998) [*Russ. Chem. Rev.* **67** 681 (1998)]
170. M K Pakter, Yu S Zaitsev, G V Borisenko, Yu M Paramonov, T K Muratov, Yu V Zelenev *Plast. Massy* (10) 7 (1987)
171. B D Fitz, J Mijovic *Macromolecules* **32** 4134 (1999)
172. H H Winter *Mater. Res. Soc. Bull.* **16** (8) 44 (1991)
173. M Böhm, W V Soden, W Heinrich, A A Yehia *Colloid Polym. Sci.* **265** 295 (1987)
174. W B Liau *Polymer* **40** 599 (1999)
175. G Williams, D C Watts *Trans. Faraday Soc.* **66** 80 (1970)
176. S Havriliak, S Negami *J. Polym. Sci., C* **14** 99 (1966)
177. S Havriliak, S Negami *Polymer* **8** 161 (1967)
178. W B Liau, K C Cheng *Polymer* **39** 6007 (1998)
179. K L Ngai, C M Roland *Macromolecules* **26** 6824 (1993)
180. C M Roland, K L Ngai, D J Plazek *Comput. Theor. Polym. Sci.* **7** 133 (1997)
181. S Andjelić, J Mijović *Macromolecules* **31** 2872 (1998)
182. A Havranek, M Ilavsky, J Nedbal, M Böhm, W V Soden, B Stoll *Colloid Polym. Sci.* **265** 8 (1987)
183. J P Elondou *Eur. Polym. J.* **38** 431 (2002)
184. M Tabellout, H Randrianantoandro, J R Emeri, D Durand, D Hayward, R A Pethrik *Polymer* **36** 4547 (1995)
185. T Koike *J. Appl. Polym. Sci.* **44** 679 (1992)
186. R A Pethrik, D Hayward *Prog. Polym. Sci.* **27** 1983 (2002)
187. L P Smirnov *Vysokomol. Soedin., Ser. B* **42** 1775 (2000) [a]
188. L J Mathias *Solid State NMR of Polymers* (New York: Plenum Press, 1991)
189. Yu Ya Gotlib, M I Lifshits, V A Shevelev, I S Lishanskii, I V Balanina *Vysokomol. Soedin., Ser. A* **18** 2299 (1976) [a]
190. G I Sandakov, V P Tarasov, N N Volkova, Yu A Ol'khov, L P Smirnov, L N Erofeev *Vysokomol. Soedin., Ser. B* **31** 821 (1989) [a]
191. G I Sandakov, L P Smirnov, A I Sosikov, K T Summanen, N N Volkova *J. Polym. Sci., Polym. Phys.* **32** 1585 (1994)
192. P T Callaghan, E T Samulski *Macromolecules* **33** 3795 (2000)
193. I N Zakirov, V I Irzhak, V M Lantsov, B A Rozenberg *Vysokomol. Soedin., Ser. A* **30** 915 (1988) [a]
194. V I Irzhak, V M Lantsov, B A Rozenberg, in *Crosslinked Epoxy*. (Eds B Sedlachek, J Kahovec) (New York, Berlin: W de Gruyter, 1987) p. 359
195. I N Zakirov, V M Lantsov, V S Derinovskii, Yu N Smirnov, A I Efremova, V I Irzhak, B A Rozenberg *Vysokomol. Soedin., Ser. A* **28** 1719 (1986) [a]
196. J-F Shi, L C Dickinson, W J McKnight, J C W Chien *Macromolecules* **26** 5908 (1993)
197. S B Ross-Murphy, in *Physical Networks. Polymers and Gels* (Eds W Burchard, S B Ross-Murphy) (London, New York: Elsevier, 1990) p. 288
198. K te Nijenhuis *Adv. Polym. Sci.* **130** 1 (1997)
199. A K Lele, R A Mashelkar *J. Non-Newtonian Fluid Mech.* **75** 99 (1998)
200. L G Baxandall *Macromolecules* **22** 1982 (1989)
201. L Leibler, M Rubinstein, R H Colby *Macromolecules* **24** 4701 (1991)
202. F Tanaka, S F Edwards *Macromolecules* **25** 1516 (1992)
203. M Rubinshtein, A N Semenov *Macromolecules* **31** 1386 (1998)
204. P J Flory *Faraday Disc. Chem. Soc.* **57** 1 (1975)
205. V I Irzhak *Vysokomol. Soedin., Ser. A* **46** 1401 (2004) [a]
206. R Stadler, L de Lucca Freitas *Colloid Polym. Sci.* **266** 1102 (1988)
207. R Stadler, L de Lucca Freitas *Macromolecules* **22** 714 (1989)
208. M Müller, R Stadler, F Kremer, G Williams *Macromolecules* **28** 6942 (1995)
209. M Müller, U Seidel, R Stadler *Polymer* **36** 3143 (1995)
210. L L de Lucca Freitas, R Stadler *Macromolecules* **20** 2478 (1987)
211. U Seidel, R Stadler, G G Fuller *Macromolecules* **27** 2066 (1994)
212. A Tobol'skii *Svoistva i Struktura Polimerov* (Properties and Structure of Polymers) (Moscow: Khimiya, 1964)
213. P E Rouse *J. Chem. Phys.* **21** 1272 (1953)
214. T F Irzhak, L I Kuzub, V I Irzhak *Vysokomol. Soedin., Ser. A* **44** 1101 (2002) [a]
215. T F Irzhak, L I Kuzub, V I Irzhak *Inzh.-Fiz. Zh.* **76** 116 (2003)
216. S Matsuoka, A Hale *J. Appl. Polym. Sci.* **65** 77 (1997)
217. K S Schweizer *J. Chem. Phys.* **91** 5802 (1989)
218. K S Schweizer *J. Chem. Phys.* **91** 5822 (1989)
219. K S Schweizer *J. Chem. Phys.* **103** 1934 (1995)
220. K S Schweizer, M Fuchs, G Szamel, M Guenza, H Tang *Macromol. Theor. Simul.* **6** 1037 (1997)
221. V I Irzhak *Dokl. Akad. Nauk* **379** 613 (2001) [b]
222. V I Irzhak *Dokl. Akad. Nauk* **380** 31 (2001) [b]
223. C Satmarel, A A Gurtovenko, A Blumen *Macromolecules* **36** 486 (2003)
224. A V Chatterjee, R F Loring *J. Chem. Phys.* **103** 4711 (1995)
225. V I Irzhak *Dokl. Akad. Nauk* **385** 470 (2002) [b]
226. A Ya Malkin *Vysokomol. Soedin., Ser. B* **44** 1598 (2002) [a]
227. N W Tschoegl, I Emri *Rheol. Acta* **32** 322 (1993)
228. H H Winter *J. Non-Newtonian Fluid Mech.* **68** 225 (1997)
229. A Ya Malkin, I Masalova *Rheol. Acta* **40** 261 (2001)
230. J J Aklonis, A V Tobolsky *J. Appl. Polym. Sci.* **36** 3483 (1965)
231. G Akovali *J. Polym. Sci., A2* **5** 875 (1967)
232. Y-H Lin *Macromolecules* **19** 159 (1986)
233. A V Tobolsky, J J Aklonis, G Akovali *J. Chem. Phys.* **42** 723 (1965)
234. M Baumgaertel, A Schausberger, H H Winter *Rheol. Acta* **29** 400 (1990)
235. Yu S Urzhumtsev, A V Putans, E V Kalnroze *Mekhan. Polim.* (4) 686 (1967)
236. F Schwarzl, A J Staverman *Physics* **18** 795 (1952)
237. G M Bartenev, A A Valishin, I I Panchuk *Vysokomol. Soedin., Ser. A* **19** 187 (1977) [a]
238. S I Vol'fson, V I Kimel'blat, M G Khakimov, I G Chebotareva *Mekhan. Kompozit. Mater.* **34** 531 (1998)
239. S I Vol'fson, V I Kimel'blat, M G Khakimov, I G Chebotareva *Mekhan. Kompozit. Mater.* **34** 691 (1998)
240. V I Kimel'blat, S I Vol'fson, I G Chebotareva, in *Struktura i Dinamika Molekulyarnykh Sistem* (Structure and Dynamics of Molecular Systems) (Ioshkar-Ola: Mordvinian State Technical University, 1998) Pt. I, p. 116
241. V I Kimel'blat, S I Vol'fson, I G Chebotareva, M G Khakimov *Kauchuk Rezina* (2) 16 (1998)
242. V I Kimel'blat *Molekulyarnye Kharakteristiki, Molekulyarnaya Podvizhnost' v Rasplavakh i Mekhanicheskie Svoistva Poliolefinovykh Kompozitsii* (Molecular Characteristics, Molecular Mobility in Melts and Mechanical Properties of Polyolefin Compositions) (Kazan': Kazan' Energy State University, 2003)
243. C A Garsia-Franco, D W Mead *Rheol. Acta* **38** 34 (1999)
244. A V Tobolsky, K Murakami *J. Polym. Sci.* **40** 443 (1959)
245. L Messe, M Pezolet, R E Prudhomme *Polymer* **42** 563 (2000)
246. R I Tanner *J. Appl. Polym. Sci.* **12** 1649 (1968)
247. D R Wiff, M Gehatia *J. Appl. Phys.* **46** 4231 (1975)
248. J Honerkamp *Rheol. Acta* **28** 363 (1989)
249. Y Liu *Rheol. Acta* **40** 256 (2001)
250. M Baumgaertel, H H Winter *J. Non-Newtonian Fluid Mech.* **44** 15 (1992)
251. S G Hatzikiriakos, M Kapnistos, D Vlassopoulos, C Chevillard, H H Winter, J Roovers *Rheol. Acta* **39** 38 (2000)
252. T Roths, D Maier, C Friedrich, M Marth, J Honerkamp *Rheol. Acta* **39** 163 (2000)
253. T Roths, M Marth, J Weese, J Honerkamp *Comput. Phys. Commun.* **139** 279 (2001)
254. J Weese *Comput. Phys. Commun.* **77** 429 (1993)
255. S W Provencher. *Comput. Phys. Commun.* **27** 213 (1982)
256. J Weese. *Comput. Phys. Commun.* **69** 99 (1992)
257. Y Liu *Rheol. Acta* **38** 357 (1999)
258. M B Peirotti, J A Deiber, J A Ressia, M A Villar, E M Valles *Rheol. Acta* **37** 449 (1998)
259. P J Davis *Interpolation and Approximation* (New York: Dover, 1975)
260. A R Davies, R S Anderssen *J. Non-Newtonian Fluid Mech.* **73** 163 (1997)

261. A R Davies, R S Anderssen *J. Non-Newtonian Fluid Mech.* **79** 235 (1998)
262. A Ya Malkin, V V Kuznetsov *Rheol. Acta* **39** 379 (2000)
263. E A Jensen *J. Non-Newtonian Fluid Mech.* **107** 1 (2002)
264. V A Dubovitskii, V I Irzhak *Dokl. Akad. Nauk* **390** 32 (2003) [b]
265. V A Dubovitskii, V I Irzhak *Vysokomol. Soedin., Ser. B* **47** 121 (2005) [a]
266. V A Dubovitskii, K V Ermolaev *Zh. Fiz. Khim.* **70** 1233 (1996) [g]
267. E Kh Gokhman *Integral Stilt'esa i ego Prilozheniya* (Integral Stiltjes and Its Applications) (Moscow: Fizmatlit, 1958)
268. G E Shilov, V A Gurevich *Integral, Mera i Proizvodnaya* (Integral, Measure and Derivative) (Moscow: Nauka, 1967)
269. C L Lawson, R J Hanson *Solving Least Squares Problems* (London: Prentice-Hall, 1974)
270. H H Winter, F Chambon *Rheol. Acta* **30** 367 (1986)
271. Y H Zang, R Muller, D Froelich *Polymer* **28** 1577 (1987)
272. W Thimm, Ch Friedrich, M Marth *Rheol. Acta* **43** 1663 (1999)
273. W Thimm, Ch Friedrich, M Marth *Rheol. Acta* **44** 429 (2000)
274. D Vlassopulos, T Pakula, G Fytas, J Roovers, K Karatasos, N Hadjichristidis *Europhys. Lett.* **39** 617 (1997)
275. T Pakula, D Vlassopulos, G Fytas, J Roovers *Macromolecules* **31** 8931 (1998)
276. V A Dubovitskii, L I Kuzub, V I Irzhak, in *Tezisy Dokladov XV Simpoziuma 'Sovremennaya Khimicheskaya Fizika'* (Abstracts of Reports of the XVth Symposium 'Modern Chemical Physics') (Moscow: Moscow State University, 2003) p. 141
277. V A Dubovitskii, L I Kuzub, V I Irzhak, in *Tezisy Dokladov XVI Simpoziuma 'Sovremennaya Khimicheskaya Fizika'* (Abstracts of Reports of the XVIth Symposium 'Modern Chemical Physics') (Moscow: Moscow State University, 2004) p. 129
278. G G Abezgauz, A P Tron', Yu N Kopenkin, I A Korovina *Spravochnik po Veroyatnostnym Raschetam* (Handbook on Probability Calculations) (Moscow: Voenizdat, 1970)
279. K S Cole, S Cole *J. Chem. Phys.* **9** 341 (1941)
280. G L Slonimskii *Dokl. Akad. Nauk SSSR* **140** 343 (1961) [b]
281. A H Jimenez, B V Jara, J H Santiago *Colloid Polym. Sci.* **280** 485 (2002)
282. R S Sabatier *Inverse Probl.* **17** 1219 (2001)

[a] — *Polym. Sci. (Engl. Transl.)*
[b] — *Dokl. Phys. (Engl. Transl.)*
[c] — *Dokl. Chem. (Engl. Transl.)*
[d] — *Dokl. Phys. Chem. (Engl. Transl.)*
[e] — *Chem. Phys. Rep. (Engl. Transl.)*
[f] — *J. Exp. Theor. Phys. (Engl. Transl.)*
[g] — *Russ. J. Phys. Chem. (Engl. Transl.)*